

ORTHOGONAL SPLINE COLLOCATION
METHODS FOR FLUID FLOW
PROBLEMS

by
Nicholas Llewellyn Fisher

© Copyright by Nicholas Llewellyn Fisher, 2019

All Rights Reserved

A thesis submitted to the Faculty and the Board of Trustees of the Colorado School of Mines in partial fulfillment of the requirements for the degree of Doctor of Philosophy (Computational and Applied Mathematics).

Golden, Colorado

Date _____

Signed: _____
Nicholas Llewellyn Fisher

Signed: _____
Dr. Bernard Bialecki
Thesis Advisor

Golden, Colorado

Date _____

Signed: _____
Dr. Gregory Fasshauer
Professor and Head
Department of Applied Mathematics and Statistics

ABSTRACT

We propose an approach for the numerical solution of the Navier-Stokes equations based on a pressure Poisson equation reformulation. Through an alternating direction implicit extrapolated Crank–Nicolson time discretization, the scheme decouples the updates for velocity and pressure terms. Moreover, the proposed scheme reduces the Navier-Stokes equations to a Burgers’ equation for the velocity terms and a singular Neumann Poisson equation for the pressure. These two sub-problems are analyzed in turn. We use extrapolated alternating direction implicit Crank-Nicolson orthogonal spline collocation with splines of order r to solve the coupled Burgers’ equations in two space variables and two unknown functions. The scheme is initialized with an alternating direction implicit predictor-corrector method. We show theoretically that the H^1 norm of the error at each time level is of order r in space and of order 2 in time. Then we use a matrix decomposition algorithm for the orthogonal spline collocation solution to Poisson’s equation with Neumann boundary conditions. We show theoretically that the H^1 semi-norm of the error is of order r . In each case, our numerical results confirm these theoretical orders. Finally, the combined scheme is implemented for the solution of the pressure Poisson reformulation of the Navier–Stokes equations using splines of equal order. Numerical results show that the scheme obtains the expected optimal order convergence rates for both the velocity and pressure terms.

TABLE OF CONTENTS

ABSTRACT	iii
LIST OF FIGURES	vi
LIST OF TABLES	vii
LIST OF ABBREVIATIONS	ix
ACKNOWLEDGMENTS	x
DEDICATION	xi
CHAPTER 1 INTRODUCTION	1
CHAPTER 2 EXTRAPOLATED ADI CRANK–NICOLSON ORTHOGONAL SPLINE COLLOCATION FOR COUPLED BURGERS’ EQUATIONS	4
2.1 Preliminaries	5
2.1.1 Definitions	5
2.1.2 Results	8
2.2 Extrapolated Crank-Nicolson Orthogonal Spline Collocation	16
2.3 Convergence Analysis	17
2.4 Implementation and Numerical Results	34
CHAPTER 3 THE ORTHOGONAL SPLINE COLLOCATION SOLUTION TO POISSON’S EQUATION WITH NEUMANN BOUNDARY CONDITIONS	41
3.1 Preliminaries	42
3.2 Neumann OSC Boundary Value Problems	46
3.2.1 Homogeneous Problems	46

3.2.2	Nonhomogeneous Problems	48
3.3	Convergence Analysis	52
3.4	An OSC Matrix Decomposition Algorithm	54
3.5	Numerical Results	56
CHAPTER 4 ADI+MDA ORTHOGONAL SPLINE COLLOCATION FOR THE PRESSURE POISSON REFORMULATION OF THE NAVIER-STOKES EQUATIONS IN TWO SPACE VARIABLES		61
4.1	Preliminaries	65
4.2	Derivation of the Pressure Poisson Reformulation	66
4.3	ADI+MDA OSC Scheme for Navier-Stokes	69
4.4	Numerical Results	72
CHAPTER 5 LID-DRIVEN CAVITY FLOW		78
CHAPTER 6 CONCLUSION		87
REFERENCES CITED		88

LIST OF FIGURES

Figure 4.1	A schematic of the ADI scheme with $N = 4$ and $r = 3$. The OSC solutions are found along the solid lines at the collocation points denoted as circles. The dashed lines denote the breaks.	73
Figure 5.1	Boundary conditions for the lid-driven cavity problem.	80
Figure 5.2	Streamlines and benchmarks of the lid-driven cavity problem for $\mu = 1/100$	83
Figure 5.3	A detail of the counter rotating eddies in the lower corners of the lid-driven cavity flow problem for $\mu = 1/100$ with the normalized velocity field given by the red arrows.	84
Figure 5.4	Streamlines and benchmarks of the lid-driven cavity problem for $\mu = 1/1000$	85
Figure 5.5	A detail of the counter rotating eddies in the lower corners of the lid-driven cavity flow problem for $\mu = 1/1000$ with the normalized velocity field given by the red arrows.	86

LIST OF TABLES

Table 2.1	Maximum norm error and convergence rates for Burgers' equation using Hermite interpolant.	37
Table 2.2	L^2 norm error and convergence rates for Burgers' equation using Hermite interpolant.	38
Table 2.3	H^1 norm error and convergence rates for Burgers' equation using Hermite interpolant.	39
Table 2.4	Maximum norm error and convergence rates for Burgers' equation using Gauss interpolant.	39
Table 2.5	L^2 norm error and convergence rates for Burgers' equation using Gauss interpolant.	40
Table 2.6	H^1 norm error and convergence rates for Burgers' equation using Gauss interpolant.	40
Table 3.1	Test Problems for OSC-MDA	57
Table 3.2	OSC-MDA H^1 semi-norm errors and rates for Problem 1.	58
Table 3.3	OSC-MDA Maximum norm errors and rates for Problem 1.	58
Table 3.4	OSC-MDA H^1 semi-norm errors and rates for Problem 2.	59
Table 3.5	OSC-MDA Maximum norm errors and rates for Problem 2.	59
Table 3.6	OSC-MDA H^1 semi-norm errors and rates for Problem 3.	60
Table 3.7	OSC-MDA Maximum norm errors and rates for Problem 3.	60
Table 4.1	L^2 norm errors and rates for ∇p using $\mu = 1$	75
Table 4.2	H^1 norm errors and rates for \mathbf{u} using $\mu = 1$	75
Table 4.3	Maximum norm errors and rates for $\nabla \cdot \mathbf{u}$ using $\mu = 1$	76

Table 4.4	Errors and rates for $\nabla \cdot \mathbf{u}$, \mathbf{u} , and p using $\mu = 1/100$ and $r = 3$. Two different values of the divergence damping coefficient γ are shown: $\gamma = 0$ (left) and $\gamma = 100$ (right).	76
Table 4.5	Errors and rates for $\nabla \cdot \mathbf{u}$, \mathbf{u} , and p using $\mu = 1/100$ and $r = 4$. Two different values of the divergence damping coefficient γ are shown: $\gamma = 0$ (left) and $\gamma = 100$ (right).	77

LIST OF ABBREVIATIONS

Alternating Direction Implicit	ADI
Extrapolated Crank-Nicolson	ECN
Matrix Decomposition Algorithm	MDA
Navier–Stokes Equations	NSE
Orthogonal Spline Collocation	OSC
Pressure Poisson Equation	PPE

ACKNOWLEDGMENTS

First and foremost, I would like to thank my advisor Prof. Bernard Bialecki. His commitment to precision and clarity—and his inimitable style—are things I greatly admire. I would be remiss if I did not mention the many intelligent and engaging friends I have been lucky enough to make along the way. Without their comradery, it would have been a rather dull journey. And, of course, I would like to thank my parents for their unwavering support and encouragement throughout these many long and difficult years.

To my parents.

CHAPTER 1
INTRODUCTION

In this dissertation, we are interested in numerical solution to the two-dimensional incompressible Navier-Stokes equations. Let $\Omega = (0, 1) \times (0, 1)$, then in standard formulation these equations are given by the nonlinear system

$$\mathbf{u}_t + (\mathbf{u} \cdot \nabla) \mathbf{u} - \mu \Delta \mathbf{u} + \nabla p = \mathbf{f}(x_1, x_2, t) \quad (x_1, x_2) \in \Omega, \quad t \in (T_0, T_1], \quad (1.1)$$

$$\nabla \cdot \mathbf{u} = 0, \quad (x_1, x_2) \in \Omega, \quad t \in (T_0, T_1], \quad (1.2)$$

for the velocity field $\mathbf{u} = \begin{bmatrix} u_1 \\ u_2 \end{bmatrix}$, pressure p , kinematic viscosity μ , and forcing term $\mathbf{f} = \begin{bmatrix} f_1 \\ f_2 \end{bmatrix}$,

where $\Delta \equiv \partial^2/\partial x_1^2 + \partial^2/\partial x_2^2$, $\nabla = \begin{bmatrix} \partial/\partial x_1 \\ \partial/\partial x_2 \end{bmatrix}$ and the domain Ω has boundary $\partial\Omega$ and closure $\bar{\Omega} = \Omega \cup \partial\Omega$. The solution \mathbf{u} of (1.1)–(1.2) is subject to the initial condition,

$$\mathbf{u}(x_1, x_2, T_0) = \mathbf{g}(x_1, x_2), \quad (x_1, x_2) \in \bar{\Omega}, \quad (1.3)$$

the nonhomogeneous Dirichlet boundary condition

$$\mathbf{u}(x_1, x_2, t) = \mathbf{d}(x_1, x_2, t), \quad (x_1, x_2, t) \in \partial\Omega \times (T_0, T_1], \quad (1.4)$$

where $\mathbf{g} = \begin{bmatrix} g_1 \\ g_2 \end{bmatrix}$ and $\mathbf{d} = \begin{bmatrix} d_1 \\ d_2 \end{bmatrix}$. Note that in what follows (cf. the second term of (1.1)),

for any functions $\mathbf{u} = \begin{bmatrix} u_1 \\ u_2 \end{bmatrix}$ in Ω we have

$$(\mathbf{u} \cdot \nabla) \mathbf{u} = \left(u_1 \frac{\partial}{\partial x_1} + u_2 \frac{\partial}{\partial x_2} \right) \begin{bmatrix} u_1 \\ u_2 \end{bmatrix} = \begin{bmatrix} u_1 \frac{\partial u_1}{\partial x_1} + u_2 \frac{\partial u_1}{\partial x_2} \\ u_1 \frac{\partial u_2}{\partial x_1} + u_2 \frac{\partial u_2}{\partial x_2} \end{bmatrix}. \quad (1.5)$$

Numerical methods for the solution of (1.1)–(1.5) face several key difficulties. For instance, the nonlinear term in (1.5) must be dealt with, either through linearization [1, 2], or by solving directly [3, 4]. Additionally, the equations do not explicitly specify any boundary

conditions for the pressure term, which has in and of itself been the source of quite a lot of research [5, 6]. As a final example, the pressure and velocity terms are coupled, requiring large systems of equations to be solved [7]. To resolve some of these complications, we propose a method based on the pressure Poisson equation (PPE) reformulation of the Navier–Stokes equations [8, 9]. That is, in place of (1.1)–(1.5), we solve the equivalent system

$$\mathbf{u}_t + (\mathbf{u} \cdot \nabla) \mathbf{u} - \mu \Delta \mathbf{u} + \nabla p = \mathbf{f}(x_1, x_2, t), \quad (x_1, x_2) \in \Omega, \quad t \in (T_0, T_1], \quad (1.6)$$

$$\mathbf{u}(x_1, x_2, t) = \mathbf{d}(x_1, x_2, t), \quad (x_1, x_2) \in \partial\Omega, \quad t \in (T_0, T_1], \quad (1.7)$$

$$\Delta p = g(\mathbf{u}, x_1, x_2, t), \quad (x_1, x_2) \in \Omega, \quad t \in (T_0, T_1], \quad (1.8)$$

$$\frac{\partial p}{\partial \mathbf{n}} = h(\mathbf{u}, x_1, x_2, t), \quad (x_1, x_2) \in \partial\Omega, \quad t \in (T_0, T_1], \quad (1.9)$$

where

$$g(\mathbf{u}, x_1, x_2, t) = -\nabla \cdot ((\mathbf{u} \cdot \nabla) \mathbf{u}) + \nabla \cdot \mathbf{f} + \gamma \nabla \cdot \mathbf{u},$$

$$h(\mathbf{u}, x_1, x_2, t) = -\mathbf{n} \cdot \mathbf{u}_t - \mathbf{n} \cdot (\mathbf{u} \cdot \nabla) \mathbf{u} - \mu \mathbf{n} \cdot \nabla \times \nabla \times \mathbf{u} + \mathbf{n} \cdot \mathbf{f},$$

γ is a nonnegative real number, \mathbf{n} is the outward unit normal vector, $\frac{\partial}{\partial \mathbf{n}} = \mathbf{n} \cdot \nabla$, and we define

$$\nabla \times \nabla \times \mathbf{u} = \begin{bmatrix} -\frac{\partial^2 u_1}{\partial x_2^2} + \frac{\partial^2 u_2}{\partial x_1 \partial x_2} \\ \frac{\partial^2 u_1}{\partial x_2 \partial x_1} - \frac{\partial^2 u_2}{\partial x_1^2} \end{bmatrix}. \quad (1.10)$$

We discretize (1.6)–(1.10) in time using an alternating direction implicit (ADI) extrapolated Crank-Nicolson (ECN) scheme and in space using orthogonal spline collocation (OSC) with spline of degree r [10, 11]. The proposed method has many important advantages. The ADI-ECN scheme linearizes the equations and, together with explicit treatment of the pressure term in (1.6), will decouple the velocity and pressure updates. Moreover the pressure term is explicitly prescribed boundary conditions which will be both straightforward to compute and physically meaningful [5]. As a result, ADI-ECN splits (1.6)–(1.10) in to two well understood sub-problems. Namely, the velocity update is obtained through Burgers’

equation with an explicit forcing term and the pressure update is obtained via Poisson's equation with Neumann boundary conditions. It is with this in mind that the remainder of the dissertation has the following structure. Chapter 2 introduces and analyses the ADI-ECN-OSC scheme for the coupled Burgers' equations. We prove that the H^1 norm of the error at each time level is of order r in space and of order 2 in time. The OSC solution to Neumann Poisson boundary value problems is discussed in Chapter 3 where we prove the error for homogeneous problems is of order r in the H^1 semi-norm and introduce an efficient matrix decomposition algorithm (MDA) for the solution of the resulting linear systems. In Chapter 4, the combined ADI+MDA scheme for the PPE reformulation of the Navier–Stokes equations is presented. We show through numerical experiments that the scheme obtains the expected optimal order convergence rates. As an application, we discuss the lid-driven cavity flow in Chapter 5. Numerical experiments show that the ADI+MDA OSC scheme matches established benchmark results. Concluding remarks are given in Chapter 6.

CHAPTER 2

EXTRAPOLATED ADI CRANK–NICOLSON ORTHOGONAL SPLINE COLLOCATION FOR COUPLED BURGERS' EQUATIONS

Assume $\Omega = (a_1, b_1) \times (a_2, b_2)$ with boundary $\partial\Omega$ and closure $\bar{\Omega} = \Omega \cup \partial\Omega$. Consider the coupled 2d Burgers' equations given by the system of nonlinear partial differential equations

$$\mathbf{u}_t - \mu\Delta\mathbf{u} = -(\mathbf{u} \cdot \nabla)\mathbf{u}, \quad (x_1, x_2) \in \Omega, \quad t \in (T_0, T_1], \quad (2.1)$$

where $\mathbf{u} = \begin{bmatrix} u_1 \\ u_2 \end{bmatrix}$, $\Delta \equiv \partial^2/\partial x_1^2 + \partial^2/\partial x_2^2$, $\nabla = \begin{bmatrix} \partial/\partial x_1 \\ \partial/\partial x_2 \end{bmatrix}$. The solution \mathbf{u} of (2.1) is subject to the initial condition

$$\mathbf{u}(x_1, x_2, T_0) = \mathbf{g}(x_1, x_2), \quad (x_1, x_2) \in \bar{\Omega}, \quad (2.2)$$

where $\mathbf{g} = \begin{bmatrix} g_1 \\ g_2 \end{bmatrix}$, and the Dirichlet boundary condition

$$\mathbf{u}(x_1, x_2, t) = \mathbf{d}(x_1, x_2, t), \quad (x_1, x_2, t) \in \partial\Omega \times (T_0, T_1], \quad (2.3)$$

where $\mathbf{d} = \begin{bmatrix} d_1 \\ d_2 \end{bmatrix}$. Note that in what follows (cf. the right-hand side in (2.1)), for any two

functions $\mathbf{v} = \begin{bmatrix} v_1 \\ v_2 \end{bmatrix}$ and $\mathbf{z} = \begin{bmatrix} z_1 \\ z_2 \end{bmatrix}$, we have

$$(\mathbf{v} \cdot \nabla)\mathbf{z} = \left(v_1 \frac{\partial}{\partial x_1} + v_2 \frac{\partial}{\partial x_2} \right) \begin{bmatrix} z_1 \\ z_2 \end{bmatrix} = \begin{bmatrix} v_1 \frac{\partial z_1}{\partial x_1} + v_2 \frac{\partial z_1}{\partial x_2} \\ v_1 \frac{\partial z_2}{\partial x_1} + v_2 \frac{\partial z_2}{\partial x_2} \end{bmatrix}. \quad (2.4)$$

The problem (2.1)–(2.3) has been solved by a variety of different methods, finite difference [12–15], finite element [13, 16], and collocation methods [17, 18]. The present chapter presents a method for solving (2.1)–(2.3) that uses orthogonal spline collocation (OSC) with splines of degree $r \geq 3$ for discretization in space and an alternating direction implicit (ADI) extrapolated Crank-Nicolson (ECN) scheme for discretization in time. At each time level this scheme leads to solving linear systems corresponding to a sequence of independent

two-point boundary value problems. A similar approach was used in [11] for scalar-valued nonlinear parabolic problems and in [19, 20] for systems of nonlinear parabolic problems, but no convergence analysis was given in either case. Maximum norm convergence analysis of the extrapolated Crank-Nicolson scheme for Burgers' equation in one space variable is given in [21]. Although the approach in [21] is similar to the present work, the results of the former paper are not directly applicable to the ADI scheme used to solve the problem (2.1)–(2.3) in two space variables. The present work gives the H^1 norm convergence analysis of the extrapolated ADI Crank-Nicolson orthogonal spline collocation scheme for the coupled Burgers' equations in two space variables. We show that the H^1 norm error at each time level is of order r in space and of order 2 in time.

In the next section definitions and basic results are given. Section 2.3 contains a description of the present scheme and the scheme's convergence analysis is given in section 2.4. A brief discussion of the implementation and results of numerical experiments are presented in section 2.5.

2.1 Preliminaries

2.1.1 Definitions

Assuming that N_{x_1} and N_{x_2} are natural numbers, in what follows, $\delta_{x_1} = \{x_1^{(i)}\}_{i=0}^{N_{x_1}}$ and $\delta_{x_2} = \{x_2^{(j)}\}_{j=0}^{N_{x_2}}$ are partitions of $[a_1, b_1]$ and $[a_2, b_2]$, respectively, such that,

$$a_1 = x_1^{(0)} < x_1^{(1)} < \dots < x_1^{(N_{x_1})} = b_1, \quad a_2 = x_2^{(0)} < x_2^{(1)} < \dots < x_2^{(N_{x_2})} = b_2.$$

For $i = 1, \dots, N_{x_1}$ and $j = 1, \dots, N_{x_2}$, we introduce

$$h_i^{x_1} = x_1^{(i)} - x_1^{(i-1)}, \quad h_j^{x_2} = x_2^{(j)} - x_2^{(j-1)},$$

and we set

$$\bar{h}_{x_1} = \max_{i=1, \dots, N_{x_1}} h_i^{x_1}, \quad \bar{h}_{x_2} = \max_{j=1, \dots, N_{x_2}} h_j^{x_2}, \quad h = \max(\bar{h}_{x_1}, \bar{h}_{x_2}),$$

$$\underline{h}_{x_1} = \min_{i=1, \dots, N_{x_1}} h_i^{x_1}, \quad \underline{h}_{x_2} = \min_{j=1, \dots, N_{x_2}} h_j^{x_2}.$$

In the following we implicitly consider a family of quasi-uniform partitions $\delta = \delta_{x_1} \times \delta_{x_2}$ of Ω , that is, we assume (cf. section 2 of [22]) that there exist positive constants $\sigma_1, \sigma_2, \sigma_3$ such that

$$\sigma_1 \bar{h}_{x_1} \leq \underline{h}_{x_1}, \quad \sigma_1 \bar{h}_{x_2} \leq \underline{h}_{x_2}, \quad \sigma_2 \leq \bar{h}_{x_1} / \bar{h}_{x_2} \leq \sigma_3 \quad (2.5)$$

for every partition δ in the family.

Let \mathcal{M}_{x_1} and \mathcal{M}_{x_2} be the spaces of C^1 splines of degree $\leq r$ with the breaks at the $x_1^{(i)}$ and $x_2^{(j)}$, respectively, that is,

$$\mathcal{M}_{x_1} = \{v \in C^1[a_1, b_1] : v|_{[x_1^{(i-1)}, x_1^{(i)}]} \in P_r, i = 1, \dots, N_{x_1}\},$$

$$\mathcal{M}_{x_2} = \{v \in C^1[a_2, b_2] : v|_{[x_2^{(j-1)}, x_2^{(j)}]} \in P_r, j = 1, \dots, N_{x_2}\},$$

where P_r is the set of polynomials of degree $\leq r$. Additionally, we introduce

$$\mathcal{M}_{x_1}^0 = \{v \in \mathcal{M}_{x_1} : v(a_1) = v(b_1) = 0\},$$

$$\mathcal{M}_{x_2}^0 = \{v \in \mathcal{M}_{x_2} : v(a_2) = v(b_2) = 0\}.$$

Let $\mathcal{M}_r = \mathcal{M}_{x_1} \otimes \mathcal{M}_{x_2}$, $\mathcal{M}_r^0 = \mathcal{M}_{x_1}^0 \otimes \mathcal{M}_{x_2}^0$, and let

$$\mathcal{M}_r \times \mathcal{M}_r = \left\{ \begin{bmatrix} v_1 \\ v_2 \end{bmatrix} : v_1, v_2 \in \mathcal{M}_r \right\}, \quad \mathcal{M}_r^0 \times \mathcal{M}_r^0 = \left\{ \begin{bmatrix} v_1 \\ v_2 \end{bmatrix} : v_1, v_2 \in \mathcal{M}_r^0 \right\}.$$

Let $\{\xi_k\}_{k=1}^{r-1}$ and $\{\omega_k\}_{k=1}^{r-1}$ be, respectively, the nodes and weights of the $(r-1)$ -point Gauss-Legendre quadrature for $(0, 1)$, and let $\mathcal{G}_{x_1} = \{\xi_{i,k}^{x_1}\}_{i=1, k=1}^{N_{x_1}, r-1}$, $\mathcal{G}_{x_2} = \{\xi_{j,l}^{x_2}\}_{j=1, l=1}^{N_{x_2}, r-1}$, where

$$\xi_{i,k}^{x_1} = x_1^{(i-1)} + h_i^{x_1} \xi_k, \quad \xi_{j,l}^{x_2} = x_2^{(j-1)} + h_j^{x_2} \xi_l. \quad (2.6)$$

Then the set of collocation points in Ω is given by,

$$\mathcal{G}_r = \{\xi = (\xi^{x_1}, \xi^{x_2}) : \xi^{x_1} \in \mathcal{G}_{x_1}, \xi^{x_2} \in \mathcal{G}_{x_2}\}.$$

For v and z defined on \mathcal{G}_r , the inner product $\langle v, z \rangle_{\mathcal{G}_r}$ and norm $\|v\|_{\mathcal{G}_r}$ are defined respectively by

$$\langle v, z \rangle_{\mathcal{G}_r} = \sum_{i=1}^{N_{x_1}} \sum_{j=1}^{N_{x_2}} h_i^{x_1} h_j^{x_2} \sum_{k=1}^{r-1} \sum_{l=1}^{r-1} \omega_k \omega_l (vz)(\xi_{i,k}^{x_1}, \xi_{j,l}^{x_2}), \quad \|v\|_{\mathcal{G}_r} = \sqrt{\langle v, v \rangle_{\mathcal{G}_r}}. \quad (2.7)$$

We also introduce

$$\|v\|_{C(\bar{\Omega})} = \max_{x \in \bar{\Omega}} |v(x)|, \quad \|v\|_{C(\mathcal{G}_r)} = \max_{\xi \in \mathcal{G}_r} |v(\xi)|, \quad (2.8)$$

$$\|v\|_{L^2(\Omega)} = \left(\int_{\Omega} v^2 dx \right)^{1/2}, \quad \|v\|_{H^1(\Omega)} = \left(\|v\|_{L^2(\Omega)}^2 + \sum_{i=1}^2 \left\| \frac{\partial v}{\partial x_i} \right\|_{L^2(\Omega)}^2 \right)^{1/2}. \quad (2.9)$$

For $\mathbf{v} = \begin{bmatrix} v_1 \\ v_2 \end{bmatrix}$ and $\mathbf{z} = \begin{bmatrix} z_1 \\ z_2 \end{bmatrix}$ defined on \mathcal{G}_r , the inner product $\langle \mathbf{v}, \mathbf{z} \rangle_{\mathcal{G}_r}$ and norm $\|\mathbf{v}\|_{\mathcal{G}_r}$ are defined by

$$\langle \mathbf{v}, \mathbf{z} \rangle_{\mathcal{G}_r} = \langle v_1, z_1 \rangle_{\mathcal{G}_r} + \langle v_2, z_2 \rangle_{\mathcal{G}_r}, \quad \|\mathbf{v}\|_{\mathcal{G}_r} = \sqrt{\langle \mathbf{v}, \mathbf{v} \rangle_{\mathcal{G}_r}}. \quad (2.10)$$

We also introduce

$$\|\mathbf{v}\|_{C(\bar{\Omega})} = \max \left\{ \|v_1\|_{C(\bar{\Omega})}, \|v_2\|_{C(\bar{\Omega})} \right\}, \quad \|\mathbf{v}\|_{C(\mathcal{G}_r)} = \max \left\{ \|v_1\|_{C(\mathcal{G}_r)}, \|v_2\|_{C(\mathcal{G}_r)} \right\}, \quad (2.11)$$

$$\|\mathbf{v}\|_{L^2(\Omega)} = \left(\|v_1\|_{L^2(\Omega)}^2 + \|v_2\|_{L^2(\Omega)}^2 \right)^{1/2}, \quad \|\mathbf{v}\|_{H^1(\Omega)} = \left(\|v_1\|_{H^1(\Omega)}^2 + \|v_2\|_{H^1(\Omega)}^2 \right)^{1/2}.$$

Let $\{t_n\}_{n=0}^{N_t}$ be a partition of $[T_0, T_1]$, where $t_n = T_0 + n\tau$ and the time step

$$\tau = \frac{T_1 - T_0}{N_t}.$$

We also introduce $t_{n+1/2} = (t_n + t_{n+1})/2$, $n = 0, \dots, N_t - 1$.

Throughout this chapter, we assume that the problem (2.1)–(2.3) has a unique, sufficiently smooth solution \mathbf{u} . In our convergence analysis we will use the piecewise polynomial Hermite interpolant \mathbf{W} of the solution \mathbf{u} of (2.1)–(2.3) as a comparison function. For $t \in [0, T]$, $\mathbf{W}(\cdot, t) = T_{r,\delta} \mathbf{u}(\cdot, t) \in \mathcal{M}_r \times \mathcal{M}_r$ is defined by

$$\begin{aligned}
(\mathbf{W} - \mathbf{u})(\zeta_{i,k}^{x_1}, \zeta_{j,l}^{x_2}, t) &= 0, \quad i = 1, \dots, N_{x_1}, \quad j = 1, \dots, N_{x_2}, \\
\frac{\partial^n}{\partial x_1^n} (\mathbf{W} - \mathbf{u})(x_1^{(i)}, \zeta_{j,l}^{x_2}, t) &= 0, \quad i = 0, \dots, N_{x_1}, \quad j = 1, \dots, N_{x_2}, \\
\frac{\partial^m}{\partial x_2^m} (\mathbf{W} - \mathbf{u})(\zeta_{i,k}^{x_1}, x_2^{(j)}, t) &= 0, \quad i = 1, \dots, N_{x_1}, \quad j = 0, \dots, N_{x_2}, \\
\frac{\partial^{n+m}}{\partial x_1^n \partial x_2^m} (\mathbf{W} - \mathbf{u})(x_1^{(i)}, x_2^{(j)}, t) &= 0, \quad i = 0, \dots, N_{x_1}, \quad j = 0, \dots, N_{x_2},
\end{aligned} \tag{2.12}$$

where $k, l = 1, \dots, r - 3$ and $n, m = 0, 1$, and where

$$\zeta_{i,k}^{x_1} = x_1^{(i-1)} + h_i^{x_1} \zeta_k, \quad i = 1, \dots, N_{x_1}, \quad k = 1, \dots, r - 3,$$

$$\zeta_{j,l}^{x_2} = x_2^{(j-1)} + h_j^{x_2} \zeta_l, \quad j = 1, \dots, N_{x_2}, \quad l = 1, \dots, r - 3,$$

and, as in [23] for $r > 3$, $0 < \zeta_1 < \zeta_2 < \dots < \zeta_{r-3} < 1$ are the simple zeros of the polynomial

$$\frac{d^{r-3}}{dt^{r-3}} [t^{r-1} (t - 1)^{r-1}].$$

2.1.2 Results

The first lemma involves bounds on (2.4).

Lemma 2.1. *If \mathbf{v} is defined on \mathcal{G}_r and \mathbf{z} is defined and differentiable on Ω , then*

$$\|(\mathbf{v} \cdot \nabla) \mathbf{z}\|_{\mathcal{G}_r}^2 \leq 2 \|\mathbf{v}\|_{C(\mathcal{G}_r)}^2 (\|\mathbf{z}_{x_1}\|_{\mathcal{G}_r}^2 + \|\mathbf{z}_{x_2}\|_{\mathcal{G}_r}^2), \tag{2.13}$$

$$\|(\mathbf{v} \cdot \nabla) \mathbf{z}\|_{\mathcal{G}_r}^2 \leq 4 \|\mathbf{v}\|_{\mathcal{G}_r}^2 \max_{j=1,2} \left\| \frac{\partial \mathbf{z}}{\partial x_j} \right\|_{C(\mathcal{G}_r)}^2, \tag{2.14}$$

$$\|\mathbf{v}\|_{\mathcal{G}_r}^2 \leq 2(b_1 - a_1)(b_2 - a_2) \|\mathbf{v}\|_{C(\mathcal{G}_r)}^2. \tag{2.15}$$

Proof. First, it follows from (2.7) that

$$\|vz\|_{\mathcal{G}_r} \leq \|v\|_{C(\mathcal{G}_r)} \|z\|_{\mathcal{G}_r}. \tag{2.16}$$

Since $\omega_k > 0$, $k = 1, \dots, r - 1$, and since $\sum_{k=1}^{r-1} \omega_k = 1$, we also have

$$\|v\|_{\mathcal{G}_r}^2 \leq (b_1 - a_1)(b_2 - a_2) \|v\|_{C(\mathcal{G}_r)}^2. \tag{2.17}$$

Using (2.4), (2.10), (2.7), the triangle inequality, and the inequality

$$(\alpha + \beta)^2 \leq 2(\alpha^2 + \beta^2), \quad \alpha, \beta \in \mathbb{R},$$

(or (2.34)), we have

$$\begin{aligned} & \|(\mathbf{v} \cdot \nabla) \mathbf{z}\|_{\mathcal{G}_r}^2 \\ &= \sum_{i=1}^2 \left\| v_1 \frac{\partial z_i}{\partial x_1} + v_2 \frac{\partial z_i}{\partial x_2} \right\|_{\mathcal{G}_r}^2 \leq \sum_{i=1}^2 \left(\left\| v_1 \frac{\partial z_i}{\partial x_1} \right\|_{\mathcal{G}_r} + \left\| v_2 \frac{\partial z_i}{\partial x_2} \right\|_{\mathcal{G}_r} \right)^2 \\ &\leq 2 \sum_{i=1}^2 \left(\left\| v_1 \frac{\partial z_i}{\partial x_1} \right\|_{\mathcal{G}_r}^2 + \left\| v_2 \frac{\partial z_i}{\partial x_2} \right\|_{\mathcal{G}_r}^2 \right) \end{aligned}$$

which yields (2.13) and (2.14) on using (2.16), (2.11), and (2.10). Finally, (2.15) follows from (2.10), (2.17), and (2.11). \square

In what follows, C denotes a generic positive constant, dependent possibly on $\mu, \sigma_1, \sigma_2, \sigma_3, r$, but independent of \mathbf{u}, h and τ . We also use $C(\mathbf{u})$ to denote a generic nonnegative constant, dependent possibly on \mathbf{u} and r , but independent of h and τ . Any specific $C(\mathbf{u})$ is denoted by $C_i(\mathbf{u})$.

The next lemma is the well known inverse inequality [24] whose simple proof we include for completeness.

Lemma 2.2. *We have*

$$\|\mathbf{v}\|_{C(\bar{\Omega})} \leq Ch^{-1} \|\mathbf{v}\|_{H^1(\Omega)}, \quad \mathbf{v} \in \mathcal{M}_r^0 \times \mathcal{M}_r^0.$$

Proof. For $i = 1, \dots, N_{x_1}$ and $j = 1, \dots, N_{x_2}$, we introduce

$$I_{i,j} = (x_1^{(i-1)}, x_1^{(i)}) \times (x_2^{(j-1)}, x_2^{(j)}), \quad \bar{I}_{i,j} = [x_1^{(i-1)}, x_1^{(i)}] \times [x_2^{(j-1)}, x_2^{(j)}].$$

First we show

$$\|v\|_{C(\bar{I}_{i,j})} \leq C (h_i^{x_1} h_j^{x_2})^{-1/2} \|v\|_{L^2(I_{i,j})}, \quad v \in P_r \otimes P_r, \quad i = 1, \dots, N_{x_1}, \quad j = 1, \dots, N_{x_2}, \quad (2.18)$$

where $\|\cdot\|_{C(\bar{I}_{i,j})}$ and $\|\cdot\|_{L^2(I_{i,j})}$ are defined by (2.8) and (2.9), respectively with Ω replaced by $I_{i,j}$. For $S = (0, 1) \times (0, 1)$, $\bar{S} = [0, 1] \times [0, 1]$, by the equivalence of norms in finite

dimensional vector spaces, we have

$$\|z\|_{C(\bar{S})} \leq C \|z\|_{L^2(S)}, \quad z \in P_r \otimes P_r, \quad (2.19)$$

where $\|\cdot\|_{C(\bar{S})}$ and $\|\cdot\|_{L^2(S)}$ are defined by (2.8) and (2.9), respectively with Ω replaced by S . For $v \in P_r \otimes P_r$ and fixed $i = 1, \dots, N_{x_1}$ and $j = 1, \dots, N_{x_2}$, we introduce

$$z(y_1, y_2) = v(x_1^{(i-1)} + h_i^{x_1} y_1, x_2^{j-1} + h_j^{x_2} y_2), \quad (y_1, y_2) \in \bar{S}.$$

Since $z \in P_r \otimes P_r$ and since

$$\|v\|_{C(\bar{I}_{i,j})} = \|z\|_{C(\bar{S})}, \quad \|z\|_{L^2(S)}^2 = (h_i^{x_1} h_j^{x_2})^{-1} \|v\|_{L^2(I_{i,j})}^2,$$

(2.19) gives (2.18). The assumption (2.5) implies

$$\frac{1}{h_i^{x_1} h_j^{x_2}} \leq \frac{1}{\underline{h}_{x_1} \underline{h}_{x_2}} \leq \frac{C}{\bar{h}_{x_1} \bar{h}_{x_2}} \leq \frac{C}{h^2}. \quad (2.20)$$

Since

$$\|\mathbf{v}\|_{C(\bar{\Omega})} = \|v_k\|_{C(\bar{I}_{i,j})}$$

for some k, i, j and since

$$\|v_k\|_{L^2(I_{i,j})} \leq \|\mathbf{v}\|_{L^2(\Omega)} \leq \|\mathbf{v}\|_{H^1(\Omega)},$$

Lemma 2.2 follows from (2.18) and (2.20). \square

The next two lemmas are concerned with properties of functions in $\mathcal{M}_r^0 \times \mathcal{M}_r^0$.

Lemma 2.3. *We have*

$$\langle \Delta \mathbf{v}, \mathbf{z} \rangle_{\mathcal{G}_r} = \langle \mathbf{v}, \Delta \mathbf{z} \rangle_{\mathcal{G}_r}, \quad \mathbf{v}, \mathbf{z} \in \mathcal{M}_r^0 \times \mathcal{M}_r^0, \quad (2.21)$$

$$\|\mathbf{v}\|_{H^1(\Omega)}^2 \leq C \langle -\Delta \mathbf{v}, \mathbf{v} \rangle_{\mathcal{G}_r}, \quad \mathbf{v} \in \mathcal{M}_r^0 \times \mathcal{M}_r^0, \quad (2.22)$$

$$\left\| \frac{\partial \mathbf{v}}{\partial x_1} \right\|_{\mathcal{G}_r}^2 + \left\| \frac{\partial \mathbf{v}}{\partial x_2} \right\|_{\mathcal{G}_r}^2 \leq \langle -\Delta \mathbf{v}, \mathbf{v} \rangle_{\mathcal{G}_r}, \quad \mathbf{v} \in \mathcal{M}_r^0 \times \mathcal{M}_r^0, \quad (2.23)$$

$$\|\mathbf{v}\|_{\mathcal{G}_r} \leq C \|\mathbf{v}\|_{L^2(\Omega)}, \quad \mathbf{v} \in \mathcal{M}_r^0 \times \mathcal{M}_r^0, \quad (2.24)$$

$$\|\mathbf{v}\|_{\mathcal{G}_r}^2 \leq \langle -\Delta \mathbf{v}, \mathbf{v} \rangle_{\mathcal{G}_r}, \quad \mathbf{v} \in \mathcal{M}_r^0 \times \mathcal{M}_r^0. \quad (2.25)$$

Proof. Equation (2.21) and the inequality (2.22) are proven for scalar valued functions and $r = 3$ in Lemma 2.2 of [25]. Corresponding proofs for arbitrary r are similar. The inequalities (2.23) and (2.24) are proven for scalar valued functions in Lemma 2.1 in [26]. The required results for vector valued functions follow from those for scalar valued functions on using the definition of $\langle \mathbf{v}, \mathbf{z} \rangle_{\mathcal{G}_r}$ in (2.10). The inequalities (2.24) and (2.22) imply (2.25). \square

Lemma 2.4. *We have,*

$$\left\langle \frac{\partial^4 \mathbf{v}}{\partial x_1^2 \partial x_2^2}, \mathbf{v} \right\rangle_{\mathcal{G}_r} \geq \left\| \frac{\partial^2 \mathbf{v}}{\partial x_1 \partial x_2} \right\|_{L^2(\Omega)}^2, \quad \mathbf{v} \in \mathcal{M}_r^0 \times \mathcal{M}_r^0.$$

Proof. To prove the claim, it suffices to show that

$$\left\langle \frac{\partial^4 v}{\partial x_1^2 \partial x_2^2}, v \right\rangle_{\mathcal{G}_r} \geq \left\| \frac{\partial^2 v}{\partial x_1 \partial x_2} \right\|_{L^2(\Omega)}^2, \quad v \in \mathcal{M}_r^0. \quad (2.26)$$

We introduce the inner products,

$$\langle f, g \rangle_{x_1} = \sum_{i=1}^{N_{x_1}} h_i^{x_1} \sum_{k=1}^{r-1} \omega_k f(\xi_{i,k}^{x_1}) g(\xi_{i,k}^{x_1}), \quad \langle f, g \rangle_{x_2} = \sum_{j=1}^{N_{x_2}} h_j^{x_2} \sum_{l=1}^{r-1} \omega_l f(\xi_{j,l}^{x_2}) g(\xi_{j,l}^{x_2}).$$

First we note that, for $p \in \mathcal{M}_{x_1}^0$,

$$p^{(r)}(\xi_{i,1}^{x_1}) = \dots = p^{(r)}(\xi_{i,r-1}^{x_1}), \quad i = 1, \dots, N_{x_1},$$

and since

$$\sum_{k=1}^{r-1} \omega_k = 1,$$

by Lemma 3.1 of [23], we have

$$-\langle p'', q \rangle_{x_1} = \int_{a_1}^{b_1} p' q' dx + C \sum_{i=1}^{N_{x_1}} (h_i^{x_1})^{2r-1} \sum_{k=1}^{r-1} \omega_k (p^{(r)} q^{(r)}) (\xi_{i,k}^{x_1}), \quad p, q \in \mathcal{M}_{x_1}^0, \quad (2.27)$$

$$-\langle p'', q \rangle_{x_2} = \int_{a_2}^{b_2} p' q' dy + C \sum_{j=1}^{N_{x_2}} (h_j^{x_2})^{2r-1} \sum_{l=1}^{r-1} \omega_l (p^{(r)} q^{(r)}) (\xi_{j,l}^{x_2}), \quad p, q \in \mathcal{M}_{x_2}^0, \quad (2.28)$$

where C is a nonnegative constant that depends on r .

Let $v \in \mathcal{M}_r^0$. Applying the definition of $\langle \cdot, \cdot \rangle_{\mathcal{G}_r}$, and (2.28) (once with $p = q$), we have

$$\begin{aligned}
\left\langle \frac{\partial^4 v}{\partial x_1^2 \partial x_2^2}, v \right\rangle_{\mathcal{G}_r} &= \sum_{i=1}^{N_{x_1}} \sum_{j=1}^{N_{x_2}} h_i^{x_1} h_j^{x_2} \sum_{k=1}^{r-1} \sum_{l=1}^{r-1} \omega_k \omega_l \left(\frac{\partial^4 v}{\partial x_1^2 \partial x_2^2} v \right) (\xi_{i,k}, \xi_{j,l}) \\
&= \sum_{i=1}^{N_{x_1}} h_i^{x_1} \sum_{k=1}^{r-1} \omega_k \left\langle \frac{\partial^4 v}{\partial x_1^2 \partial x_2^2} (\xi_{i,k}, \cdot), v(\xi_{i,k}, \cdot) \right\rangle_{x_2} \\
&= \sum_{i=1}^{N_{x_1}} h_i^{x_1} \sum_{k=1}^{r-1} \omega_k \left[- \int_{a_2}^{b_2} \frac{\partial^3 v}{\partial x_1^2 \partial x_2} (\xi_{i,k}, x_2) \frac{\partial v}{\partial x_2} (\xi_{i,k}, x_2) dx_2 \right. \\
&\quad \left. - C \sum_{j=1}^{N_{x_2}} (h_j^{x_2})^{2r-1} \sum_{l=1}^{r-1} \omega_l \left(\frac{\partial^{r+2} v}{\partial x_2^r \partial x_1^2} \frac{\partial^r v}{\partial x_2^r} \right) (\xi_{i,k}^{x_1}, \xi_{j,l}^{x_2}) \right] \\
&= - \int_{a_2}^{b_2} \sum_{i=1}^{N_{x_1}} h_i^{x_1} \sum_{k=1}^{r-1} \omega_k \frac{\partial^3 v}{\partial x_2 \partial x_1^2} (\xi_{i,k}, x_2) \frac{\partial v}{\partial x_2} (\xi_{i,k}, x_2) dx_2 \\
&\quad - C \sum_{j=1}^{N_{x_2}} (h_j^{x_2})^{2r-1} \sum_{l=1}^{r-1} \omega_l \sum_{i=1}^{N_{x_1}} h_i^{x_1} \sum_{k=1}^{r-1} \omega_k \left(\frac{\partial^{r+2} v}{\partial x_1^2 \partial x_2^r} \frac{\partial^r v}{\partial x_2^r} \right) (\xi_{i,k}^{x_1}, \xi_{j,l}^{x_2}) \\
&= - \int_{a_2}^{b_2} \left\langle \frac{\partial^3 v}{\partial x_2 \partial x_1^2} (\cdot, x_2) \frac{\partial v}{\partial x_2} (\cdot, x_2) \right\rangle_{x_1} dx_2 \\
&\quad - C \sum_{j=1}^{N_{x_2}} (h_j^{x_2})^{2r-1} \sum_{l=1}^{r-1} \omega_l \left\langle \frac{\partial^{r+2} v}{\partial x_1^2 \partial x_2^r} (\cdot, \xi_{j,l}^{x_2}), \frac{\partial^r v}{\partial x_2^r} (\cdot, \xi_{j,l}^{x_2}) \right\rangle_{x_1} \\
&\geq - \int_{a_2}^{b_2} \left\langle \frac{\partial^3 v}{\partial x_2 \partial x_1^2} (\cdot, x_2) \frac{\partial v}{\partial x_2} (\cdot, x_2) \right\rangle_{x_1} dx_2.
\end{aligned}$$

An additional application of (2.27) proves (2.26). \square

Remark 2.1. Lemma 2.4 is stated as (3.10) in [27]. It is claimed before Lemma 3.4 in [27] that the proof of Lemma 2.4 uses the same techniques as the derivation of equation (3.7) in the proof of Lemma 3.3 in [27]. Since we were unable to verify correctness of this claim, for the sake of completeness, we present our proof of Lemma 2.4.

The next few lemmas involve bounds of the error $\mathbf{u} - \mathbf{W}$ in several different norms.

Lemma 2.5. *If \mathbf{u} is sufficiently smooth, then*

$$\left\| \frac{\partial^{k+l}(\mathbf{u} - \mathbf{W})}{\partial x_1^k \partial x_2^l}(\cdot, t) \right\|_{C(\bar{\Omega})} \leq C(\mathbf{u}) h^{r+1-k-l}, \quad 0 \leq k+l \leq 1, \quad t \in [T_0, T_1]. \quad (2.29)$$

Proof. We prove (2.29) for scalar valued functions by modifying the proof of Theorem 1.2 in [28]. We set $S = (0, 1) \times (0, 1)$, that is, S is Ω with $a_1 = a_2 = 0$ and $b_1 = b_2 = 1$. Assume $v \in W_\infty^{r+1}(S)$ and let $T_r v(y_1, y_2)$ be the interpolant of $v(y_1, y_2)$, $(y_1, y_2) \in \bar{S}$, corresponding to the partition of S with $N_{y_1} = N_{y_2} = 1$. Introduce

$$F_{y_1, y_2}(v) = \frac{\partial^{k+l}}{\partial y_1^k \partial y_2^l} (v - T_r v)(y_1, y_2), \quad (y_1, y_2) \in \bar{S}.$$

Since $\| \frac{\partial^{k+l}}{\partial y_1^k \partial y_2^l} T_r v \|_{C(\bar{S})} \leq C \|v\|_{C^2(\bar{S})}$, and since $H^{r+1}(S)$ and $W_\infty^{r+1}(S)$ are continuously imbedded in $C^2(\bar{S})$ and $H^{r+1}(S)$, respectively, (in short $C^2(\bar{S})$ is continuously imbedded in $W_\infty^{r+1}(S)$), we have

$$|F_{y_1, y_2}(v)| \leq C \|v\|_{W_\infty^{r+1}(S)}, \quad (y_1, y_2) \in \bar{S}.$$

Clearly $F_{y_1, y_2}(v)$ is linear and $F_{y_1, y_2}(p) = 0$ for all polynomials p of degree $\leq r$ since such polynomials are in $P_r \otimes P_r$ and since $F_{y_1, y_2}(q) = 0$, $q \in P_r \otimes P_r$. Therefore it follows from Bramble-Hilbert lemma (see, e.g., Theorem 9.3 in [29]) that

$$|F_{y_1, y_2}(v)| \leq C |v|_{W_\infty^{r+1}(S)}, \quad (y_1, y_2) \in \bar{S}.$$

Assume $u \in W_\infty^{r+1}$. For fixed $i = 1, \dots, N_{x_1}$, $j = 1, \dots, N_{x_2}$, introduce

$$v(y_1, y_2) = u(x_1^{(i-1)} + h_i^{x_1} y_1, x_2^{(j-1)} + h_j^{x_2} y_2), \quad (y_1, y_2) \in \bar{S}.$$

Then $v \in W_\infty^{r+1}(S)$ and

$$\frac{\partial^{k+l}}{\partial y_1^k \partial y_2^l} v(y_1, y_2) = \frac{\partial^{k+l}}{\partial x_1^k \partial x_2^l} u(x_1^{(i-1)} + h_i^{x_1} y_1, x_2^{(j-1)} + h_j^{x_2} y_2) (h_i^{x_1})^k (h_j^{x_2})^l, \quad (y_1, y_2) \in \bar{S}.$$

Moreover, since

$$T_r v(y_1, y_2) = T_{r, \delta} u(x_1^{(i-1)} + h_i^{x_1} y_1, x_2^{(j-1)} + h_j^{x_2} y_2), \quad (y_1, y_2) \in \bar{S},$$

we also have

$$\frac{\partial^{k+l}}{\partial y_1^k \partial y_2^l} T_r v(y_1, y_2) = \frac{\partial^{k+l}}{\partial x_1^k \partial x_2^l} T_{r,\delta} u(x_1^{(i-1)} + h_i^{x_1} y_1, x_2^{(j-1)} + h_j^{x_2} y_2) (h_i^{x_1})^k (h_j^{x_2})^l, \quad (y_1, y_2) \in \bar{S}.$$

Therefore

$$\frac{\partial^{k+l}}{\partial x_1^k \partial x_2^l} (u - T_{r,\delta} u)(x_1, x_2) = (h_i^{x_1})^{-k} (h_j^{x_2})^{-l} F_{y_1, y_2}(v), \quad (x_1, x_2) \in \bar{I}_{i,j},$$

where x_1, x_2 and y_1, y_2 are related by

$$x_1 = x_1^{(i-1)} + h_i^{x_1} y_1, \quad x_2 = x_2^{(j-1)} + h_j^{x_2} y_2.$$

Hence

$$\begin{aligned} \left| \frac{\partial^{k+l}}{\partial x_1^k \partial x_2^l} (u - T_{r,\delta} u)(x_1, x_2) \right| &= (h_i^{x_1})^{-k} (h_j^{x_2})^{-l} |v|_{W_\infty^{r+1}(S)} \\ &\leq C h^{r+1-k-l} |u|_{W_\infty^{r+1}(I_{i,j})}, \quad (x_1, x_2) \in \bar{I}_{i,j}, \end{aligned}$$

which yields the desired result. The result for vector valued functions follows immediately. \square

Lemma 2.6. *If \mathbf{u} is sufficiently smooth, then*

$$\left\| \frac{\partial^{i+j}(\mathbf{u} - \mathbf{W})}{\partial x_1^i \partial x_2^j}(\cdot, t) \right\|_{\mathcal{G}_r} \leq C(\mathbf{u}) h^{r+1-i-j}, \quad 0 \leq i+j \leq 1, \quad t \in [T_0, T_1], \quad (2.30)$$

$$\left\| \frac{\partial^2(\mathbf{u} - \mathbf{W})}{\partial x_1^i \partial x_2^{2-i}}(\cdot, t) \right\|_{\mathcal{G}_r} \leq C(\mathbf{u}) h^r, \quad i = 0, 1, 2, \quad t \in [T_0, T_1], \quad (2.31)$$

$$\|\Delta(\mathbf{u} - \mathbf{W})_t(\cdot, t)\|_{\mathcal{G}_r} \leq C(\mathbf{u}) h^r, \quad t \in [T_0, T_1], \quad (2.32)$$

$$\left\| \frac{\partial^4}{\partial x_1^2 \partial x_2^2}(\mathbf{u} - \mathbf{W})_t(\cdot, t) \right\|_{\mathcal{G}_r} \leq C(\mathbf{u}), \quad t \in [T_0, T_1]. \quad (2.33)$$

Proof. The first two inequalities follow from (2.19) and (2.20) of Lemma 2.3 in [26], respectively. The inequality (2.32) follows from $\mathbf{W}_t = T_{r,\delta} \mathbf{u}_t$, (2.31) with $i = 0, 2$, and the triangle inequality. The last inequality is (2.16) in [30] with $k = 1$. \square

Lemma 2.7. *If \mathbf{u} is sufficiently smooth, then*

$$\|\mathbf{u} - \mathbf{W}\|_{H^1(\Omega)} \leq C(u)h^{r+1}.$$

Proof. This is Lemma 2.5 with $k = 1$ in [26]. □

Lemma 2.8. *If \mathbf{u} is sufficiently smooth, then*

$$\|\mathbf{W}^n\|_{C(\mathcal{G}_r)} \leq C(\mathbf{u}), \quad n = 0, \dots, N_t,$$

$$\left\| \frac{\partial \mathbf{W}^n}{\partial x_k} \right\|_{C(\mathcal{G}_r)} \leq C(\mathbf{u}), \quad k = 1, 2, \quad n = 0, \dots, N_t,$$

where $\mathbf{W}^n = \mathbf{W}(\cdot, t_n)$.

Proof. For $\mathbf{u}^n = \mathbf{u}(\cdot, t_n)$, the first inequality follows from

$$\mathbf{W}^n = \mathbf{W}^n - \mathbf{u}^n + \mathbf{u}^n,$$

the triangle inequality, and (2.29) with $k = l = 0$. Similarly, the second inequality follows from

$$\frac{\partial \mathbf{W}^n}{\partial x_k} = \frac{\partial \mathbf{W}^n}{\partial x_k} - \frac{\partial \mathbf{u}^n}{\partial x_k} + \frac{\partial \mathbf{u}^n}{\partial x_k}, \quad k = 1, 2,$$

the triangle inequality, and (2.29) with $k = 1, l = 0$ and $k = 0, l = 1$. □

The next result is the discrete Gronwall inequality [31].

Lemma 2.9. *Assume $\alpha_k \geq 0$ and $\beta_k \geq 0$ for $k = 0, \dots, m$, $\beta_k \leq \beta_{k+1}$ for $k = 0, \dots, m-1$, and*

$$\alpha_k \leq \beta_k + C\tau \sum_{n=0}^{k-1} \alpha_n, \quad k = 0, \dots, m.$$

Then

$$\alpha_n \leq e^{C\tau n} \beta_n, \quad n = 0, \dots, m.$$

In our convergence analysis, we will frequently use the inequality

$$\alpha\beta \leq \epsilon\alpha^2 + \frac{\beta^2}{4\epsilon}, \quad \alpha, \beta \in R, \quad \epsilon > 0. \quad (2.34)$$

2.2 Extrapolated Crank-Nicolson Orthogonal Spline Collocation

The ADI-ECN-OSC scheme for (2.1)–(2.3) consists in finding $\mathbf{U}^n \in \mathcal{M}_r \times \mathcal{M}_r$, $n = 2, \dots, N_t$, such that for $n = 1, \dots, N_t - 1$,

$$\frac{\mathbf{U}^{n, \frac{1}{2}}(\xi) - \mathbf{U}^n(\xi)}{0.5\tau} - \mu \mathbf{U}_{x_1 x_1}^{n, \frac{1}{2}}(\xi) - \mu \mathbf{U}_{x_2 x_2}^n(\xi) = - \left[\left(\tilde{\mathbf{U}}^n \cdot \nabla \right) \tilde{\mathbf{U}}^n \right](\xi), \quad \xi \in \mathcal{G}_r, \quad (2.35)$$

$$\frac{\mathbf{U}^{n+1}(\xi) - \mathbf{U}^{n, \frac{1}{2}}(\xi)}{0.5\tau} - \mu \mathbf{U}_{x_1 x_1}^{n, \frac{1}{2}}(\xi) - \mu \mathbf{U}_{x_2 x_2}^{n+1}(\xi) = - \left[\left(\tilde{\mathbf{U}}^n \cdot \nabla \right) \tilde{\mathbf{U}}^n \right](\xi), \quad \xi \in \mathcal{G}_r, \quad (2.36)$$

where

$$\tilde{\mathbf{U}}^n = \frac{3\mathbf{U}^n - \mathbf{U}^{n-1}}{2}, \quad (2.37)$$

and $\mathbf{U}^0, \mathbf{U}^1 \in \mathcal{M}_r \times \mathcal{M}_r$. For $n = 1, \dots, N_t - 1$ and $\xi^{x_2} \in \mathcal{G}_{x_2}$, $\mathbf{U}^{n, \frac{1}{2}}(\cdot, \xi^{x_2}) \in \mathcal{M}_{x_1} \times \mathcal{M}_{x_1}$ and

$$\mathbf{U}^{n, \frac{1}{2}}(x_1, \xi^{x_2}) = \mathbf{U}^{n+1/2}(x_1, \xi^{x_2}) - \frac{\tau^2 \mu}{4} (d_t \mathbf{U}^n)_{x_2 x_2}(x_1, \xi^{x_2}), \quad x_1 = a_1, b_1, \quad (2.38)$$

where

$$\mathbf{U}^{n+1/2} = \frac{\mathbf{U}^n + \mathbf{U}^{n+1}}{2}, \quad d_t \mathbf{U}^n = \frac{\mathbf{U}^{n+1} - \mathbf{U}^n}{\tau}.$$

With $\mathbf{W}(\cdot, t) \in \mathcal{M}_r \times \mathcal{M}_r$, $t \in [0, T]$, defined in (2.12) and $\mathbf{W}^n = \mathbf{W}(\cdot, t_n)$, $n = 0, \dots, N_t$, we assume that

$$\mathbf{U}^n|_{\partial\Omega} = \mathbf{W}^n|_{\partial\Omega}, \quad n = 2, \dots, N_t. \quad (2.39)$$

To initialize the scheme (2.35)–(2.36), we set

$$\mathbf{U}^0 = \mathbf{W}^0, \quad (2.40)$$

and compute $\mathbf{U}^1 \in \mathcal{M}_r \times \mathcal{M}_r$ using an ADI predictor-corrector method. Specifically, we solve the equations

$$\frac{\mathbf{V}^{0,\frac{1}{2}}(\xi) - \mathbf{V}^0(\xi)}{0.5\tau} - \mu \mathbf{V}_{x_1 x_1}^{0,\frac{1}{2}}(\xi) - \mu \mathbf{V}_{x_2 x_2}^0(\xi) = - [(\mathbf{V}^0 \cdot \nabla) \mathbf{V}^0](\xi), \quad \xi \in \mathcal{G}_r, \quad (2.41)$$

$$\frac{\mathbf{V}^1(\xi) - \mathbf{V}^{0,\frac{1}{2}}(\xi)}{0.5\tau} - \mu \mathbf{V}_{x_1 x_1}^{0,\frac{1}{2}}(\xi) - \mu \mathbf{V}_{x_2 x_2}^1(\xi) = - [(\mathbf{V}^0 \cdot \nabla) \mathbf{V}^0](\xi), \quad \xi \in \mathcal{G}_r, \quad (2.42)$$

$$\frac{\mathbf{U}^{0,\frac{1}{2}}(\xi) - \mathbf{U}^0(\xi)}{0.5\tau} - \mu \mathbf{U}_{x_1 x_1}^{0,\frac{1}{2}}(\xi) - \mu \mathbf{U}_{x_2 x_2}^0(\xi) = - [(\mathbf{V}^{1/2} \cdot \nabla) \mathbf{V}^{1/2}](\xi), \quad \xi \in \mathcal{G}_r, \quad (2.43)$$

$$\frac{\mathbf{U}^1(\xi) - \mathbf{U}^{0,\frac{1}{2}}(\xi)}{0.5\tau} - \mu \mathbf{U}_{x_1 x_1}^{0,\frac{1}{2}}(\xi) - \mu \mathbf{U}_{x_2 x_2}^1(\xi) = - [(\mathbf{V}^{1/2} \cdot \nabla) \mathbf{V}^{1/2}](\xi), \quad \xi \in \mathcal{G}_r, \quad (2.44)$$

where

$$\mathbf{V}^0 = \mathbf{U}^0, \quad (2.45)$$

$\mathbf{V}^1 \in \mathcal{M}_r \times \mathcal{M}_r$,

$$\mathbf{V}^1|_{\partial\Omega} = \mathbf{U}^1|_{\partial\Omega} = \mathbf{W}^1|_{\partial\Omega}, \quad (2.46)$$

$$\mathbf{V}^{1/2} = \frac{\mathbf{V}^0 + \mathbf{V}^1}{2}, \quad (2.47)$$

for each $\xi^{x_2} \in \mathcal{G}_{x_2}$, $\mathbf{V}^{0,\frac{1}{2}}(\cdot, \xi^{x_2}) \in \mathcal{M}_{x_1} \times \mathcal{M}_{x_1}$, $\mathbf{U}^{0,\frac{1}{2}}(\cdot, \xi^{x_2}) \in \mathcal{M}_{x_1} \times \mathcal{M}_{x_1}$,

$$\mathbf{V}^{0,\frac{1}{2}}(x_1, \xi^{x_2}) = \mathbf{V}^{1/2}(x_1, \xi^{x_2}) - \frac{\tau^2 \mu}{4} (d_t \mathbf{V}^0)_{x_2 x_2}(x_1, \xi_{j,l}^{x_2}), \quad x_1 = a_1, b_1, \quad (2.48)$$

and (2.38) holds for $n = 0$. The last terms on the right-hand sides in (2.38), (2.48) are the perturbation terms.

2.3 Convergence Analysis

We introduce

$$\boldsymbol{\eta}^n = \mathbf{u}^n - \mathbf{W}^n, \quad n = 0, \dots, N_t, \quad (2.49)$$

$$\boldsymbol{\nu}^n = \mathbf{W}^n - \mathbf{U}^n, \quad n = 0, \dots, N_t, \quad (2.50)$$

where $\mathbf{u}^n = \mathbf{u}(\cdot, t_n)$, $\mathbf{W}^n = \mathbf{W}(\cdot, t_n)$.

It follows from (2.50), (2.40), (2.39), and (2.46) that

$$\boldsymbol{\nu}^0 = 0, \quad \boldsymbol{\nu}^n \in \mathcal{M}_r^0 \times \mathcal{M}_r^0, \quad n = 1, \dots, N_t. \quad (2.51)$$

The first theorem gives a bound on $\langle -\Delta \boldsymbol{\nu}^{n+1}, \boldsymbol{\nu}^{n+1} \rangle_{\mathcal{G}_r}$.

Theorem 2.1. *Assume that $\mathbf{U}^n \in \mathcal{M}_r \times \mathcal{M}_r$, $n = 2, \dots, N_t$, are defined by (2.35)–(2.39).*

Then $\boldsymbol{\nu}^n$, $n = 0, \dots, N_t$, defined by (2.50), satisfy

$$\begin{aligned} & \langle -\Delta \boldsymbol{\nu}^{n+1}, \boldsymbol{\nu}^{n+1} \rangle_{\mathcal{G}_r} + \langle \Delta \boldsymbol{\nu}^n, \boldsymbol{\nu}^n \rangle_{\mathcal{G}_r} \leq C(\mathbf{u})(h^{2r} + \tau^4) \\ & + \left[C(\mathbf{u}) + C\|\tilde{\mathbf{U}}^n\|_{C(\mathcal{G}_r)}^2 \right] \tau \sum_{j=0}^1 \langle -\Delta \boldsymbol{\nu}^{n-j}, \boldsymbol{\nu}^{n-j} \rangle_{\mathcal{G}_r}, \quad n = 1, \dots, N_t - 1. \end{aligned}$$

Proof. Subtracting (2.36) from (2.35) and multiplying by $\tau/4$, we get

$$\mathbf{U}^{n, \frac{1}{2}}(\xi) = \mathbf{U}^{n+1/2}(\xi) - \frac{\tau^2 \mu}{4} (d_t \mathbf{U}^n)_{x_2 x_2}(\xi), \quad \xi \in \mathcal{G}_r. \quad (2.52)$$

Since for each $\xi^{x_2} \in \mathcal{G}_{x_2}$, $\mathbf{U}^{n, \frac{1}{2}}(\cdot, \xi^{x_2}) \in \mathcal{M}_{x_1} \times \mathcal{M}_{x_1}$ is determined uniquely by $\mathbf{U}^{n, \frac{1}{2}}(x_1, \xi^{x_2})$, $x_1 \in \mathcal{G}_{x_1} \cup \{a_1, b_1\}$ and since for each $\xi^{x_2} \in \mathcal{G}_{x_2}$, $\mathbf{U}^{n+1/2}(\cdot, \xi^{x_2}), (d_t \mathbf{U}^n)_{x_2 x_2}(\cdot, \xi^{x_2}) \in \mathcal{M}_{x_1} \times \mathcal{M}_{x_1}$, (2.52), (2.38) imply that

$$\mathbf{U}^{n, \frac{1}{2}}(x_1, \xi^{x_2}) = \mathbf{U}^{n+1/2}(x_1, \xi^{x_2}) - \frac{\tau^2 \mu}{4} (d_t \mathbf{U}^n)_{x_2 x_2}(x_1, \xi^{x_2}), \quad x_1 \in [a_1, b_1], \quad \xi^{x_2} \in \mathcal{G}_{x_2}. \quad (2.53)$$

Substituting (2.53) into (2.35), we get

$$d_t \mathbf{U}^n(\xi) - \mu \Delta \mathbf{U}^{n+1/2}(\xi) + \frac{\tau^2 \mu^2}{4} (d_t \mathbf{U}^n)_{x_1 x_1 x_2 x_2}(\xi) = - \left[(\tilde{\mathbf{U}}^n \cdot \nabla) \tilde{\mathbf{U}}^n \right](\xi), \quad \xi \in \mathcal{G}_r. \quad (2.54)$$

Using (2.50), (2.54), (2.49), and (2.1), we have, for $\xi \in \mathcal{G}_r$, $n = 1, \dots, N_t - 1$,

$$\begin{aligned}
& d_t \boldsymbol{\nu}^n(\xi) - \mu \Delta \boldsymbol{\nu}^{n+1/2}(\xi) + \frac{\tau^2 \mu^2}{4} (d_t \boldsymbol{\nu}^n)_{x_1 x_1 x_2 x_2}(\xi) \tag{2.55} \\
&= d_t \mathbf{W}^n(\xi) - \mu \Delta \mathbf{W}^{n+1/2}(\xi) + \\
&+ \left[\left(\tilde{\mathbf{U}}^n \cdot \nabla \right) \tilde{\mathbf{U}}^n \right](\xi) + \frac{\tau^2 \mu^2}{4} (d_t \mathbf{W}^n)_{x_1 x_1 x_2 x_2}(\xi) \\
&= -d_t \boldsymbol{\eta}^n(\xi) + d_t \mathbf{u}^n(\xi) - \mathbf{u}_t(\xi, t_{n+1/2}) \\
&+ \mu \Delta \mathbf{u}(\xi, t_{n+1/2}) - \mu \Delta \mathbf{u}^{n+1/2}(\xi) + \mu \Delta \boldsymbol{\eta}^{n+1/2}(\xi) \\
&- [(\mathbf{u} \cdot \nabla) \mathbf{u}](\xi, t_{n+1/2}) + \left[\left(\tilde{\mathbf{U}}^n \cdot \nabla \right) \tilde{\mathbf{U}}^n \right](\xi) \\
&+ \frac{\tau^2 \mu^2}{4} (d_t \mathbf{W}^n)_{x_1 x_1 x_2 x_2}(\xi).
\end{aligned}$$

It follows from (2.4), (2.37), (2.49), and (2.50) that the second and third to last terms on the right-hand side in (2.55) can be written as

$$\begin{aligned}
& - [(\mathbf{u} \cdot \nabla) \mathbf{u}] (\xi, t_{n+1/2}) + \left[(\tilde{\mathbf{U}}^n \cdot \nabla) \tilde{\mathbf{U}}^n \right] (\xi) \tag{2.56} \\
& = - [(\mathbf{u} \cdot \nabla) \mathbf{u}] (\xi, t_{n+1/2}) + [(\tilde{\mathbf{u}}^n \cdot \nabla) \mathbf{u}] (\xi, t_{n+1/2}) \\
& \quad - [(\tilde{\mathbf{u}}^n \cdot \nabla) \mathbf{u}(\cdot, t_{n+1/2})] (\xi) + \left[(\tilde{\mathbf{W}}^n \cdot \nabla) \mathbf{u}(\cdot, t_{n+1/2}) \right] (\xi) \\
& \quad - \left[(\tilde{\mathbf{W}}^n \cdot \nabla) \mathbf{u}(\cdot, t_{n+1/2}) \right] (\xi) + \left[(\tilde{\mathbf{W}}^n \cdot \nabla) \tilde{\mathbf{u}}^n \right] (\xi) \\
& \quad - \left[(\tilde{\mathbf{W}}^n \cdot \nabla) \tilde{\mathbf{u}}^n \right] (\xi) + \left[(\tilde{\mathbf{W}}^n \cdot \nabla) \tilde{\mathbf{W}}^n \right] (\xi) \\
& \quad - \left[(\tilde{\mathbf{W}}^n \cdot \nabla) \tilde{\mathbf{W}}^n \right] (\xi) + (\tilde{\mathbf{U}}^n(\xi) \cdot \nabla) \tilde{\mathbf{W}}^n(\xi) \\
& \quad - \left[(\tilde{\mathbf{U}}^n \cdot \nabla) \tilde{\mathbf{W}}^n \right] (\xi) + \left[(\tilde{\mathbf{U}}^n \cdot \nabla) \tilde{\mathbf{U}}^n \right] (\xi) \\
& = - \left[(\{\mathbf{u}(\cdot, t_{n+1/2}) - \tilde{\mathbf{u}}^n\} \cdot \nabla) \mathbf{u}(\cdot, t_{n+1/2}) \right] (\xi) \\
& \quad - [(\tilde{\boldsymbol{\eta}}^n \cdot \nabla) \mathbf{u}(\cdot, t_{n+1/2})] (\xi) \\
& \quad - \left[(\tilde{\mathbf{W}}^n \cdot \nabla) \{\mathbf{u}(\cdot, t_{n+1/2}) - \tilde{\mathbf{u}}^n\} \right] (\xi) \\
& \quad - \left[(\tilde{\mathbf{W}}^n \cdot \nabla) \tilde{\boldsymbol{\eta}}^n \right] (\xi) - [(\tilde{\boldsymbol{\nu}}^n \cdot \nabla) \tilde{\mathbf{W}}^n] (\xi) \\
& \quad - \left[(\tilde{\mathbf{U}}^n \cdot \nabla) \tilde{\boldsymbol{\nu}}^n \right] (\xi), \quad \xi \in \mathcal{G}_r, \quad n = 1, \dots, N_t - 1.
\end{aligned}$$

Taking the discrete inner product (2.10) of both sides of (2.55) with $d_t \boldsymbol{\nu}^n$ and using (2.56), we obtain

$$\begin{aligned}
& \|d_t \boldsymbol{\nu}^n\|_{\mathcal{G}_r}^2 - \mu \langle \Delta \boldsymbol{\nu}^{n+1/2}, d_t \boldsymbol{\nu}^n \rangle_{\mathcal{G}_r} + \frac{\tau^2 \mu^2}{4} \langle (d_t \boldsymbol{\nu}^n)_{x_1 x_1 x_2 x_2}, d_t \boldsymbol{\nu}^n \rangle_{\mathcal{G}_r} \\
&= - \langle d_t \boldsymbol{\eta}^n, d_t \boldsymbol{\nu}^n \rangle_{\mathcal{G}_r} + \langle d_t \mathbf{u}^n - \mathbf{u}_t(\cdot, t_{n+1/2}), d_t \boldsymbol{\nu}^n \rangle_{\mathcal{G}_r} \\
&\quad + \mu \langle \Delta \mathbf{u}(\cdot, t_{n+1/2}) - \Delta \mathbf{u}^{n+1/2}, d_t \boldsymbol{\nu}^n \rangle_{\mathcal{G}_r} + \mu \langle \Delta \boldsymbol{\eta}^{n+1/2}, d_t \boldsymbol{\nu}^n \rangle_{\mathcal{G}_r} \\
&\quad - \langle [(\{\mathbf{u}(\cdot, t_{n+1/2}) - \tilde{\mathbf{u}}^n\} \cdot \nabla) \mathbf{u}](\cdot, t_{n+1/2}), d_t \boldsymbol{\nu}^n \rangle_{\mathcal{G}_r} \\
&\quad - \langle [(\tilde{\boldsymbol{\eta}}^n \cdot \nabla) \mathbf{u}](\cdot, t_{n+1/2}), d_t \boldsymbol{\nu}^n \rangle_{\mathcal{G}_r} \\
&\quad - \langle (\tilde{\mathbf{W}}^n \cdot \nabla) \{\mathbf{u}(\cdot, t_{n+1/2}) - \tilde{\mathbf{u}}^n\}, d_t \boldsymbol{\nu}^n \rangle_{\mathcal{G}_r} \\
&\quad - \langle (\tilde{\mathbf{W}}^n \cdot \nabla) \tilde{\boldsymbol{\eta}}^n, d_t \boldsymbol{\nu}^n \rangle_{\mathcal{G}_r} - \langle (\tilde{\boldsymbol{\nu}}^n \cdot \nabla) \tilde{\mathbf{W}}^n, d_t \boldsymbol{\nu}^n \rangle_{\mathcal{G}_r} \\
&\quad - \langle (\tilde{\mathbf{U}}^n \cdot \nabla) \tilde{\boldsymbol{\nu}}^n, d_t \boldsymbol{\nu}^n \rangle_{\mathcal{G}_r} + \frac{\tau^2 \mu^2}{4} \langle (d_t \mathbf{W}^n)_{x_1 x_1 x_2 x_2}, d_t \boldsymbol{\nu}^n \rangle_{\mathcal{G}_r}, \quad n = 1, \dots, N_t - 1.
\end{aligned} \tag{2.57}$$

We bound the terms on the right-hand side of (2.57). It follows from (2.49), the inequality

$$\left\| \int_{t_n}^{t_{n+1}} \mathbf{v}(s) ds \right\|_{\mathcal{G}_r}^2 \leq \tau \int_{t_n}^{t_{n+1}} \|\mathbf{v}(s)\|_{\mathcal{G}_r}^2 ds \tag{2.58}$$

(derived for \mathbf{v} defined on \mathcal{G}_r using the Cauchy-Schwarz inequality), $\mathbf{W}_t = T_{r,\delta} \mathbf{u}_t$, (2.30) with $i = j = 0$ and \mathbf{u} replaced by \mathbf{u}_t that

$$\begin{aligned}
\|d_t \boldsymbol{\eta}^n\|_{\mathcal{G}_r}^2 &= \left\| \tau^{-1} \int_{t_n}^{t_{n+1}} (\mathbf{u} - \mathbf{W})_t(\cdot, s) ds \right\|_{\mathcal{G}_r}^2 \\
&\leq \tau^{-1} \int_{t_n}^{t_{n+1}} \|\mathbf{u}_t - \mathbf{W}_t(\cdot, s)\|_{\mathcal{G}_r}^2 ds \leq C(\mathbf{u}) h^{2r+2}, \quad n = 1, \dots, N_t - 1.
\end{aligned} \tag{2.59}$$

Using the Cauchy-Schwarz inequality, (2.34), and (2.59), we obtain

$$|\langle d_t \boldsymbol{\eta}^n, d_t \boldsymbol{\nu}^n \rangle_{\mathcal{G}_r}| \leq \epsilon \|d_t \boldsymbol{\nu}^n\|_{\mathcal{G}_r}^2 + \frac{C(\mathbf{u})}{\epsilon} h^{2r+2}, \quad n = 1, \dots, N_t - 1, \quad \epsilon > 0. \tag{2.60}$$

For $n = 1, \dots, N_t - 1$, it follows from Taylor's theorem that

$$\|d_t \mathbf{u}^n - \mathbf{u}_t(\cdot, t_{n+1/2})\|_{C(\mathcal{G}_r)} \leq C(\mathbf{u})\tau^2, \quad (2.61)$$

$$\|\mathbf{u}(\cdot, t_{n+1/2}) - \tilde{\mathbf{u}}^n\|_{C(\mathcal{G}_r)} \leq C(\mathbf{u})\tau^2, \quad (2.62)$$

$$\|\Delta \mathbf{u}(\cdot, t_{n+1/2}) - \Delta \mathbf{u}^{n+1/2}\|_{C(\mathcal{G}_r)} \leq C(\mathbf{u})\tau^2, \quad (2.63)$$

$$\left\| \frac{\partial \mathbf{u}(\cdot, t_{n+1/2})}{\partial x_j} - \frac{\partial \tilde{\mathbf{u}}^n}{\partial x_j} \right\|_{C(\mathcal{G}_r)} \leq C(\mathbf{u})\tau^2, \quad j = 1, 2. \quad (2.64)$$

Using the Cauchy-Schwarz inequality, (2.34), (2.61), (2.63), and (2.15), we obtain

$$|\langle d_t \mathbf{u}^n - \mathbf{u}_t(\cdot, t_{n+1/2}), d_t \boldsymbol{\nu}^n \rangle_{\mathcal{G}_r}| \quad (2.65)$$

$$\leq \epsilon \|d_t \boldsymbol{\nu}^n\|_{\mathcal{G}_r}^2 + \frac{C(\mathbf{u})}{\epsilon} \tau^4, \quad n = 1, \dots, N_t - 1, \quad \epsilon > 0,$$

$$\mu |\langle \Delta \mathbf{u}(\cdot, t_{n+1/2}) - \Delta \mathbf{u}^{n+1/2}, d_t \boldsymbol{\nu}^n \rangle_{\mathcal{G}_r}| \quad (2.66)$$

$$\leq \epsilon \|d_t \boldsymbol{\nu}^n\|_{\mathcal{G}_r}^2 + \frac{C(\mathbf{u})}{\epsilon} \tau^4, \quad n = 1, \dots, N_t - 1, \quad \epsilon > 0.$$

It follows from Cauchy-Schwarz inequality, (2.34), (2.49), and (2.32) that

$$\mu \left| \langle \Delta \boldsymbol{\eta}^{n+1/2}, d_t \boldsymbol{\nu}^n \rangle_{\mathcal{G}_r} \right| \leq \epsilon \|d_t \boldsymbol{\nu}^n\|_{\mathcal{G}_r}^2 + \frac{C(\mathbf{u})}{\epsilon} h^{2r}, \quad n = 1, \dots, N_t - 1, \quad \epsilon > 0. \quad (2.67)$$

Using the Cauchy-Schwarz inequality, (2.34), (2.14), (2.15), (2.62), and boundedness of $\partial u_i / \partial x_j$, $i, j = 1, 2$, we obtain

$$\left| \langle [(\{\mathbf{u}(\cdot, t_{n+1/2}) - \tilde{\mathbf{u}}^n\} \cdot \nabla) \mathbf{u}](\cdot, t_{n+1/2}), d_t \boldsymbol{\nu}^n \rangle_{\mathcal{G}_r} \right| \quad (2.68)$$

$$\leq \epsilon \|d_t \boldsymbol{\nu}^n\|_{\mathcal{G}_r}^2 + \frac{C(\mathbf{u})}{\epsilon} \tau^4, \quad n = 1, \dots, N_t - 1, \quad \epsilon > 0.$$

It follows from (2.37), the triangle inequality, (2.49), and (2.30) with $i = j = 0$ that

$$\|\tilde{\boldsymbol{\eta}}^n\|_{\mathcal{G}_r} \leq \frac{3}{2} \|\boldsymbol{\eta}^n\|_{\mathcal{G}_r} + \frac{1}{2} \|\boldsymbol{\eta}^{n-1}\|_{\mathcal{G}_r} \leq C(\mathbf{u})h^{r+1}, \quad n = 1, \dots, N_t - 1. \quad (2.69)$$

Using the Cauchy-Schwarz inequality, (2.34), (2.14), (2.69), and boundedness of $\partial u_i/\partial x_j$, $i, j = 1, 2$, we obtain,

$$\left| \left\langle [(\tilde{\boldsymbol{\eta}}^n \cdot \nabla) \mathbf{u}](\cdot, t_{n+1/2}), d_t \boldsymbol{\nu}^n \right\rangle_{\mathcal{G}_r} \right| \leq \epsilon \|d_t \boldsymbol{\nu}^n\|_{\mathcal{G}_r}^2 + \frac{C(\mathbf{u})}{\epsilon} h^{2r+2}, \quad n = 1, \dots, N_t - 1, \quad \epsilon > 0. \quad (2.70)$$

It follows from (2.37), the triangle inequality, (2.49), and (2.30) with $i = 1, j = 0$ and $i = 0, j = 1$ that

$$\left\| \frac{\partial \tilde{\boldsymbol{\eta}}^n}{\partial x_j} \right\|_{\mathcal{G}_r} \leq \frac{3}{2} \left\| \frac{\partial \boldsymbol{\eta}^n}{\partial x_j} \right\|_{\mathcal{G}_r} + \frac{1}{2} \left\| \frac{\partial \boldsymbol{\eta}^{n-1}}{\partial x_j} \right\|_{\mathcal{G}_r} \leq C(\mathbf{u}) h^r, \quad j = 1, 2, \quad n = 1, \dots, N_t - 1. \quad (2.71)$$

It follows from (2.37), the triangle inequality, and Lemma 2.8 that

$$\left\| \widetilde{\mathbf{W}}^n \right\|_{C(\mathcal{G}_r)} \leq \frac{3}{2} \left\| \mathbf{W}^n \right\|_{C(\mathcal{G}_r)} + \frac{1}{2} \left\| \mathbf{W}^{n-1} \right\|_{C(\mathcal{G}_r)} \leq C(\mathbf{u}), \quad n = 1, \dots, N_t - 1. \quad (2.72)$$

$$\begin{aligned} \left\| \frac{\partial \widetilde{\mathbf{W}}^n}{\partial x_j} \right\|_{C(\mathcal{G}_r)} &\leq \frac{3}{2} \left\| \frac{\partial \mathbf{W}^n}{\partial x_j} \right\|_{C(\mathcal{G}_r)} + \frac{1}{2} \left\| \frac{\partial \mathbf{W}^{n-1}}{\partial x_j} \right\|_{C(\mathcal{G}_r)} \\ &\leq C(\mathbf{u}), \quad j = 1, 2, \quad n = 1, \dots, N_t - 1. \end{aligned} \quad (2.73)$$

Using the Cauchy-Schwarz inequality, (2.34), (2.13), (2.72), (2.15), and (2.64), we obtain

$$\begin{aligned} &\left| \left\langle \left(\widetilde{\mathbf{W}}^n \cdot \nabla \right) \{ \mathbf{u}(\cdot, t_{n+1/2}) - \tilde{\mathbf{u}}^n \}, d_t \boldsymbol{\nu}^n \right\rangle_{\mathcal{G}_r} \right| \\ &\leq \epsilon \|d_t \boldsymbol{\nu}^n\|_{\mathcal{G}_r}^2 + \frac{C(\mathbf{u})}{\epsilon} \tau^4, \quad n = 1, \dots, N_t - 1, \quad \epsilon > 0. \end{aligned} \quad (2.74)$$

Using the Cauchy-Schwarz inequality, (2.34), (2.13), (2.72), and (2.71), we obtain

$$\left| \left\langle \left(\widetilde{\mathbf{W}}^n \cdot \nabla \right) \tilde{\boldsymbol{\eta}}^n, d_t \boldsymbol{\nu}^n \right\rangle_{\mathcal{G}_r} \right| \leq \epsilon \|d_t \boldsymbol{\nu}^n\|_{\mathcal{G}_r}^2 + \frac{C(\mathbf{u})}{\epsilon} h^{2r}, \quad n = 1, \dots, N_t - 1, \quad \epsilon > 0. \quad (2.75)$$

Using the Cauchy-Schwarz inequality, (2.34), (2.14), and (2.73), we obtain

$$\left| \left\langle (\tilde{\boldsymbol{\nu}}^n \cdot \nabla) \tilde{\mathbf{W}}^n, d_t \boldsymbol{\nu}^n \right\rangle_{\mathcal{G}_r} \right| \leq \epsilon \|d_t \boldsymbol{\nu}^n\|_{\mathcal{G}_r}^2 + \frac{C(\mathbf{u})}{\epsilon} \|\tilde{\boldsymbol{\nu}}^n\|_{\mathcal{G}_r}^2, \quad n = 1, \dots, N_t - 1, \quad \epsilon > 0. \quad (2.76)$$

Using the Cauchy-Schwarz inequality, (2.34), and (2.13), we obtain

$$\begin{aligned} \left| \left\langle (\tilde{\mathbf{U}}^n \cdot \nabla) \tilde{\boldsymbol{\nu}}^n, d_t \boldsymbol{\nu}^n \right\rangle_{\mathcal{G}_r} \right| &\leq \epsilon \|d_t \boldsymbol{\nu}^n\|_{\mathcal{G}_r}^2 \\ + 2 \frac{\|\tilde{\mathbf{U}}^n\|_{C(\mathcal{G}_r)}^2}{\epsilon} (\|\tilde{\boldsymbol{\nu}}_{x_1}^n\|_{\mathcal{G}_r}^2 + \|\tilde{\boldsymbol{\nu}}_{x_2}^n\|_{\mathcal{G}_r}^2), &n = 1, \dots, N_t - 1, \quad \epsilon > 0. \end{aligned} \quad (2.77)$$

For $n = 1, \dots, N_t - 1$, using (2.37), the triangle inequality, (2.34), (2.51), (2.25), and (2.23), we have

$$\|\tilde{\boldsymbol{\nu}}^n\|_{\mathcal{G}_r}^2 \leq C \sum_{j=0}^1 \|\boldsymbol{\nu}^{n-j}\|_{\mathcal{G}_r}^2 \leq C \sum_{j=0}^1 \langle -\Delta \boldsymbol{\nu}^{n-j}, \boldsymbol{\nu}^{n-j} \rangle_{\mathcal{G}_r}, \quad (2.78)$$

$$\|\tilde{\boldsymbol{\nu}}_{x_1}^n\|_{\mathcal{G}_r}^2 + \|\tilde{\boldsymbol{\nu}}_{x_2}^n\|_{\mathcal{G}_r}^2 \leq C \sum_{j=0}^1 \left[\|\boldsymbol{\nu}_{x_1}^{n-j}\|_{\mathcal{G}_r}^2 + \|\boldsymbol{\nu}_{x_2}^{n-j}\|_{\mathcal{G}_r}^2 \right] \leq C \sum_{j=0}^1 \langle -\Delta \boldsymbol{\nu}^{n-j}, \boldsymbol{\nu}^{n-j} \rangle_{\mathcal{G}_r}. \quad (2.79)$$

Using (2.58), the triangle inequality, (2.34), and (2.33), we have

$$\begin{aligned} \|(d_t \mathbf{W}^n)_{x_1 x_1 x_2 x_2}\|_{\mathcal{G}_r}^2 &= \left\| \tau^{-1} \int_{t_n}^{t_{n+1}} \mathbf{W}_{tx_1 x_1 x_2 x_2}(\cdot, s) ds \right\|_{\mathcal{G}_r}^2 \\ &\leq \tau^{-1} \int_{t_n}^{t_{n+1}} \|\mathbf{W}_{tx_1 x_1 x_2 x_2}(\cdot, s)\|_{\mathcal{G}_r}^2 ds \\ &\leq \tau^{-1} 2 \int_{t_n}^{t_{n+1}} \|(\mathbf{u} - \mathbf{W})_{tx_1 x_1 x_2 x_2}(\cdot, s)\|_{\mathcal{G}_r}^2 ds + \tau^{-1} 2 \int_{t_n}^{t_{n+1}} \|\mathbf{u}_{tx_1 x_1 x_2 x_2}(\cdot, s)\|_{\mathcal{G}_r}^2 ds \\ &\leq C(\mathbf{u}), \quad n = 1, \dots, N_t - 1. \end{aligned} \quad (2.80)$$

Using the Cauchy-Schwarz inequality, (2.34), and (2.80), we have

$$\frac{\tau^2 \mu^2}{4} \langle (d_t \mathbf{W}^n)_{x_1 x_1 x_2 x_2}, d_t \boldsymbol{\nu}^n \rangle_{\mathcal{G}_r} \leq \epsilon \|d_t \boldsymbol{\nu}^n\|_{\mathcal{G}_r}^2 + \frac{C(\mathbf{u})}{\epsilon} \tau^4, \quad n = 1, \dots, N_t - 1, \quad \epsilon > 0. \quad (2.81)$$

Using (2.57), (2.51), Lemma 2.4, (2.60), (2.65), (2.66), (2.67), (2.68), (2.70), (2.74), (2.75), (2.76), (2.77), (2.78), (2.79), (2.81), and taking ϵ sufficiently small, we obtain

$$\begin{aligned} \mu \langle -\Delta \boldsymbol{\nu}^{n+1/2}, d_t \boldsymbol{\nu}^n \rangle_{\mathcal{G}_r} &\leq C(\mathbf{u})(h^{2r} + \tau^4) \\ &+ \left[C(\mathbf{u}) + C \|\tilde{\mathbf{U}}^n\|_{C(\mathcal{G}_r)}^2 \right] \sum_{j=0}^1 \langle -\Delta \boldsymbol{\nu}^{n-j}, \boldsymbol{\nu}^{n-j} \rangle_{\mathcal{G}_r}, \quad n = 1, \dots, N_t - 1. \end{aligned} \quad (2.82)$$

Using (2.51), (2.21), we have

$$\langle -\Delta (\boldsymbol{\nu}^n + \boldsymbol{\nu}^{n+1}), \boldsymbol{\nu}^{n+1} - \boldsymbol{\nu}^n \rangle_{\mathcal{G}_r} = \langle -\Delta \boldsymbol{\nu}^{n+1}, \boldsymbol{\nu}^{n+1} \rangle_{\mathcal{G}_r} + \langle \Delta \boldsymbol{\nu}^n, \boldsymbol{\nu}^n \rangle_{\mathcal{G}_r}, \quad n = 1, \dots, N_t - 1.$$

Therefore, the desired result follows on multiplying (2.82) by $2\tau/\mu$ and on using the last unnumbered equation. \square

In the next lemma we bound $\langle -\Delta \boldsymbol{\nu}^1, \boldsymbol{\nu}^1 \rangle_{\mathcal{G}_r}$.

Lemma 2.10. *Assume that \mathbf{U}^0 and \mathbf{U}^1 in $\mathcal{M}_r \times \mathcal{M}_r$ are defined by (2.40)–(2.48), (2.38) with $n = 0$, and that $h^{-2}\tau^3 \leq C$. Then*

$$\langle -\Delta \boldsymbol{\nu}^1, \boldsymbol{\nu}^1 \rangle_{\mathcal{G}_r} \leq C(\mathbf{u})\tau(h^{2r} + \tau^4).$$

Proof. We set

$$\hat{\boldsymbol{\nu}}^n = \mathbf{W}^n - \mathbf{V}^n, \quad n = 0, 1. \quad (2.83)$$

It follows from (2.83), (2.45), (2.40), and (2.46) that

$$\hat{\boldsymbol{\nu}}^0 = \mathbf{0}, \quad \hat{\boldsymbol{\nu}}^1 \in \mathcal{M}_r^0 \times \mathcal{M}_r^0. \quad (2.84)$$

Following the derivation of (2.54) and using (2.41)–(2.42) and (2.48), we get

$$d_t \mathbf{V}^0(\xi) - \mu \Delta \mathbf{V}^{1/2}(\xi) + \frac{\tau^2 \mu^2}{4} (d_t \mathbf{V}^0)_{x_1 x_1 x_2 x_2}(\xi) = - [(\mathbf{V}^0 \cdot \nabla) \mathbf{V}^0](\xi), \quad \xi \in \mathcal{G}_r, \quad (2.85)$$

and using (2.43)–(2.44) and (2.38) with $n = 0$, we get

$$d_t \mathbf{U}^0(\xi) - \mu \Delta \mathbf{U}^{1/2}(\xi) + \frac{\tau^2 \mu^2}{4} (d_t \mathbf{U}^0)_{x_1 x_1 x_2 x_2}(\xi) = - (\mathbf{V}^{1/2}(\xi) \cdot \nabla) \mathbf{V}^{1/2}(\xi), \quad \xi \in \mathcal{G}_r. \quad (2.86)$$

Using (2.83), (2.85), (2.45), (2.49), and (2.1), we have

$$\begin{aligned}
& d_t \widehat{\boldsymbol{\nu}}^0(\xi) - \mu \Delta \widehat{\boldsymbol{\nu}}^{1/2}(\xi) + \frac{\tau^2 \mu^2}{4} (d_t \widehat{\boldsymbol{\nu}}^0)_{x_1 x_1 x_2 x_2}(\xi) \\
&= d_t \mathbf{W}^0(\xi) - \mu \Delta \mathbf{W}^{1/2}(\xi) + [(\mathbf{U}^0 \cdot \nabla) \mathbf{U}^0](\xi) + \frac{\tau^2 \mu^2}{4} (d_t \mathbf{W}^0)_{x_1 x_1 x_2 x_2}(\xi) \\
&= -d_t \boldsymbol{\eta}^0(\xi) + d_t \mathbf{u}^0(\xi) - \mathbf{u}_t(\xi, t_{1/2}) + \mu \Delta \mathbf{u}(\xi, t_{1/2}) \\
&\quad - \mu \Delta \mathbf{u}^{1/2}(\xi) + \mu \Delta \boldsymbol{\eta}^{1/2}(\xi) - [(\mathbf{u} \cdot \nabla) \mathbf{u}](\xi, t_{1/2}) \\
&\quad + [(\mathbf{U}^0 \cdot \nabla) \mathbf{U}^0](\xi) + \frac{\tau^2 \mu^2}{4} (d_t \mathbf{W}^0)_{x_1 x_1 x_2 x_2}(\xi), \quad \xi \in \mathcal{G}_r.
\end{aligned} \tag{2.87}$$

Using (2.49), (2.40), and (2.84) we have

$$\begin{aligned}
& - [(\mathbf{u} \cdot \nabla) \mathbf{u}](\xi, t_{1/2}) + [(\mathbf{U}^0 \cdot \nabla) \mathbf{U}^0](\xi) \\
&= - [(\mathbf{u} \cdot \nabla) \mathbf{u}](\xi, t_{1/2}) + [(\mathbf{u}^0 \cdot \nabla) \mathbf{u}](\xi, t_{1/2}) \\
&\quad - [(\mathbf{u}^0 \cdot \nabla) \mathbf{u}](\xi, t_{1/2}) + [(\mathbf{W}^0 \cdot \nabla) \mathbf{u}](\xi, t_{1/2}) \\
&\quad - [(\mathbf{W}^0 \cdot \nabla) \mathbf{u}](\xi, t_{1/2}) + [(\mathbf{W}^0 \cdot \nabla) \mathbf{u}^0](\xi) \\
&\quad - [(\mathbf{W}^0 \cdot \nabla) \mathbf{u}^0](\xi) + [(\mathbf{W}^0 \cdot \nabla) \mathbf{W}^0](\xi) \\
&= - [(\{\mathbf{u}(\cdot, t_{1/2}) - \mathbf{u}^0\} \cdot \nabla) \mathbf{u}(\cdot, t_{1/2})](\xi) \\
&\quad - [(\boldsymbol{\eta}^0 \cdot \nabla) \mathbf{u}(\cdot, t_{1/2})](\xi) \\
&\quad - [(\mathbf{W}^0 \cdot \nabla) \{\mathbf{u}(\cdot, t_{1/2})(\xi) - \mathbf{u}^0\}](\xi) \\
&\quad - [(\mathbf{W}^0 \cdot \nabla) \boldsymbol{\eta}^0](\xi), \quad \xi \in \mathcal{G}_r.
\end{aligned} \tag{2.88}$$

Taking the discrete inner product (2.10) of (2.87) with $d_t \widehat{\boldsymbol{\nu}}^0$ and using (2.88), we obtain

$$\begin{aligned}
& \|d_t \widehat{\mathbf{v}}^0\|_{\mathcal{G}_r}^2 - \mu \langle \Delta \widehat{\mathbf{v}}^{1/2}, d_t \widehat{\mathbf{v}}^0 \rangle_{\mathcal{G}_r} + \frac{\tau^2 \mu^2}{4} \langle (d_t \widehat{\mathbf{v}}^0)_{x_1 x_1 x_2 x_2}, d_t \widehat{\mathbf{v}}^0 \rangle_{\mathcal{G}_r} \\
&= - \langle d_t \boldsymbol{\eta}^0, d_t \widehat{\mathbf{v}}^0 \rangle_{\mathcal{G}_r} + \langle d_t \mathbf{u}^0 - \mathbf{u}_t(\cdot, t_{1/2}), d_t \widehat{\mathbf{v}}^0 \rangle_{\mathcal{G}_r} \\
&\quad + \mu \langle \Delta \mathbf{u}(\cdot, t_{1/2}) - \Delta \mathbf{u}^{1/2}, d_t \widehat{\mathbf{v}}^0 \rangle_{\mathcal{G}_r} + \mu \langle \Delta \boldsymbol{\eta}^{1/2}, d_t \widehat{\mathbf{v}}^0 \rangle_{\mathcal{G}_r} \\
&\quad - \langle [(\{\mathbf{u}(\cdot, t_{1/2}) - \mathbf{u}^0\} \cdot \nabla) \mathbf{u}] (\cdot, t_{1/2}), d_t \widehat{\mathbf{v}}^0 \rangle_{\mathcal{G}_r} \\
&\quad - \langle [(\boldsymbol{\eta}^0 \cdot \nabla) \mathbf{u}] (\cdot, t_{1/2}), d_t \widehat{\mathbf{v}}^0 \rangle_{\mathcal{G}_r} \\
&\quad - \langle (\mathbf{W}^0 \cdot \nabla) \{\mathbf{u}(\cdot, t_{1/2}) - \mathbf{u}^0\}, d_t \widehat{\mathbf{v}}^0 \rangle_{\mathcal{G}_r} \\
&\quad - \langle (\mathbf{W}^0 \cdot \nabla) \boldsymbol{\eta}^0, d_t \widehat{\mathbf{v}}^0 \rangle + \frac{\tau^2 \mu^2}{4} \langle (d_t \mathbf{W}^0)_{x_1 x_1 x_2 x_2}, d_t \widehat{\mathbf{v}}^0 \rangle_{\mathcal{G}_r}.
\end{aligned} \tag{2.89}$$

By Taylor's theorem, we have

$$\|\mathbf{u}(\cdot, t_{1/2}) - \mathbf{u}^0\|_{C(\mathcal{G}_r)} \leq C(\mathbf{u})\tau, \tag{2.90}$$

$$\left\| \frac{\partial \mathbf{u}(\cdot, t_{1/2})}{\partial x_j} - \frac{\partial \mathbf{u}^0}{\partial x_j} \right\|_{C(\mathcal{G}_r)} \leq C(\mathbf{u})\tau. \tag{2.91}$$

Using the Cauchy-Schwarz inequality, (2.34), (2.14), (2.15), (2.90), and boundedness of $\partial u_i / \partial x_j$, $i, j = 1, 2$, we obtain

$$\begin{aligned}
& \left| \langle [(\{\mathbf{u}(\cdot, t_{1/2}) - \mathbf{u}^0\} \cdot \nabla) \mathbf{u}] (\cdot, t_{1/2}), d_t \widehat{\mathbf{v}}^0 \rangle_{\mathcal{G}_r} \right| \\
& \leq \epsilon \|d_t \widehat{\mathbf{v}}^0\|_{\mathcal{G}_r}^2 + \frac{C(\mathbf{u})}{\epsilon} \tau^2, \quad \epsilon > 0.
\end{aligned} \tag{2.92}$$

Using the Cauchy-Schwarz inequality, (2.34), (2.13), Lemma 2.8, (2.91), and (2.15), we obtain

$$\begin{aligned}
& \left| \langle (\mathbf{W}^0 \cdot \nabla) \{\mathbf{u}(\cdot, t_{1/2}) - \mathbf{u}^0\}, d_t \widehat{\mathbf{v}}^0 \rangle_{\mathcal{G}_r} \right| \\
& \leq \epsilon \|d_t \widehat{\mathbf{v}}^0\|_{\mathcal{G}_r}^2 + \frac{C(\mathbf{u})}{\epsilon} \tau^2, \quad \epsilon > 0.
\end{aligned} \tag{2.93}$$

Using (2.89), (2.84), Lemma 2.4, using (2.60), (2.65), (2.66), and (2.81) with $n = 0$ and $\widehat{\boldsymbol{\nu}}$ replacing $\boldsymbol{\nu}$, using (2.92), using (2.70) with $n = 0$ and $\boldsymbol{\eta}$, $\boldsymbol{\nu}$ replacing $\widetilde{\boldsymbol{\eta}}$, $\boldsymbol{\nu}$, respectively, using (2.93), using (2.75) with $n = 0$ and \mathbf{W} , $\boldsymbol{\eta}$, $\widetilde{\boldsymbol{\nu}}$ replacing $\widetilde{\mathbf{W}}$, $\widetilde{\boldsymbol{\eta}}$, $\boldsymbol{\nu}$, respectively, and taking ϵ sufficiently small, we obtain

$$\mu \langle -\Delta \widehat{\boldsymbol{\nu}}^{1/2}, d_t \widehat{\boldsymbol{\nu}}^0 \rangle_{\mathcal{G}_r} \leq C(\mathbf{u})(h^{2r} + \tau^2).$$

Multiplying the last unnumbered equation by $2\tau/\mu$ and using $\widehat{\boldsymbol{\nu}}^0 = \mathbf{0}$ of (2.84), we get

$$\langle -\Delta \widehat{\boldsymbol{\nu}}^1, \widehat{\boldsymbol{\nu}}^1 \rangle_{\mathcal{G}_r} \leq C(\mathbf{u})\tau(h^{2r} + \tau^2). \quad (2.94)$$

Using (2.50), (2.86), (2.49), and (2.1), we have

$$\begin{aligned} & d_t \boldsymbol{\nu}^0(\xi) - \mu \Delta \boldsymbol{\nu}^{1/2}(\xi) + \frac{\tau^2 \mu^2}{4} (d_t \boldsymbol{\nu}^0)_{x_1 x_1 x_2 x_2}(\xi) \\ &= d_t \mathbf{W}^0(\xi) - \mu \Delta \mathbf{W}^{1/2}(\xi) + [(\mathbf{V}^{1/2} \cdot \nabla) \mathbf{V}^{1/2}](\xi) + \frac{\tau^2 \mu^2}{4} (d_t \mathbf{W}^0)_{x_1 x_1 x_2 x_2}(\xi) \\ &= -d_t \boldsymbol{\eta}^0(\xi) + d_t \mathbf{u}^0(\xi) - \mathbf{u}_t(\xi, t_{1/2}) + \mu \Delta \mathbf{u}(\xi, t_{1/2}) - \mu \Delta \mathbf{u}^{1/2}(\xi) + \mu \Delta \boldsymbol{\eta}^{1/2}(\xi) \\ &\quad - [(\mathbf{u} \cdot \nabla) \mathbf{u}](\xi, t_{1/2}) + [(\mathbf{V}^{1/2} \cdot \nabla) \mathbf{V}^{1/2}](\xi) + \frac{\tau^2 \mu^2}{4} (d_t \mathbf{W}^0)_{x_1 x_1 x_2 x_2}(\xi), \quad \xi \in \mathcal{G}_r. \end{aligned} \quad (2.95)$$

Using (2.49) and (2.83), we have

$$\begin{aligned}
& - [(\mathbf{u} \cdot \nabla) \mathbf{u}] (\xi, t_{1/2}) + [(\mathbf{V}^{1/2} \cdot \nabla) \mathbf{V}^{1/2}] (\xi) \tag{2.96} \\
& = - [(\mathbf{u} \cdot \nabla) \mathbf{u}(\cdot, t_{1/2})] (\xi) + [(\mathbf{u}^{1/2} \cdot \nabla) \mathbf{u}(\cdot, t_{1/2})] (\xi) \\
& \quad - [(\mathbf{u}^{1/2} \cdot \nabla) \mathbf{u}(\cdot, t_{1/2})] (\xi) + [(\mathbf{W}^{1/2} \cdot \nabla) \mathbf{u}(\cdot, t_{1/2})] (\xi) \\
& \quad - [(\mathbf{W}^{1/2} \cdot \nabla) \mathbf{u}(\cdot, t_{1/2})] (\xi) + [(\mathbf{W}^{1/2} \cdot \nabla) \mathbf{u}^{1/2}] (\xi) \\
& \quad - [(\mathbf{W}^{1/2} \cdot \nabla) \mathbf{u}^{1/2}] (\xi) + [(\mathbf{W}^{1/2} \cdot \nabla) \mathbf{W}^{1/2}] (\xi) \\
& \quad - [(\mathbf{W}^{1/2} \cdot \nabla) \mathbf{W}^{1/2}] (\xi) + [(\mathbf{V}^{1/2} \cdot \nabla) \mathbf{W}^{1/2}] (\xi) \\
& \quad - [(\mathbf{V}^{1/2} \cdot \nabla) \mathbf{W}^{1/2}] (\xi) + [(\mathbf{V}^{1/2} \cdot \nabla) \mathbf{V}^{1/2}] (\xi) \\
& = - [(\{\mathbf{u}(\cdot, t_{1/2}) - \mathbf{u}^{1/2}\} \cdot \nabla) \mathbf{u}(\cdot, t_{1/2})] (\xi) - [(\boldsymbol{\eta}^{1/2} \cdot \nabla) \mathbf{u}(\cdot, t_{1/2})] (\xi) \\
& \quad - [(\mathbf{W}^{1/2} \cdot \nabla) \{\mathbf{u}(\cdot, t_{1/2}) - \mathbf{u}^{1/2}\}] (\xi) - [(\mathbf{W}^{1/2} \cdot \nabla) \boldsymbol{\eta}^{1/2}] (\xi) \\
& \quad - [(\widehat{\boldsymbol{\nu}}^{1/2} \cdot \nabla) \mathbf{W}^{1/2}] (\xi) - [(\mathbf{V}^{1/2} \cdot \nabla) \widehat{\boldsymbol{\nu}}^{1/2}] (\xi), \quad \xi \in \mathcal{G}_r.
\end{aligned}$$

Taking the discrete inner product (2.10) of (2.95) with $d_t \boldsymbol{\nu}^0$ and using (2.96), we obtain

$$\begin{aligned}
& \|d_t \boldsymbol{\nu}^0\|_{\mathcal{G}_r}^2 - \mu \langle \Delta \boldsymbol{\nu}^{1/2}, d_t \boldsymbol{\nu}^0 \rangle_{\mathcal{G}_r} + \frac{\tau^2 \mu^2}{4} \left\langle (d_t \boldsymbol{\nu}^0)_{x_1 x_1 x_2 x_2}, d_t \boldsymbol{\nu}^0 \right\rangle_{\mathcal{G}_r} \quad (2.97) \\
& = - \langle d_t \boldsymbol{\eta}^0, d_t \boldsymbol{\nu}^0 \rangle_{\mathcal{G}_r} + \langle d_t \mathbf{u}^0 - \mathbf{u}_t(\cdot, t_{1/2}), d_t \boldsymbol{\nu}^0 \rangle_{\mathcal{G}_r} \\
& \quad + \mu \langle \Delta \mathbf{u}(\cdot, t_{1/2}) - \Delta \mathbf{u}^{1/2}, d_t \boldsymbol{\nu}^0 \rangle_{\mathcal{G}_r} + \mu \langle \Delta \boldsymbol{\eta}^{1/2}, d_t \boldsymbol{\nu}^0 \rangle_{\mathcal{G}_r} \\
& \quad - \left\langle [(\{\mathbf{u}(\cdot, t_{1/2}) - \mathbf{u}^{1/2}\} \cdot \nabla) \mathbf{u}] (\cdot, t_{1/2}), d_t \boldsymbol{\nu}^0 \right\rangle_{\mathcal{G}_r} \\
& \quad - \left\langle [(\boldsymbol{\eta}^{1/2} \cdot \nabla) \mathbf{u}] (\cdot, t_{1/2}), d_t \boldsymbol{\nu}^0 \right\rangle_{\mathcal{G}_r} \\
& \quad - \left\langle (\mathbf{W}^{1/2} \cdot \nabla) \{\mathbf{u}(\cdot, t_{1/2}) - \mathbf{u}^{1/2}\}, d_t \boldsymbol{\nu}^0 \right\rangle_{\mathcal{G}_r} \\
& \quad - \left\langle (\mathbf{W}^{1/2} \cdot \nabla) \boldsymbol{\eta}^{1/2}, d_t \boldsymbol{\nu}^0 \right\rangle_{\mathcal{G}_r} - \left\langle (\widehat{\boldsymbol{\nu}}^{1/2} \cdot \nabla) \mathbf{W}^{1/2}, d_t \boldsymbol{\nu}^0 \right\rangle_{\mathcal{G}_r} \\
& \quad - \left\langle (\mathbf{V}^{1/2} \cdot \nabla) \widehat{\boldsymbol{\nu}}^{1/2}, d_t \boldsymbol{\nu}^0 \right\rangle_{\mathcal{G}_r} + \frac{\tau^2 \mu^2}{4} \left\langle (d_t \mathbf{W}^0)_{x_1 x_1 x_2 x_2}, d_t \boldsymbol{\nu}^0 \right\rangle_{\mathcal{G}_r}.
\end{aligned}$$

By Taylor's theorem and the triangle inequality, we have

$$\|\mathbf{u}(\cdot, t_{1/2}) - \mathbf{u}^{1/2}\|_{C(\mathcal{G}_r)} \leq C(\mathbf{u})\tau^2, \quad (2.98)$$

$$\left\| \frac{\partial \mathbf{u}(\cdot, t_{1/2})}{\partial x_j} - \frac{\partial \mathbf{u}^{1/2}}{\partial x_j} \right\|_{C(\mathcal{G}_r)} \leq C(\mathbf{u})\tau^2, \quad j = 1, 2. \quad (2.99)$$

Using the Cauchy-Schwarz inequality, (2.34), (2.14), (2.15), (2.98), and boundedness of $\partial u_i / \partial x_j$, $i, j = 1, 2$, we obtain

$$\left| \left\langle [(\{\mathbf{u}(\cdot, t_{1/2}) - \mathbf{u}^{1/2}\} \cdot \nabla) \mathbf{u}] (\cdot, t_{1/2}), d_t \boldsymbol{\nu}^0 \right\rangle_{\mathcal{G}_r} \right| \leq \epsilon \|d_t \boldsymbol{\nu}^0\|_{\mathcal{G}_r}^2 + \frac{C(\mathbf{u})}{\epsilon} \tau^4, \quad \epsilon > 0. \quad (2.100)$$

The triangle inequality and Lemma 2.8 give

$$\|\mathbf{W}^{1/2}\|_{C(\mathcal{G}_r)} \leq \frac{1}{2} \|\mathbf{W}^1\|_{C(\mathcal{G}_r)} + \frac{1}{2} \|\mathbf{W}^0\|_{C(\mathcal{G}_r)} \leq C(\mathbf{u}). \quad (2.101)$$

Using the Cauchy-Schwarz inequality, (2.34), (2.14), (2.15), (2.101), and (2.99), we obtain

$$\left| \left\langle (\mathbf{W}^{1/2} \cdot \nabla) \{\mathbf{u}(\cdot, t_{1/2}) - \mathbf{u}^{1/2}\}, d_t \boldsymbol{\nu}^0 \right\rangle_{\mathcal{G}_r} \right| \leq \epsilon \|d_t \boldsymbol{\nu}^0\|_{\mathcal{G}_r}^2 + \frac{C(\mathbf{u})}{\epsilon} \tau^4. \quad (2.102)$$

The triangle inequality, (2.49), and (2.30) with $i = j = 0$ give

$$\|\boldsymbol{\eta}^{1/2}\|_{\mathcal{G}_r} \leq \frac{1}{2} \|\boldsymbol{\eta}^1\|_{\mathcal{G}_r} + \frac{1}{2} \|\boldsymbol{\eta}^0\|_{\mathcal{G}_r} \leq C(\mathbf{u})h^{r+1}. \quad (2.103)$$

Using the Cauchy-Schwarz inequality, (2.34), (2.14), (2.103), and boundedness of $\partial u_i/\partial x_j$, $i, j = 1, 2$, we obtain

$$\left| \langle (\boldsymbol{\eta}^{1/2} \cdot \nabla) \mathbf{u}(\cdot, t_{1/2}), d_t \boldsymbol{\nu}^0 \rangle_{\mathcal{G}_r} \right| \leq \epsilon \|d_t \boldsymbol{\nu}^0\|_{\mathcal{G}_r}^2 + \frac{C(\mathbf{u})}{\epsilon} h^{2r+2}, \quad \epsilon > 0. \quad (2.104)$$

The triangle inequality, (2.49) and (2.30) with $i = j = 0$ give

$$\left\| \frac{\partial \boldsymbol{\eta}^{1/2}}{\partial x_j} \right\|_{\mathcal{G}_r} \leq \frac{1}{2} \left\| \frac{\partial \boldsymbol{\eta}^1}{\partial x_j} \right\|_{\mathcal{G}_r} + \frac{1}{2} \left\| \frac{\partial \boldsymbol{\eta}^0}{\partial x_j} \right\|_{\mathcal{G}_r} \leq C(\mathbf{u})h^r, \quad j = 1, 2. \quad (2.105)$$

Using the Cauchy-Schwarz inequality, (2.34), (2.13), (2.101), and (2.105), we obtain

$$\left| \langle (\mathbf{W}^{1/2} \cdot \nabla) \boldsymbol{\eta}^{1/2}, d_t \boldsymbol{\nu}^0 \rangle_{\mathcal{G}_r} \right| \leq \epsilon \|d_t \boldsymbol{\nu}^0\|_{\mathcal{G}_r}^2 + \frac{C(\mathbf{u})}{\epsilon} h^{2r}. \quad (2.106)$$

The triangle inequality and Lemma 2.8 give

$$\left\| \frac{\partial \mathbf{W}^{1/2}}{\partial x_j} \right\|_{C(\mathcal{G}_r)} \leq \frac{1}{2} \left\| \frac{\partial \mathbf{W}^1}{\partial x_j} \right\|_{C(\mathcal{G}_r)} + \frac{1}{2} \left\| \frac{\partial \mathbf{W}^0}{\partial x_j} \right\|_{C(\mathcal{G}_r)} \leq C(\mathbf{u}), \quad j = 1, 2. \quad (2.107)$$

Using the Cauchy-Schwarz inequality, (2.34), (2.14), (2.107), (2.84), and (2.25), we obtain

$$\left| \langle (\widehat{\boldsymbol{\nu}}^{1/2} \cdot \nabla) \mathbf{W}^{1/2}, d_t \boldsymbol{\nu}^0 \rangle_{\mathcal{G}_r} \right| \leq \epsilon \|d_t \boldsymbol{\nu}^0\|_{\mathcal{G}_r}^2 + \frac{C(\mathbf{u})}{\epsilon} \langle -\Delta \widehat{\boldsymbol{\nu}}^{1/2}, \widehat{\boldsymbol{\nu}}^{1/2} \rangle_{\mathcal{G}_r}. \quad (2.108)$$

Using (2.47), (2.45), (2.40), and (2.83) with $n = 1$, we have

$$\mathbf{V}^{1/2} = \frac{1}{2} (\mathbf{W}^0 + \mathbf{W}^1 - \widehat{\boldsymbol{\nu}}^1).$$

Hence the triangle inequality, Lemma 2.8, (2.84), Lemma 2.2, (2.22), (2.94), $r \geq 3$, and $h^{-2}\tau^3 \leq C$ give

$$\begin{aligned} \|\mathbf{V}^{1/2}\|_{C(\mathcal{G}_r)} &\leq C (\|\mathbf{W}^0\|_{C(\mathcal{G}_r)} + \|\mathbf{W}^1\|_{C(\mathcal{G}_r)} + h^{-1} \|\widehat{\boldsymbol{\nu}}^1\|_{H^1(\Omega)}) \quad (2.109) \\ &\leq C(u) + C(u)h^{-1}(h^r + \tau^{3/2}) \leq C(\mathbf{u}). \end{aligned}$$

Using the Cauchy-Schwarz inequality, (2.34), (2.13), (2.109), (2.84), and (2.23), we obtain

$$\left| \left\langle (\mathbf{V}^{1/2} \cdot \nabla) \widehat{\boldsymbol{\nu}}^{1/2}, d_t \boldsymbol{\nu}^0 \right\rangle_{\mathcal{G}_r} \right| \leq \epsilon \|d_t \boldsymbol{\nu}^0\|_{\mathcal{G}_r}^2 + \frac{C(\mathbf{u})}{\epsilon} \langle -\Delta \widehat{\boldsymbol{\nu}}^{1/2}, \widehat{\boldsymbol{\nu}}^{1/2} \rangle_{\mathcal{G}_r}. \quad (2.110)$$

Using (2.97), (2.51), Lemma 2.4, using (2.60), (2.65), (2.66), (2.67), and (2.81), all with $n = 0$, (2.100), (2.104), (2.102), (2.106), (2.108), (2.110), and taking ϵ sufficiently small, we obtain

$$\langle -\Delta \boldsymbol{\nu}^{1/2}, d_t \boldsymbol{\nu}^0 \rangle_{\mathcal{G}_r} \leq C(\mathbf{u}) \left(h^{2r} + \tau^4 + \langle -\Delta \widehat{\boldsymbol{\nu}}^{1/2}, \widehat{\boldsymbol{\nu}}^{1/2} \rangle_{\mathcal{G}_r} \right).$$

Multiplying the last unnumbered equation by 2τ and using $\boldsymbol{\nu}^0 = \widehat{\boldsymbol{\nu}}^0 = \mathbf{0}$ of (2.51) and (2.84), we get

$$\langle -\Delta \boldsymbol{\nu}^1, \boldsymbol{\nu}^1 \rangle_{\mathcal{G}_r} \leq C(\mathbf{u}) \tau \left(h^{2r} + \tau^4 + \langle -\Delta \widehat{\boldsymbol{\nu}}^1, \widehat{\boldsymbol{\nu}}^1 \rangle_{\mathcal{G}_r} \right).$$

The desired result follows from the last unnumbered equation and (2.94). \square

Finally, we prove that, at each time level, the H^1 norm error in our ADI-ECN-OSC scheme of section 2.2 for solving the coupled Burgers' equation is of order r in space and of order 2 in time.

Theorem 2.2. *Assume that $\mathbf{U}^n \in \mathcal{M}_r \times \mathcal{M}_r$, $n = 2, \dots, N_t$, are defined by (2.35)–(2.39), and that \mathbf{U}^0 and \mathbf{U}^1 in $\mathcal{M}_r \times \mathcal{M}_r$ are defined by (2.40)–(2.48), (2.38) with $n = 0$. Assume also that $h^{-2}\tau^3 \leq C$, and that h and τ are sufficiently small. Then*

$$\|\mathbf{u}^n - \mathbf{U}^n\|_{H^1(\Omega)} \leq C(\mathbf{u})(h^r + \tau^2).$$

Proof. First we show that

$$\|\widetilde{\mathbf{U}}^n\|_{C(\mathcal{G}_r)} \leq C_4(\mathbf{u}), \quad n = 1, \dots, N_t. \quad (2.111)$$

Lemmas 2.8 and 2.10 give

$$\|\mathbf{W}^n\|_{C(\mathcal{G}_r)} \leq C_1(\mathbf{u}), \quad n = 0, \dots, N_t, \quad (2.112)$$

$$\langle -\Delta \boldsymbol{\nu}^1, \boldsymbol{\nu}^1 \rangle_{\mathcal{G}_r} \leq C_2(\mathbf{u})(h^{2r} + \tau^4). \quad (2.113)$$

It follows from (2.37), (2.50), and (2.40) that

$$\tilde{\mathbf{U}}^1 = \frac{1}{2} [3(\mathbf{W}^1 - \boldsymbol{\nu}^1) - \mathbf{W}^0]. \quad (2.114)$$

Using (2.114), the triangle inequality, (2.51), Lemma 2.2, (2.22), (2.113), $r \geq 3$, and $h^{-2}\tau^3 \leq C$, we have

$$\begin{aligned} \|\tilde{\mathbf{U}}^1\|_{C(\mathcal{G}_r)} &\leq C(\|\mathbf{W}^0\|_{C(\mathcal{G}_r)} + \|\mathbf{W}^1\|_{C(\mathcal{G}_r)} + h^{-1}\|\boldsymbol{\nu}^1\|_{H^1(\Omega)}) \quad (2.115) \\ &\leq C(u) + C(U)h^{-1}(h^r + \tau^2) \leq C_3(\mathbf{u}). \end{aligned}$$

With $C_i(\mathbf{u})$, $i = 1, 2, 3$, as in (2.112), (2.113), and (2.115), we set

$$C_4(\mathbf{u}) = \max \left\{ 4C_1(\mathbf{u}), \sqrt{1 + C_2(\mathbf{u})}, C_3(\mathbf{u}) \right\}, \quad (2.116)$$

and use mathematical induction to prove (2.111). First, (2.115) and (2.116) show that $\|\tilde{\mathbf{U}}^1\|_{C(\bar{\Omega})} \leq C_4(\mathbf{u})$. Next we assume that $\|\tilde{\mathbf{U}}^n\|_{C(\mathcal{G}_r)} \leq C_4(\mathbf{u})$, $n = 1, \dots, l$ for some l such that $1 \leq l \leq N_t - 1$. Then Theorem 4.1 gives

$$\begin{aligned} \langle -\Delta \boldsymbol{\nu}^{n+1}, \boldsymbol{\nu}^{n+1} \rangle_{\mathcal{G}_r} + \langle \Delta \boldsymbol{\nu}^n, \boldsymbol{\nu}^n \rangle_{\mathcal{G}_r} &\leq C(\mathbf{u})\tau(h^{2r} + \tau^4) \\ &+ C(\mathbf{u})\tau \sum_{j=0}^1 \langle -\Delta \boldsymbol{\nu}^{n-j}, \boldsymbol{\nu}^{n-j} \rangle_{\mathcal{G}_r}, \quad n = 1, \dots, l. \end{aligned} \quad (2.117)$$

Summing (2.117) for $n = 1, \dots, k-1$, where fixed k is such that $2 \leq k \leq l+1$, we get

$$\begin{aligned} \langle -\Delta \boldsymbol{\nu}^k, \boldsymbol{\nu}^k \rangle_{\mathcal{G}_r} &\leq \langle -\Delta \boldsymbol{\nu}^1, \boldsymbol{\nu}^1 \rangle_{\mathcal{G}_r} + C(\mathbf{u})(h^{2r} + \tau^4) \\ &+ C(\mathbf{u})\tau \sum_{n=0}^{k-1} \langle -\Delta \boldsymbol{\nu}^n, \boldsymbol{\nu}^n \rangle_{\mathcal{G}_r}, \quad k = 2, \dots, l+1. \end{aligned} \quad (2.118)$$

It follows from (2.51) and (2.25) that (2.118) holds for $k = 0, 1$. We set

$$m = l+1, \quad \alpha_k = \langle -\Delta \boldsymbol{\nu}^k, \boldsymbol{\nu}^k \rangle_{\mathcal{G}_r}, \quad \beta_k = \langle -\Delta \boldsymbol{\nu}^1, \boldsymbol{\nu}^1 \rangle_{\mathcal{G}_r} + C(\mathbf{u})(h^{2r} + \tau^4),$$

and use (2.118) (also with $k = 0, 1$) and Lemma 2.9 to obtain

$$\langle -\Delta \boldsymbol{\nu}^n, \boldsymbol{\nu}^n \rangle_{\mathcal{G}_r} \leq C(\mathbf{u}) (\langle -\Delta \boldsymbol{\nu}^1, \boldsymbol{\nu}^1 \rangle_{\mathcal{G}_r} + h^{2r} + \tau^4), \quad n = 0, \dots, l+1. \quad (2.119)$$

Using (2.51), Lemma 2.2, (2.22), (2.119), (2.113), (2.116), $r \geq 3$, $h^{-2}\tau^3 \leq C$ and taking τ and h sufficiently small so that $C(\mathbf{u})(h^{2r-2} + C\tau) \leq 1/16$, we obtain

$$\|\boldsymbol{\nu}^n\|_{C(\mathcal{G}_r)}^2 \leq C(\mathbf{u})(1 + C_2(\mathbf{u}))h^{-2}(h^{2r} + \tau^4) \leq \frac{C_4^2(\mathbf{u})}{16}, \quad n = l, l+1. \quad (2.120)$$

It follows from (2.37) and (2.50) that

$$\tilde{\mathbf{U}}^{l+1} = \frac{3}{2}\mathbf{W}^{l+1} - \frac{1}{2}\mathbf{W}^l - \frac{3}{2}\boldsymbol{\nu}^{l+1} + \frac{1}{2}\boldsymbol{\nu}^l.$$

Hence using the triangle inequality, (2.112), (2.116), and (2.120), we get

$$\|\tilde{\mathbf{U}}^{l+1}\|_{C(\mathcal{G}_r)} \leq \frac{3}{2}\|\mathbf{W}^{l+1}\|_{C(\mathcal{G}_r)} + \frac{1}{2}\|\mathbf{W}^l\|_{C(\mathcal{G}_r)} + \frac{3}{2}\|\boldsymbol{\nu}^{l+1}\|_{C(\mathcal{G}_r)} + \frac{1}{2}\|\boldsymbol{\nu}^l\|_{C(\bar{\Omega})} \leq 2C_1(\mathbf{u}) + \frac{C_4(\mathbf{u})}{2} \leq C_4(\mathbf{u}) \quad (2.121)$$

which completes the proof of (2.111) by induction.

Next we use (2.111) and follow the derivation of (2.119) to show that

$$\langle -\Delta\boldsymbol{\nu}^n, \boldsymbol{\nu}^n \rangle_{\mathcal{G}_r} \leq C(\mathbf{u}) (\langle -\Delta\boldsymbol{\nu}^1, \boldsymbol{\nu}^1 \rangle_{\mathcal{G}_r} + h^{2r} + \tau^4), \quad n = 0, \dots, N_t. \quad (2.122)$$

Then (2.51), (2.22), (2.122), and Lemma 2.10 give

$$\|\boldsymbol{\nu}^n\|_{H^1(\Omega)} \leq C(\mathbf{u})(h^r + \tau^2), \quad n = 0, \dots, N_t. \quad (2.123)$$

It follows from (2.49) and (2.50) that $\mathbf{u}^n - \mathbf{U}^n = \boldsymbol{\eta}^n + \boldsymbol{\nu}^n$. Hence, using the triangle inequality, (2.49), Lemma 2.7, and (2.123), we have

$$\|\mathbf{u}^n - \mathbf{U}^n\|_{H^1(\Omega)} \leq \|\boldsymbol{\eta}^n\|_{H^1(\Omega)} + \|\boldsymbol{\nu}^n\|_{H^1(\Omega)} \leq C(\mathbf{u})(h^r + \tau^2), \quad n = 0, \dots, N_t,$$

which is the desired result. \square

2.4 Implementation and Numerical Results

We briefly discuss the implementation of the scheme of section 2.2 and begin by outlining the computation of \mathbf{U}^0 in (2.40). Following (2.12), we first compute \mathbf{W}^0 at all points $(\xi_{i,k}^{x_1}, a_2)$, $(\xi_{i,k}^{x_1}, b_2)$, $(\xi_{i,k}^{x_1}, \xi_{j,l}^{x_2})$ since then this allows us to obtain \mathbf{W}^0 on vertical line segments passing through the Gauss points. We compute \mathbf{W}^0 at all points $(\xi_{i,k}^{x_1}, a_2)$ and $(\xi_{i,k}^{x_1}, b_2)$ using the 1d Hermite interpolants of $\mathbf{u}(\cdot, a_2)$ and $\mathbf{u}(\cdot, b_2)$, respectively. Next we explain how to

compute \mathbf{W}^0 at all points $(\xi_{i,k}^{x_1}, \xi_{j,l}^{x_2})$ in the fixed cell $[x_1^{(i-1)}, x_1^{(i)}] \times [x_2^{(j-1)}, x_2^{(j)}]$. We begin by computing \mathbf{W}^0 and $\mathbf{W}_{x_1}^0$ at all $\xi_{j,l}^{x_2}$ corresponding to vertical sides of the cell. (These computations involve 1d Hermite interpolants of $\mathbf{u}^0(x_1^{i-1}, \cdot)$, $\mathbf{u}^0(x_1^i, \cdot)$ and $\mathbf{u}_{x_1}^0(x_1^{i-1}, \cdot)$, $\mathbf{u}_{x_1}^0(x_1^i, \cdot)$ on $[x_2^{(j-1)}, x_2^{(j)}]$.) Next, for each $k = 1, \dots, r-3$, we compute $\mathbf{W}^0(\zeta_{i,k}^{x_2}, \xi_{j,l}^{x_2})$, $l = 1, \dots, r-1$. (Each computation involves 1d Hermite interpolant of $\mathbf{u}^0(\zeta_{i,k}^{x_1}, \cdot)$ on $[x_2^{(j-1)}, x_2^{(j)}]$.) Finally for each $\xi_{j,l}^{x_2}$, $l = 1, \dots, r-1$, we compute $\mathbf{W}^0(\xi_{i,k}^{x_1}, \xi_{j,l}^{x_2})$, $k = 1, \dots, r-1$. (This computation involves 1d Hermite interpolant of $\mathbf{W}^0(\cdot, \xi_{j,l}^{x_2})$ on $[x_1^{(i-1)}, x_1^{(i)}]$.)

We implement (2.35)–(2.39) as follows. First, for each $\xi^{x_2} \in \mathcal{G}_{x_2}$, we compute $\mathbf{U}^{n, \frac{1}{2}}(\cdot, \xi^{x_2}) \in \mathcal{M}_{x_1} \times \mathcal{M}_{x_1}$ using (2.35), (2.38), (2.39). Then, for each $\xi^{x_1} \in \mathcal{G}_{x_1}$, we compute $\mathbf{U}^{n+1}(\xi^{x_1}, \cdot) \in \mathcal{M}_{x_2} \times \mathcal{M}_{x_2}$ using (2.36), (2.39). Finally, for each $\xi^{x_2} \in \mathcal{G}_{x_2}$, we compute $\mathbf{U}^{n+1}(\cdot, \xi^{x_2}) \in \mathcal{M}_{x_1} \times \mathcal{M}_{x_1}$ using (2.39). Note that $\mathbf{U}^{n+1}(\xi^{x_1}, \cdot)$, $\xi^{x_1} \in \mathcal{G}_{x_1}$, and $\mathbf{U}^{n+1}(\cdot, \xi^{x_2})$, $\xi^{x_2} \in \mathcal{G}_{x_2}$, are needed to compute the right-hand side in (2.35) and (2.36) with n replaced by $n+1$. Throughout, the required collocation matrices are set up using the B-spline package of de Boor [32]. These matrices have almost block diagonal structure and linear systems with such matrices can be solved using the package COLROW [33, 34] which has been implemented in Matlab by P. Keast [35].

To compute the L^2 , H^1 , global maximum norm errors in \mathbf{U}^{N_t} , we evaluate \mathbf{U}^{N_t} at points of a partition of $\bar{\Omega}$. For example, if $\{\tilde{\xi}_k\}_{k=1}^{r+1}$ and $\{\tilde{\omega}_k\}_{k=1}^{r+1}$ are the nodes and weights of the $(r+1)$ -point Gauss-Legendre quadrature rule for $(0, 1)$, we define $\tilde{\mathcal{G}}_{x_1} = \{\tilde{\xi}_{i,k}^{x_1}\}_{i=1, k=1}^{N_{x_1}, r+1}$ and $\tilde{\mathcal{G}}_{x_2} = \{\tilde{\xi}_{j,l}^{x_2}\}_{j=1, l=1}^{N_{x_2}, r+1}$, where the $\tilde{\xi}_{i,k}^{x_1}$ and $\tilde{\xi}_{j,l}^{x_2}$ are given by (2.6) with ξ_k replaced by $\tilde{\xi}_k$. We introduce

$$\tilde{\mathcal{G}}_r = \{\xi = (\tilde{\xi}^{x_1}, \tilde{\xi}^{x_2}) : \tilde{\xi}^{x_1} \in \tilde{\mathcal{G}}_{x_1}, \tilde{\xi}^{x_2} \in \tilde{\mathcal{G}}_{x_2}\}. \quad (2.124)$$

Then the L^2 norm error is computed as follows. First, for each $\xi^{x_1} \in \mathcal{G}_{x_1}$, we evaluate, $\mathbf{U}^{N_t}(\xi^{x_1}, \cdot) \in \mathcal{M}_{x_2} \times \mathcal{M}_{x_2}$ at the points $\tilde{\xi}^{x_2} \in \tilde{\mathcal{G}}_{x_2}$, and for each $\tilde{\xi}^{x_2} \in \tilde{\mathcal{G}}_{x_2}$, we evaluate $\mathbf{U}^{N_t}(\cdot, \tilde{\xi}^{x_2}) \in \mathcal{M}_{x_1} \times \mathcal{M}_{x_1}$ at the points $\tilde{\xi}^{x_1} \in \tilde{\mathcal{G}}_{x_1}$. Thus we evaluate \mathbf{U}^{N_t} at the points of $\tilde{\mathcal{G}}_r$ in (2.124) and then we approximate $\|\mathbf{u}^{N_t} - \mathbf{U}^{N_t}\|_{L^2(\Omega)}$ by $\|\mathbf{u}^{N_t} - \mathbf{U}^{N_t}\|_{\tilde{\mathcal{G}}_r}$, where $\|\cdot\|_{\tilde{\mathcal{G}}_r}$ is defined by (2.10) and (2.7) with $r-1$, ω_k , ω_l , $\xi_{i,k}^{x_1}$, $\xi_{j,l}^{x_2}$ replaced by $r+1$, $\tilde{\omega}_k$, $\tilde{\omega}_l$, $\tilde{\xi}_{i,k}^{x_1}$, $\tilde{\xi}_{j,l}^{x_2}$,

respectively. The maximum and H^1 norm errors are computed in a similar manner.

To test our method, we use $\mu = 1/100$ and

$$\Omega = [0, 1] \times [0, 1], \quad T_0 = 0, \quad T_1 = 1,$$

in (2.1) and choose \mathbf{g} in (2.2) and \mathbf{d} in (2.3) so that

$$u_1(x_1, x_2, t) = \frac{3}{4} - \frac{1}{4(1 + e^{\mu^{-1}(-t-4x_1+4x_2)/32})}, \quad (2.125)$$

$$u_2(x_1, x_2, t) = \frac{3}{4} + \frac{1}{4(1 + e^{\mu^{-1}(-t-4x_1+4x_2)/32})}, \quad (2.126)$$

(see [36]) is the exact solution of (2.1)–(2.3). For $r = 3, 4, 5, 6$, the error at the final time T_1 is computed in three ways. First, using uniform 500×500 partition of Ω , we compute the maximum norm error

$$\|\mathbf{u}(\cdot, T_1) - \mathbf{U}^{N_t}\|_{C(\Omega)}.$$

Then we computed the errors in the L^2 and H^1 norms,

$$\|\mathbf{u}(\cdot, T_1) - \mathbf{U}^{N_t}\|_{L^2(\Omega)}, \quad \|\mathbf{u}(\cdot, T_1) - \mathbf{U}^{N_t}\|_{H^1(\Omega)},$$

respectively.

Since we expect the L^2 and maximum norm errors in space to be of order $r + 1$, we compute these errors by selecting $N_t = N^{(r+1)/2}$ so that

$$O(h^{r+1}) + O(\tau^2) = O(N^{-(r+1)}).$$

The H^1 norm error is computed using $N_t = N^{r/2}$ so that

$$O(h^r) + O(\tau^2) = O(N^{-r}).$$

(Note that the assumption $h^{-2}\tau^3 \leq C$ of Theorem 2.2 is satisfied for these two choices of N and N_t .) When computing the L^2 and maximum norm errors we select $N = 9, 16, 25, 36$ for $r = 3, 4, 5$. For these values of N , we have $N_t = (\sqrt{N})^{r+1} = 3^{r+1}, 4^{r+1}, 5^{r+1}, 6^{r+1}$. However, to avoid reaching machine precision, we select $N = 4, 9, 16, 25$ when $r = 6$. In this case, we have $N_t = 2^{r+1}, 3^{r+1}, 4^{r+1}, 5^{r+1}$. When computing the H^1 norm errors we select $N = 25, 36, 49, 64$ for $r = 3, 4, 5$. Likewise, for $r = 6$, we select $N = 4, 9, 16, 25$. For these

values of N , we have $N_t = (\sqrt{N})^r = 5^r, 6^r, 7^r, 8^r$ and $N_t = 2^r, 3^r, 4^r, 5^r$, respectively. We compute the corresponding convergence rates using the formula

$$\text{rate} = \frac{\log(\epsilon_{N_1}/\epsilon_{N_2})}{\log(N_1/N_2)},$$

where $N_1 < N_2$ are two consecutive values of N . Tables Table 2.1 and Table 2.2 show that error behaves like $N^{-(r+1)}$, as expected, in both the maximum and L^2 norms, respectively. Table 2.1 and Table 2.2 show that error behaves like $N^{-(r+1)}$, as expected, in both the maximum and L^2 norms, respectively. The results of Table 2.3 confirm that the H^1 norm error behaves like N^{-r} .

Table 2.1: Maximum norm error and convergence rates for Burgers' equation using Hermite interpolant.

$r = 3$			$r = 4$		
N	error	rate	N	error	rate
9	4.2628e-02	-	9	3.4867e-03	-
16	5.0353e-03	3.7125	16	2.1036e-04	4.8802
25	9.1549e-04	3.8199	25	2.0527e-05	5.2143
36	2.1669e-04	3.9518	36	2.9801e-06	5.2923
$r = 5$			$r = 6$		
N	error	rate	N	error	rate
9	3.0273e-04	-	4	4.5251e-03	-
16	8.5086e-06	6.2078	9	2.6486e-05	6.3394
25	5.1540e-07	6.2827	16	3.7297e-07	7.4090
36	5.2296e-08	6.2747	25	1.6731e-08	6.9557

The convergence analysis of section 4 relies on the use of the Hermite interpolant for boundary conditions (2.39) and the initial condition (2.40). The use of the Hermite interpolant greatly simplifies the convergence proof, but complicates the implementation of the overall scheme. As an alternative, we show, via numerical experiments, that one may use the Gauss interpolant in place of the Hermite interpolant and still obtain the expected optimal convergence rates. Specifically, in place of (2.39) and (2.46), for $n = 1, \dots, N_t$, we use

$$\mathbf{U}^n(a, \xi^{x_2}) = \mathbf{d}(a, \xi^{x_2}, t^n), \quad \xi^{x_2} \in \mathcal{G}_{x_2} \cup \{0, 1\}, \quad a = 0, 1,$$

Table 2.2: L^2 norm error and convergence rates for Burgers' equation using Hermite interpolant.

$r = 3$			$r = 4$		
N	error	rate	N	error	rate
9	1.1269e-04	-	9	8.4772e-06	-
16	1.3207e-05	3.7261	16	4.7237e-07	5.0184
25	2.0179e-06	4.2097	25	5.2324e-08	4.9302
36	4.3623e-07	4.2003	36	8.4863e-09	4.9884
$r = 5$			$r = 6$		
N	error	rate	N	error	rate
9	6.8741e-07	-	4	1.3340e-05	-
16	2.2931e-08	5.9100	9	6.5934e-08	6.5479
25	1.5932e-09	5.9754	16	1.2307e-09	6.9192
36	1.7992e-10	5.9812	25	5.4877e-11	6.9691

$$\mathbf{U}^n(\xi^{x_1}, b) = \mathbf{d}(\xi^{x_1}, b, t^n), \quad \xi^{x_1} \in \mathcal{G}_{x_1} \cup \{0, 1\}, \quad b = 0, 1.$$

Then, in place of (2.40), for each $\xi^{x_1} \in \mathcal{G}_{x_1}$, we compute $\mathbf{U}^0(\xi^{x_1}, \cdot) \in \mathcal{M}_{x_2} \times \mathcal{M}_{x_2}$ (on the vertical line $\xi^{x_1} \times [0, 1]$) such that

$$\mathbf{U}^0(\xi^{x_1}, \xi^{x_2}) = \mathbf{g}(\xi^{x_1}, \xi^{x_2}), \quad \xi^{x_2} \in \mathcal{G}_{x_2} \cup \{0, 1\}.$$

The replacement of the Hermite interpolant in (2.39) and (2.40) with the Gauss interpolant is not consistent with the current theoretical results, but such considerations are beyond the scope of this dissertation. Instead, we offer numerical evidence to demonstrate that the use of the Gauss interpolant for initial and boundary conditions in the ADI-ECN-OSC scheme for Burgers' equations preserves the expected convergence rates. To that end, we repeat our numerical experiments using the Gauss interpolant in place of the Hermite interpolant. The results corresponding to Table 2.1, Table 2.2, and Table 2.3 are given in Table 2.4, Table 2.5, and Table 2.6, respectively. It is clear from these results that the expected convergence rates are obtained and that, in fact, the errors and rates do not differ that much.

Table 2.3: H^1 norm error and convergence rates for Burgers' equation using Hermite interpolant.

$r = 3$			$r = 4$		
N	error	rate	N	error	rate
25	2.2810e-04	-	25	9.2523e-06	-
36	7.3572e-05	3.1030	36	2.1468e-06	4.0064
49	2.8596e-05	3.0652	49	6.2531e-07	4.0090
64	1.2715e-05	3.0348	64	2.1532e-07	3.9920
$r = 5$			$r = 6$		
N	error	rate	N	error	rate
25	4.0977e-07	-	4	9.3322e-04	-
36	6.5956e-08	5.0093	9	8.2221e-06	5.8350
49	1.4147e-08	4.9935	16	2.5892e-07	6.0102
64	3.7404e-09	4.9812	25	1.7768e-08	6.0031

Table 2.4: Maximum norm error and convergence rates for Burgers' equation using Gauss interpolant.

$r = 3$			$r = 4$		
N	error	rate	N	error	rate
9	4.1922e-02	-	9	3.3292e-03	-
16	4.6146e-03	3.8351	16	2.0198e-04	4.8705
25	7.0427e-04	4.2121	25	2.0021e-05	5.1792
36	1.5662e-04	4.1227	36	2.9219e-06	5.2780
$r = 5$			$r = 6$		
N	error	rate	N	error	rate
9	2.9456e-04	-	4	4.5012e-03	-
16	8.3935e-06	6.1840	9	2.6246e-05	6.3440
25	5.0427e-07	6.3011	16	3.7296e-07	7.3932
36	5.2303e-08	6.2145	25	1.6733e-08	6.9553

Table 2.5: L^2 norm error and convergence rates for Burgers' equation using Gauss interpolant.

$r = 3$			$r = 4$		
N	error	rate	N	error	rate
9	1.0898e-04	-	9	8.3547e-06	-
16	1.2604e-05	3.7492	16	4.6862e-07	5.0069
25	1.8956e-06	4.2450	25	5.2162e-08	4.9193
36	4.0455e-07	4.2356	36	8.4740e-09	4.9839
$r = 5$			$r = 6$		
N	error	rate	N	error	rate
9	6.8334e-07	-	4	1.3310e-05	-
16	2.2926e-08	5.9001	9	6.5921e-08	6.5454
25	1.5924e-09	5.9761	16	1.2303e-09	6.9194
36	1.7983e-10	5.9811	25	5.4871e-11	6.9687

Table 2.6: H^1 norm error and convergence rates for Burgers' equation using Gauss interpolant.

$r = 3$			$r = 4$		
N	error	rate	N	error	rate
25	2.2650e-04	-	25	9.2424e-06	-
36	7.3234e-05	3.0964	36	2.1456e-06	4.0050
49	2.8518e-05	3.0591	49	6.2507e-07	4.0003
64	1.2698e-05	3.0295	64	2.1526e-07	3.9916
$r = 5$			$r = 6$		
N	error	rate	N	error	rate
25	4.0961e-07	-	4	9.2525e-04	-
36	6.5933e-08	5.0092	9	8.2203e-06	5.8247
49	1.4143e-08	4.9933	16	2.5886e-07	6.0103
64	3.7396e-09	4.9810	25	1.7767e-08	6.0027

CHAPTER 3

THE ORTHOGONAL SPLINE COLLOCATION SOLUTION TO POISSON'S EQUATION WITH NEUMANN BOUNDARY CONDITIONS

In this chapter we consider the Neumann boundary value problem consisting of Poisson's equation

$$-\Delta u = f(x_1, x_2), \quad (x_1, x_2) \in \Omega = (0, 1) \times (0, 1), \quad (3.1)$$

where $\Delta \equiv \partial^2/\partial x_1^2 + \partial^2/\partial x_2^2$, and the nonhomogeneous Neumann boundary condition

$$\frac{\partial u}{\partial \mathbf{n}} = g(x_1, x_2), \quad (x_1, x_2) \in \partial\Omega, \quad (3.2)$$

where $\partial\Omega$ denotes the boundary of Ω , \mathbf{n} is the outward unit normal vector on $\partial\Omega$ and $\frac{\partial}{\partial \mathbf{n}} = \mathbf{n} \cdot \nabla$. Note that, for the choice of $\Omega = (0, 1) \times (0, 1)$, the normal vector \mathbf{n} is well defined on $\partial\Omega$ except at the corners. To that end, we set $\mathbf{n} = \begin{bmatrix} 0 \\ 1 \end{bmatrix}$ at the corners $(1, 0)$ and

$(1, 1)$, and $\mathbf{n} = \begin{bmatrix} 0 \\ -1 \end{bmatrix}$ at the points $(0, 0)$ and $(0, 1)$. Throughout it is assumed that

$$\int_{\Omega} f = - \int_0^1 [g(1, x_2) + g(0, x_2)] dx_2 - \int_0^1 [g(x_1, 1) + g(x_1, 0)] dx_1 \quad (3.3)$$

which is a necessary condition for the existence of the sufficiently smooth solution u on $\bar{\Omega}$ satisfying (3.1)–(3.2). (3.3) is derived by integrating (3.1) and (3.2) when using integration by parts in the x_1 and x_2 directions.

The numerical solution to Poisson's equation with Neumann boundary conditions is of great importance to computational fluid dynamics. For example, methods based on the pressure Poisson reformulation for the solution of the Navier-Stokes equation rely on solving a Poisson equation for the pressure term satisfying nonhomogeneous Neumann boundary conditions at each time step [9]. Orthogonal spline collocation (OSC) methods for the solution to Neumann Poisson problems using a matrix decomposition algorithm (MDA) are

described in [37] and [38]. However, the convergence analysis in [38] only applies to the special choice of piecewise Hermite cubic basis functions, and, while the method presented in [37] uses B-spline basis functions of arbitrary order, no convergence analysis is given. The present chapter gives an H^1 semi-norm convergence analysis of the OSC solution to Poisson's equation using a matrix decomposition algorithm and B-splines of degree $r \geq 3$.

The chapter is outlined as follows. Section 3.1 gives some preliminary results used in the convergence analysis and section 3.2 introduces an orthogonal spline collocation method for solving singular Neumann collocation problems. Error bounds for the method are derived in section 3.4 and a description of the matrix decomposition algorithm is given in section 3.4. Finally, numerical results are shown in section 3.5.

3.1 Preliminaries

In what follows, $\delta_{x_1} = \{x_1^{(i)}\}_{i=0}^{N_{x_1}}$ and $\delta_{x_2} = \{x_2^{(j)}\}_{j=0}^{N_{x_2}}$ are partitions of $[0, 1]$, such that,

$$0 = x_1^{(0)} < x_1^{(1)} < \dots < x_1^{(N_{x_1})} = 1, \quad 0 = x_2^{(0)} < x_2^{(1)} < \dots < x_2^{(N_{x_2})} = 1.$$

We define $\delta = \delta_{x_1} \times \delta_{x_2}$, and introduce $h_i^{x_1} = x_1^{(i)} - x_1^{(i-1)}$, $i = 1, \dots, N_{x_1}$ and $h_j^{x_2} = x_2^{(j)} - x_2^{(j-1)}$, $j = 1, \dots, N_{x_2}$. We set

$$h_{x_1} = \max_{i=1, \dots, N_{x_1}} h_i^{x_1}, \quad h_{x_2} = \max_{j=1, \dots, N_{x_2}} h_j^{x_2}, \quad h = \max(h_{x_1}, h_{x_2}).$$

Let \mathcal{M}_{x_1} and \mathcal{M}_{x_2} be the spaces of C^1 splines of degree $\leq r$ with the breaks at the $x_1^{(i)}$ and $x_2^{(j)}$, respectively, that is,

$$\mathcal{M}_{x_1} = \{v \in C^1[0, 1] : v|_{[x_1^{(i-1)}, x_1^{(i)}]} \in P_r, i = 1, \dots, N_{x_1}\},$$

$$\mathcal{M}_{x_2} = \{v \in C^1[0, 1] : v|_{[x_2^{(j-1)}, x_2^{(j)}]} \in P_r, j = 1, \dots, N_{x_2}\},$$

where P_r is the set of polynomials of degree $\leq r$. Note that $\dim \mathcal{M}_{x_i} = (r - 1)N_{x_i} + 2$, $i = 1, 2$.

Additionally, we introduce

$$\mathcal{M}_{x_1}^{\mathcal{N}} = \{v \in \mathcal{M}_{x_1} : v'(0) = v'(1) = 0\}, \quad \mathcal{M}_{x_2}^{\mathcal{N}} = \{v \in \mathcal{M}_{x_2} : v'(0) = v'(1) = 0\}.$$

Let $\mathcal{M}_r = \mathcal{M}_{x_1} \otimes \mathcal{M}_{x_2}$, $\mathcal{M}_r^{\mathcal{N}} = \mathcal{M}_{x_1}^{\mathcal{N}} \otimes \mathcal{M}_{x_2}^{\mathcal{N}}$.

Let $\{\xi_k\}_{k=1}^{r-1}$ be the nodes of the $(r-1)$ -point Gauss-Legendre quadrature for $(0, 1)$, and let $\mathcal{G}_{x_1} = \{\xi_{i,k}^{x_1}\}_{i=1,k=1}^{N_{x_1}, r-1}$, $\mathcal{G}_{x_2} = \{\xi_{j,l}^{x_2}\}_{j=1,l=1}^{N_{x_2}, r-1}$ where

$$\xi_{i,k}^{x_1} = x_1^{(i-1)} + h_i^{x_1} \xi_k, \quad \xi_{j,l}^{x_2} = x_2^{(j-1)} + h_j^{x_2} \xi_l. \quad (3.4)$$

Then the set of collocation points in Ω is given by

$$\mathcal{G}_r = \{\xi = (\xi^{x_1}, \xi^{x_2}) : \xi^{x_1} \in \mathcal{G}_{x_1}, \xi^{x_2} \in \mathcal{G}_{x_2}\}.$$

For v and z defined on \mathcal{G}_r , the inner product $\langle v, z \rangle_{\mathcal{G}_r}$ and norm $\|v\|_{\mathcal{G}_r}$ are defined by

$$\langle v, z \rangle_{\mathcal{G}_r} = \sum_{i=1}^{N_{x_1}} \sum_{j=1}^{N_{x_2}} h_i^{x_1} h_j^{x_2} \sum_{k=1}^{r-1} \sum_{l=1}^{r-1} \omega_k \omega_l (vz)(\xi_{i,k}, \xi_{j,l}), \quad \|v\|_{\mathcal{G}_r} = \sqrt{\langle v, v \rangle_{\mathcal{G}_r}}, \quad (3.5)$$

and we define

$$\langle v, z \rangle_{x_1} = \sum_{i=1}^{N_{x_1}} h_i^{x_1} \sum_{k=1}^{r-1} \omega_k v(\xi_{i,k}^{x_1}) z(\xi_{i,k}^{x_1}), \quad \langle v, z \rangle_{x_2} = \sum_{j=1}^{N_{x_2}} h_j^{x_2} \sum_{l=1}^{r-1} \omega_l v(\xi_{j,l}^{x_2}) z(\xi_{j,l}^{x_2}).$$

We introduce,

$$\|\nabla v\|_{L^2(\Omega)} = \left(\int_{\Omega} v_{x_1}^2 + \int_{\Omega} v_{x_2}^2 \right)^{1/2}, \quad \|v\|_{C(\bar{\Omega})} = \max_{x \in \bar{\Omega}} |v(x)|.$$

For $i = 1, 2$, we will make use of $\{\sigma_j^{x_i}\}_{j=0}^{(r-1)N_{x_i}+1}$ where

$$\sigma_{(l-1)(r-1)+k}^{x_i} = \xi_{i,k}^{x_i}, \quad l = 1, \dots, N_{x_i}, \quad k = 1, \dots, r-1, \quad (3.6)$$

with

$$\sigma_0^{x_i} = 0, \quad \sigma_{(r-1)N_{x_i}+1}^{x_i} = 1. \quad (3.7)$$

Throughout this chapter, we assume that the exact solution u of (3.1)–(3.2) is sufficiently smooth. In what follows, C denotes a generic positive constant, dependent possibly on r , but independent of u and h . We also use $C(u)$ to denote a generic positive constant, dependent possibly on u and r , but independent of h . Any specific $C(u)$ is denoted by $C_i(u)$.

Lemma 3.1. *We have,*

$$\|\nabla v\|_{L^2(\Omega)}^2 \leq C \langle -\Delta v, v \rangle_{\mathcal{G}_r}, \quad v \in \mathcal{M}_r^{\mathcal{N}}.$$

Proof. It follows from Lemma 3.1 in [23] that

$$-\langle p'', p \rangle_{x_i} \geq \int_0^1 (p')^2(x_i) dx_i, \quad p \in \mathcal{M}_{x_i}^N, \quad (3.8)$$

and modifying the proof of Theorem 5.5 in [22], we can show that

$$\langle p, p \rangle_{x_i} \geq C \int_0^1 p^2(x_i) dx_i, \quad p \in \mathcal{M}_{x_i}^N. \quad (3.9)$$

Assume $v \in \mathcal{M}_r^N$. Using (3.5), (3.8), and (3.9), we have

$$\begin{aligned} \langle -v_{x_1 x_1}, v \rangle_{\mathcal{G}_r} &= \sum_{i=1}^{N_{x_1}} \sum_{j=1}^{N_{x_2}} h_i^{x_1} h_j^{x_2} \sum_{k=1}^{r-1} \sum_{l=1}^{r-1} \omega_k \omega_l (-v_{x_1 x_1} v)(\xi_{i,k}, \xi_{j,l}) \\ &= \sum_{j=1}^{N_{x_2}} h_j^{x_2} \sum_{l=1}^{r-1} \omega_l \langle -v_{x_1 x_1}(\cdot, \xi_{j,l}), v(\cdot, \xi_{j,l}) \rangle_{x_1} \\ &\geq \int_0^1 \sum_{j=1}^{N_{x_2}} h_j^{x_2} \sum_{l=1}^{r-1} \omega_l v_{x_1}^2(x_1, \xi_{j,l}) dx_1 \\ &= \int_0^1 \langle v_{x_1}(x_1, \cdot), v_{x_1}(x_1, \cdot) \rangle_{x_2} dx_1 \\ &\geq \int_0^1 \int_0^1 v_{x_1}^2(x_1, x_2) dx_2 dx_1 \end{aligned}$$

In a similar way, using (3.5) and (3.8), we have

$$\langle -v_{x_2 x_2}, v \rangle_{\mathcal{G}_r} \geq \int_0^1 \int_0^1 v_{x_2}^2(x_1, x_2) dx_1 dx_2$$

It follows from the last two unnumbered equations that

$$\langle -\Delta v, v \rangle_{\mathcal{G}_r} = \sum_{i=1}^2 \langle -v_{x_i x_i}, v \rangle_{\mathcal{G}_r} \geq \int_0^1 \int_0^1 v_{x_1}^2(x_1, x_2) dx_2 dx_1 + \int_0^1 \int_0^1 v_{x_2}^2(x_1, x_2) dx_1 dx_2$$

which completes the proof of the lemma. \square

Lemma 3.2. *We have,*

$$\langle -\Delta v, z \rangle_{\mathcal{G}_r} = \langle v, -\Delta z \rangle_{\mathcal{G}_r}, \quad v, z \in \mathcal{M}_r^N. \quad (3.10)$$

Proof. Equation (3.10) follows directly from Lemma 3.1 in [23]. \square

The following lemma is the OSC analog of the Poincaré inequality.

Lemma 3.3. *We have*

$$\langle -\Delta v, v \rangle_{\mathcal{G}_r} \geq \|v\|_{\mathcal{G}_r}^2 - \langle v, 1 \rangle_{\mathcal{G}_r}^2, \quad v \in \mathcal{M}_r^N.$$

Proof. For $x_1 = \xi_{i,k}^{x_1}$, $x_2 = \xi_{j,l}^{x_2}$, $y_1, y_2 \in [0, 1]$, we have

$$\begin{aligned} v^2(x_1, x_2) + v^2(y_1, y_2) - 2v(x_1, x_2)v(y_1, y_2) &= [v(x_1, x_2) - v(y_1, y_2)]^2 \\ &= \left[\int_{y_1}^{x_1} v_{x_1}(s_1, x_2) ds_1 + \int_{y_2}^{x_2} v_{x_2}(y_1, s_2) ds_2 \right]^2 \\ &\leq \left[\left| \int_{y_1}^{x_1} v_{x_1}(s_1, x_2) ds_1 \right| + \left| \int_{y_2}^{x_2} v_{x_2}(y_1, s_2) ds_2 \right| \right]^2 \\ &\leq 2 \left(\int_{y_1}^{x_1} v_{x_1}(s_1, x_2) ds_1 \right)^2 + 2 \left(\int_{y_2}^{x_2} v_{x_2}(y_1, s_2) ds_2 \right)^2 \\ &\leq 2|x_1 - y_1| \int_0^1 v_{x_1}^2(s_1, x_2) ds_1 + 2|x_2 - y_2| \int_0^1 v_{x_2}^2(y_1, s_2) ds_2. \end{aligned}$$

Multiplying by $h_i^{x_1} \omega_k h_j^{x_2} \omega_l$ and summing over i, k, j, l and using

$$\sum_{i=1}^{N_{x_1}} h_i^{x_1} \sum_{k=1}^{r-1} \omega_k = 1, \quad \sum_{j=1}^{N_{x_2}} h_j^{x_2} \sum_{l=1}^{r-1} \omega_l = 1, \quad (3.11)$$

we obtain

$$\begin{aligned} &\|v\|_{\mathcal{G}_r}^2 + v^2(y_1, y_2) - 2v(y_1, y_2)\langle v, 1 \rangle_{\mathcal{G}_r} \\ &\leq 2 \sum_{i=1}^{N_{x_1}} h_i^{x_1} \sum_{k=1}^{r-1} \omega_k |\xi_{i,k}^{x_1} - y_1| \sum_{j=1}^{N_{x_2}} h_j^{x_2} \sum_{l=1}^{r-1} \omega_l \int_0^1 v_{x_1}^2(s_1, \xi_{j,l}^{x_2}) ds_1 \\ &\quad + 2 \sum_{j=1}^{N_{x_2}} h_j^{x_2} \sum_{l=1}^{r-1} \omega_l |\xi_{j,l}^{x_2} - y_2| \int_0^1 v_{x_2}^2(y_1, s_2) ds_2. \end{aligned}$$

Using $|\xi_{i,k}^{x_1} - y_1| \leq 1$, $|\xi_{j,l}^{x_2} - y_2| \leq 1$, and (3.11), we get

$$\sum_{i=1}^{N_{x_1}} h_i^{x_1} \sum_{k=1}^{r-1} \omega_k |\xi_{i,k}^{x_1} - y_1| \leq 1, \quad \sum_{j=1}^{N_{x_2}} h_j^{x_2} \sum_{l=1}^{r-1} \omega_l |\xi_{j,l}^{x_2} - y_2| \leq 1.$$

The last two unnumbered equations and (3.8) yield

$$\|v\|_{\mathcal{G}_r}^2 + v^2(y_1, y_2) - 2v(y_1, y_2)\langle v, 1 \rangle_{\mathcal{G}_r} \leq 2\langle -v_{x_1 x_1}, v \rangle_{\mathcal{G}_r} + 2 \int_0^1 v_{x_2}^2(y_1, s_2) ds_2.$$

Taking $y_1 = \xi_{i,k}^{x_1}$, $y_2 = \xi_{j,l}^{x_2}$, multiplying by $h_i^{x_1} \omega_k h_j^{x_2} \omega_l$ summing over i, k, j, l , using (3.11) and (3.8), we obtain

$$2\|v\|_{\mathcal{G}_r}^2 - 2\langle v, 1 \rangle_{\mathcal{G}_r}^2 \leq 2\langle -v_{x_1 x_1}, v \rangle_{\mathcal{G}_r} + 2 \sum_{i=1}^{N_{x_1}} h_i^{x_1} \sum_{k=1}^{r-1} \omega_k \int_0^1 v_{x_2}^2(\xi_{i,k}, s_2) ds_2 \leq 2\langle -\Delta v, v \rangle_{\mathcal{G}_r},$$

which yields the required result. \square

This final lemma will be helpful in determining the matrix-vector form of discrete OSC problems.

Lemma 3.4. *The matrix-vector form of*

$$\phi_{i,j} = \sum_{m=1}^{M'} c_{i,m}^{(1)} \sum_{n=1}^{N'} c_{j,n}^{(2)} \psi_{m,n}, \quad i = 1, \dots, I', \quad j = 1, \dots, J',$$

is

$$\Phi = (C_1 \otimes C_2) \Psi,$$

where \otimes denotes the matrix tensor product,

$$C_1 = [c_{i,m}^{(1)}]_{i=1, m=1}^{I', M'}, \quad C_2 = [c_{j,n}^{(2)}]_{j=1, n=1}^{J', N'},$$

and

$$\Phi = [\phi_{1,1}, \dots, \phi_{1,J'}, \dots, \phi_{I',1}, \dots, \phi_{I',J'}], \quad \Psi = [\psi_{1,1}, \dots, \psi_{1,N'}, \dots, \psi_{M',1}, \dots, \psi_{M',N'}].$$

3.2 Neumann OSC Boundary Value Problems

3.2.1 Homogeneous Problems

Consider (3.1)–(3.2) with $g = 0$. Then the orthogonal spline collocation solution $U \in \mathcal{M}_r^{\mathcal{N}}$ is defined by

$$-\Delta U(\xi) = f(\xi), \quad \xi \in \mathcal{G}_r. \quad (3.12)$$

Note that (3.12) may not have a solution in the classical sense. Since the operator $-\Delta$ is self-adjoint on $\mathcal{M}_r^{\mathcal{N}}$ with respect to $\langle \cdot, \cdot \rangle_{\mathcal{G}_r}$ and since $-\Delta 1 = 0$, $\langle f, 1 \rangle_{\mathcal{G}_r} = 0$, the discrete analog of (3.3) for $g = 0$, is a necessary and sufficient condition for the existence of the solution of (3.12).

Given that (3.12) may not have a classical solution, we introduce

$$f^* = f - \langle f, 1 \rangle_{\mathcal{G}_r}. \quad (3.13)$$

and seek a solution $U \in \mathcal{M}_r^{\mathcal{N}}$ of

$$-\Delta U(\xi) = f^*(\xi), \quad \xi \in \mathcal{G}_r. \quad (3.14)$$

Since $\langle f^*, 1 \rangle_{\mathcal{G}_r} = 0$, (since $\langle 1, 1 \rangle_{\mathcal{G}_r} = 1$) it follows that (3.14) has a solution $U \in \mathcal{M}_r^{\mathcal{N}}$.

We now describe an appropriate choice of B-spline basis functions for $\mathcal{M}_{x_1}^{\mathcal{N}}$ and $\mathcal{M}_{x_2}^{\mathcal{N}}$. For $i = 1, 2$, let $\{B_j^{x_i}\}_{j=0}^{(r-1)N_{x_i}+1}$ be B-spline basis functions for \mathcal{M}_{x_i} . Recall that

$$B_0^{x_i}(0) \neq 0, \quad [B_0^{x_i}]'(0) \neq 0, \quad B_1^{x_i}(0) = 0, \quad [B_1^{x_i}]'(0) \neq 0,$$

$$B_j^{x_i}(0) = [B_j^{x_i}]'(0) = B_j^{x_i}(1) = [B_j^{x_i}]'(1) = 0, \quad j = 2, \dots, (r-1)N_{x_i} - 1,$$

$$B_{(r-1)N_{x_i}}^{x_i}(1) = 0, \quad [B_{(r-1)N_{x_i}}^{x_i}]'(1) \neq 0, \quad B_{(r-1)N_{x_i}+1}^{x_i}(1) \neq 0, \quad [B_{(r-1)N_{x_i}+1}^{x_i}]'(1) \neq 0.$$

We set

$$\phi_1^{x_i} = [B_1^{x_i}]'(0)B_0^{x_i} - [B_0^{x_i}]'(0)B_1^{x_i}, \quad (3.15)$$

$$\phi_j^{x_i} = B_j^{x_i}, \quad j = 2, \dots, (r-1)N_{x_i} - 1, \quad (3.16)$$

$$\phi_{(r-1)N_{x_i}}^{x_i} = \left[B_{(r-1)N_{x_i}}^{x_i} \right]'(1)B_{(r-1)N_{x_i}+1}^{x_i} - \left[B_{(r-1)N_{x_i}+1}^{x_i} \right]'(1)B_{(r-1)N_{x_i}}^{x_i}. \quad (3.17)$$

Then $[\phi_1^{x_i}]'(0) = 0$, $[\phi_{(r-1)N_{x_i}}^{x_i}]'(1) = 0$ and hence $\{\phi_j^{x_i}\}_{j=1}^{(r-1)N_{x_i}}$ is a basis for $\mathcal{M}_{x_i}^{\mathcal{N}}$.

Then we can write

$$U(x_1, x_2) = \sum_{m=1}^{(r-1)N_{x_1}} \sum_{n=1}^{(r-1)N_{x_2}} U_{m,n} \phi_m^{x_1}(x_1) \phi_n^{x_2}(x_2). \quad (3.18)$$

Substituting (3.18) into (3.14) we obtain,

$$\sum_{m=1}^{(r-1)N_{x_1}} \sum_{n=1}^{(r-1)N_{x_2}} U_{m,n} \left[-[\phi_m^{x_1}]''(\sigma_i^{x_1}) \phi_n^{x_2}(\sigma_j^{x_2}) - \phi_m^{x_1}(\sigma_i^{x_1}) [\phi_n^{x_2}]''(\sigma_j^{x_2}) \right] = f^*(\sigma_i^{x_1}, \sigma_j^{x_2})$$

where $i = 1, \dots, (r-1)N_{x_1}$ and $j = 1, \dots, (r-1)N_{x_2}$. Using Lemma 3.4, the corresponding matrix-vector form of (3.14)

$$(A_{x_1} \otimes B_{x_2} + B_{x_1} \otimes A_{x_2}) \mathbf{u} = \mathbf{f}^*, \quad (3.19)$$

where,

$$\mathbf{u} = [U_{1,1}, \dots, U_{1,(r-1)N_{x_2}}, \dots, U_{(r-1)N_{x_1},1}, \dots, U_{(r-1)N_{x_1},(r-1)N_{x_2}}]^T,$$

$$\mathbf{f}^* = [f_{1,1}^*, \dots, f_{1,(r-1)N_{x_2}}^*, \dots, f_{(r-1)N_{x_1},1}^*, \dots, f_{(r-1)N_{x_1},(r-1)N_{x_2}}^*]^T,$$

with $f_{i,j}^* = f^*(\sigma_i^{x_1}, \sigma_j^{x_2})$ and where

$$A_{x_1} = [-\phi_m^{x_1}]''(\sigma_i^{x_1})_{m,i=1}^{(r-1)N_{x_1}}, \quad B_{x_1} = [\phi_m^{x_1}(\sigma_i^{x_1})]_{m,i=1}^{(r-1)N_{x_1}},$$

$$A_{x_2} = [-\phi_j^{x_2}]''(\sigma_n^{x_2})_{j,n=1}^{(r-1)N_{x_2}}, \quad B_{x_2} = [\phi_j^{x_2}(\sigma_n^{x_2})]_{j,n=1}^{(r-1)N_{x_2}}.$$

3.2.2 Nonhomogeneous Problems

We consider a problem with nonhomogeneous Neumann boundary conditions (3.1)–(3.2).

Recall that we set $\mathbf{n} = \begin{bmatrix} 0 \\ 1 \end{bmatrix}$ at $(0, 1), (1, 1)$ and $\mathbf{n} = \begin{bmatrix} 0 \\ -1 \end{bmatrix}$ at $(0, 0), (1, 0)$. Hence, writing (3.2) as

$$u_{x_2}(x_1, 0) = -g(x_1, 0), \quad u_{x_2}(x_1, 1) = g(x_1, 1), \quad x_1 \in [0, 1], \quad (3.20)$$

$$u_{x_1}(0, x_2) = -g(0, x_2), \quad u_{x_1}(1, x_2) = g(0, x_2), \quad x_2 \in (0, 1), \quad (3.21)$$

will be helpful in determining the OSC approximate solution $U \in \mathcal{M}_r$ for which we have

$$U(x_1, x_2) = \sum_{m=0}^{(r-1)N_{x_1+1}} \sum_{n=0}^{(r-1)N_{x_2+1}} U_{n,m} \phi_m^{x_1}(x_1) \phi_n^{x_2}(x_2), \quad (3.22)$$

where $\{\phi_n^{x_i}\}_{n=1}^{(r-1)N_{x_i}}$ are defined in (3.15), (3.17), (3.16) and

$$\phi_0^{x_i} = B_0^{x_i}, \quad \phi_{(r-1)N_{x_i}+1}^{x_i} = B_{(r-1)N_{x_i}+1}^{x_i}.$$

The $\{U_{m,n}\}_{m=0}^{(r-1)N_{x_1}+1}$, $n = 0, (r-1)N_{x_2} + 1$, in (3.22) are determined using (cf., (3.20))

$$U_{x_2}(\xi^{x_1}, 0) = -g(\xi^{x_1}, 0), \quad \xi^{x_1} \in \mathcal{G}_{x_1} \cup \{0, 1\},$$

$$U_{x_2}(\xi^{x_1}, 1) = g(\xi^{x_1}, 1), \quad \xi^{x_1} \in \mathcal{G}_{x_1} \cup \{0, 1\}.$$

Note, e.g., that

$$U_{x_2}(0, 0) = [\phi_0^{x_2}]'(0) [\phi_0^{x_1}(0)U_{0,0} + \phi_1^{x_1}(0)U_{1,0}],$$

$$U_{x_2}(\xi^{x_1}, 0) = [\phi_0^{x_2}]'(0) \sum_{m=0}^{(r-1)N_{x_1}+1} \phi_m^{x_1}(\xi^{x_1})U_{m,0}, \quad \xi^{x_1} \in \mathcal{G}_{x_1},$$

$$U_{x_2}(1, 0) = [\phi_0^{x_2}]'(0) \left[\phi_{(r-1)N_{x_1}}^{x_1}(1)U_{(r-1)N_{x_1},0} + \phi_{(r-1)N_{x_1}+1}^{x_1}(1)U_{(r-1)N_{x_1}+1,0} \right].$$

The last three unnumbered equations give rise to a linear system in

$$\mathbf{U}_{\cdot,0} = [U_{0,0}, U_{1,0}, \dots, U_{(r-1)N_{x_1},0}, U_{(r-1)N_{x_1}+1,0}]^T.$$

That is, the entries of $\mathbf{U}_{\cdot,0}$ are obtained by solving

$$B_{x_1}^* \mathbf{U}_{\cdot,0} = \mathbf{g}_{\cdot,0},$$

where

$$B_{x_1}^* = [\phi_j^{x_1}(\sigma_i^{x_1})]_{i,j=0}^{(r-1)N_{x_1}+1}, \quad \mathbf{g}_{\cdot,0} = -[g(\sigma_0^{x_1}, 0), \dots, g(\sigma_{(r-1)N_{x_1}+1}^{x_1}, 0)]^T / [\phi_0^{x_2}]'(0).$$

In a similar way we obtain a linear system in

$$[U_{0,(r-1)N_{x_2}+1}, U_{1,(r-1)N_{x_2}+1}, \dots, U_{(r-1)N_{x_1},(r-1)N_{x_2}+1}, U_{(r-1)N_{x_1}+1,(r-1)N_{x_2}+1}]^T.$$

Since

$$U_{0,0}, \quad U_{0,(r-1)N_{x_2}+1}, \quad U_{(r-1)N_{x_1}+1,0}, \quad U_{(r-1)N_{x_1}+1,(r-1)N_{x_2}+1},$$

are known at this point, the $\{U_{m,n}\}_{n=1}^{(r-1)N_{x_2}}$, $m = 0, (r-1)N_{x_2} + 1$ in (3.22) are determined using (cf., (3.21))

$$U_{x_2}(0, \xi^{x_2}) = -g(0, \xi^{x_2}), \quad \xi^{x_2} \in \mathcal{G}_{x_2},$$

$$U_{x_2}(1, \xi^{x_2}) = g(1, \xi^{x_2}), \quad \xi^{x_2} \in \mathcal{G}_{x_2}.$$

Note that

$$U_{x_1}(0, \xi^{x_2}) = [\phi_0^{x_1}]'(0) \sum_{n=0}^{(r-1)N_{x_2}+1} \phi_n^{x_2}(\xi^{x_2}) U_{0,n}, \quad \xi^{x_2} \in \mathcal{G}_{x_2}.$$

The last unnumbered equation, involving known $U_{0,0}$, $U_{0,(r-1)N_{x_1}+1}$, gives rise to a linear system in

$$[U_{0,1}, \dots, U_{0,(r-1)N_{x_2}}]^T.$$

To avoid moving terms to the right-hand side, this system can be solved by solving a system in

$$\mathbf{U}_{0,\cdot} = [U_{0,0}, U_{0,1}, \dots, U_{0,(r-1)N_{x_2}}, U_{0,(r-1)N_{x_2}+1}]^T,$$

with the first and last equations corresponding to known $U_{0,0}$, $U_{0,(r-1)N_{x_1}+1}$, respectively.

That is, the entries of $\mathbf{U}_{0,\cdot}$ are obtained by solving

$$B_{x_2}^{**} \mathbf{U}_{0,\cdot} = \mathbf{g}_{0,\cdot},$$

where

$$B_{x_2}^{**} = \begin{bmatrix} 1 & 0 & \dots & 0 \\ \overline{B}_{x_2}^{**} \\ 0 & \dots & 0 & 1 \end{bmatrix}, \quad \mathbf{g}_{0,\cdot} = [U_{0,0}, -g(0, \sigma_1^{x_2}), \dots, -g(0, \sigma_{(r-1)N_{x_2}}^{x_2}), U_{0,(r-1)N_{x_2}+1}]^T / [\phi_0^{x_1}]'(0),$$

with the $(r-1)N_{x_2} \times (r-1)N_{x_2} + 2$ matrix $\overline{B}_{x_2}^{**}$ defined by

$$\overline{B}_{x_2}^{**} = [\phi_j^{x_2}(\sigma_i^{x_2})]_{i=1, j=0}^{(r-1)N_{x_2}, (r-1)N_{x_2}+1}.$$

In a similar way we obtain a linear system in

$$[U_{(r-1)N_{x_1}+1,1}, \dots, U_{(r-1)N_{x_1}+1,(r-1)N_{x_2}}]^T.$$

Then

$$U = \bar{U} + \hat{U},$$

where

$$\begin{aligned} \bar{U}(x_1, x_2) &= \sum_{m=1}^{(r-1)N_{x_1}} \sum_{n=1}^{(r-1)N_{x_2}} U_{m,n} \phi_m^{x_1}(x_1) \phi_n^{x_2}(x_2), \\ \hat{U}(x_1, x_2) &= \sum_{m=0}^{(r-1)N_{x_1}+1} \sum_{n=0, (r-1)N_{x_2}+1} U_{m,n} \phi_m^{x_1}(x_1) \phi_n^{x_2}(x_2) \\ &+ \sum_{m=0, (r-1)N_{x_2}+1} \sum_{n=1}^{(r-1)N_{x_2}} U_{m,n} \phi_m^{x_1}(x_1) \phi_n^{x_2}(x_2), \end{aligned}$$

and (3.12) becomes

$$-\Delta \bar{U}(\xi) = f(\xi) + \Delta \hat{U}(\xi), \quad \xi \in \mathcal{G}_r,$$

where $\bar{U} \in \mathcal{M}_r^{\mathcal{N}}$. As in (3.13) let

$$f^{**} = f^* + \Delta \hat{U} - \langle \Delta \hat{U}, 1 \rangle_{\mathcal{G}_r} \quad (3.23)$$

The counterpart of (3.14) is

$$-\Delta \bar{U}(\xi) = f^{**}(\xi), \quad \xi \in \mathcal{G}_r. \quad (3.24)$$

Since $\langle f^{**}, 1 \rangle_{\mathcal{G}_r} = 0$, it follows that (3.24) has a solution $\bar{U} \in \mathcal{M}_r^{\mathcal{N}}$.

Note that for $\xi = (\xi^{x_1}, \xi^{x_2}) \in \mathcal{G}_r$,

$$\begin{aligned} \Delta \hat{U}(\xi^{x_1}, \xi^{x_2}) &= \sum_{m=0}^{(r-1)N_{x_1}+1} [\phi_m^{x_1}]''(\xi^{x_1}) \sum_{n=0, (r-1)N_{x_2}+1} \phi_n^{x_2}(\xi^{x_2}) U_{m,n} \\ &+ \sum_{m=0}^{(r-1)N_{x_1}+1} \phi_m^{x_1}(\xi^{x_1}) \sum_{n=1, (r-1)N_{x_2}+1} [\phi_n^{x_2}]''(\xi^{x_2}) U_{m,n} \\ &+ \sum_{m=0, (r-1)N_{x_1}+1} [\phi_m^{x_1}]''(\xi^{x_1}) \sum_{n=1}^{(r-1)N_{x_2}} \phi_n^{x_2}(\xi^{x_2}) U_{m,n} \\ &+ \sum_{m=0, (r-1)N_{x_1}+1} \phi_m^{x_1}(\xi^{x_1}) \sum_{n=1}^{(r-1)N_{x_2}} [\phi_n^{x_2}]''(\xi^{x_2}) U_{m,n} \end{aligned}$$

which, by Lemma 3.14, can be computed using matrix tensor products.

3.3 Convergence Analysis

In this section we present convergence analysis of the OSC method for the homogeneous Neumann Poisson problem only.

As in [23], for $r > 3$, let $0 < \zeta_1 < \zeta_2 < \dots < \zeta_{r-3} < 1$ be the simple zeros of the polynomial

$$\frac{d^{r-3}}{dt^{r-3}} [t^{r-1} (t-1)^{r-1}]$$

and let

$$\zeta_{i,k}^{x_1} = x_1^{(i-1)} + h_i^{x_1} \zeta_k, \quad i = 1, \dots, N_{x_1}, \quad k = 1, \dots, r-3,$$

$$\zeta_{j,l}^{x_2} = x_2^{(j-1)} + h_j^{x_2} \zeta_l, \quad j = 1, \dots, N_{x_2}, \quad l = 1, \dots, r-3.$$

For u (the solution to (3.1)-(3.20)) sufficiently smooth, let $W \in \mathcal{M}_r$ be the comparison function such that

$$W = T_{r,\delta} u,$$

where $T_{r,\delta} u \in \mathcal{M}_r$ is the piecewise polynomial interpolant of u , that is

$$\begin{aligned} (W - u)(\zeta_{i,k}^{x_1}, \zeta_{j,l}^{x_2}) &= 0, & i = 1, \dots, N_{x_1}, & \quad j = 1, \dots, N_{x_2}, \\ \frac{\partial^n}{\partial x_1^n} (W - u)(x_1^{(i)}, \zeta_{j,l}^{x_2}) &= 0, & i = 0, \dots, N_{x_1}, & \quad j = 1, \dots, N_{x_2}, \\ \frac{\partial^m}{\partial x_2^m} (W - u)(\zeta_{i,k}^{x_1}, x_2^{(j)}) &= 0, & i = 1, \dots, N_{x_1}, & \quad j = 0, \dots, N_{x_2}, \\ \frac{\partial^{n+m}}{\partial x_1^n \partial x_2^m} (W - u)(x_1^{(i)}, x_2^{(j)}) &= 0, & i = 0, \dots, N_{x_1}, & \quad j = 0, \dots, N_{x_2}, \end{aligned} \tag{3.25}$$

where $k, l = 1, \dots, r-3$ and $n, m = 0, 1$.

Lemma 3.5. *For f sufficiently smooth, we have*

$$\left| \sum_{i=1}^{N_{x_1}} \sum_{j=1}^{N_{x_2}} h_i^{x_1} h_j^{x_2} \sum_{k=1}^{r-1} \sum_{l=1}^{r-1} \omega_k \omega_l f(\xi_{i,k}, \xi_{j,l}) \right| \leq Ch^r$$

Proof. This follows from (3.3) with $g = 0$ and the error bounds on the composite Gauss quadrature rule. See, for example, section 7.4 in [39]. \square

Theorem 3.1. *If u , the solution to (3.1)–(3.20), is sufficiently smooth, and $U \in \mathcal{M}_r^N$ is a solution to (3.14) then*

$$\|\nabla(u - U)\|_{L^2(\Omega)} \leq C(u)h^r.$$

Proof. It follows from (2.20) and Lemma 2.5 in [26] that

$$\|\Delta(u - W)\|_{\mathcal{G}_r} \leq Ch^r, \quad (3.26)$$

$$\|\nabla(u - W)\|_{L^2(\Omega)} \leq C(u)h^r. \quad (3.27)$$

We set

$$\nu = W - U - c, \quad c = \langle W - U, 1 \rangle_{\mathcal{G}_r}. \quad (3.28)$$

It follows from (3.25) and (3.21)–(3.20) that

$$W_{x_1}(\alpha, x_2) = 0, \quad \alpha = 0, 1, \quad x_2 \in [0, 1], \quad W_{x_2}(x_1, \beta) = 0, \quad x_1 \in [0, 1], \quad \beta = 0, 1.$$

Hence, $W \in \mathcal{M}_r^N$ by definition of \mathcal{M}_r^N and the last unnumbered equation. Since $U + c \in \mathcal{M}_r^N$, it follows that $\nu \in \mathcal{M}_r^N$. Next, using (3.14), (3.13), (3.1), the Cauchy-Schwarz inequality, (3.26), and Lemma 3.5, we have

$$\begin{aligned} & \langle -\Delta\nu, \nu \rangle_{\mathcal{G}_r} \\ &= \langle -\Delta W + \Delta U, \nu \rangle_{\mathcal{G}_r} = \langle -\Delta W - f + \langle f, 1 \rangle_{\mathcal{G}_r}, \nu \rangle_{\mathcal{G}_r} \\ &= \langle \Delta(u - W), \nu \rangle_{\mathcal{G}_r} + \langle f, 1 \rangle_{\mathcal{G}_r} \langle 1, \nu \rangle_{\mathcal{G}_r} \\ &\leq Ch^r \|\nu\|_{\mathcal{G}_r} \end{aligned} \quad (3.29)$$

It follows from (3.28) that

$$\langle \nu, 1 \rangle_{\mathcal{G}_r} = \langle W - U, 1 \rangle_{\mathcal{G}_r} - c \langle 1, 1 \rangle_{\mathcal{G}_r} = c - c = 0.$$

Hence Lemma 3.3 implies

$$\|\nu\|_{\mathcal{G}_r} \leq \langle -\Delta\nu, \nu \rangle_{\mathcal{G}_r}^{1/2}. \quad (3.30)$$

It follows from (3.29), (3.30), and Lemma 3.1 that

$$\|\nabla\nu\|_{L^2(\Omega)} \leq C(u)h^r.$$

Since $\nabla(u - U) = \nabla(u - W) + \nabla\nu$, the desired result follows from the triangle inequality, (3.27) and the last unnumbered equation. □

3.4 An OSC Matrix Decomposition Algorithm

We present an efficient method for solving (3.19).

Let the diagonal matrices W_1 and W_2 be defined by

$$\begin{aligned} W_1 &= \text{diag} \left(h_1^{x_1} \omega_1, \dots, h_1^{x_1} \omega_{r-1}, \dots, h_{N_{x_1}}^{x_1} \omega_1, \dots, h_{N_{x_1}}^{x_1} \omega_{r-1} \right), \\ W_2 &= \text{diag} \left(h_1^{x_2} \omega_1, \dots, h_1^{x_2} \omega_{r-1}, \dots, h_{N_{x_2}}^{x_2} \omega_1, \dots, h_{N_{x_2}}^{x_2} \omega_{r-1} \right), \end{aligned}$$

Additionally, we introduce

$$F_1 = B_{x_1}^T W_1 B_{x_1}, \quad G_1 = B_{x_1}^T W_1 A_{x_1},$$

Note that F_1 and G_1 are symmetric and F_1 is positive definite [37].

Next, we use the decomposition $F_1 = LL^T$ with $L = B_{x_1}^T W_1^{1/2}$, and define the symmetric matrix

$$C = L^{-1} G_1 L^{-T} = W_1^{1/2} A_{x_1} B_{x_1}^{-1} W_1^{-1/2}.$$

We solve the eigenvalue problem for orthogonal Q and diagonal Λ such that

$$Q^T C Q = \Lambda.$$

We set $Z = B_{x_1}^{-1} W^{-1/2} Q$. Then, from the last three unnumbered equations, the following equalities hold

$$Z^T G_1 Z = \Lambda, \quad Z^T F_1 Z = I_{(r-1)N_{x_1}},$$

where $I_{(r-1)N_{x_1}}$ is the identity matrix of size $(r-1)N_{x_1}$. From the last unnumbered equation and the properties of tensor product matrices this leads to

$$\begin{aligned} & [Z^T B_{x_1} W_1 \otimes I_{(r-1)N_{x_2}}] (A_{x_1} \otimes B_{x_2} + B_{x_1} \otimes A_{x_2}) (Z \otimes I_{(r-1)N_{x_2}}) \\ &= (\Lambda \otimes B_{x_2} + I_{(r-1)N_{x_1}} \otimes A_{x_2}). \end{aligned}$$

Hence, (3.19) may be written as

$$(\Lambda \otimes B_{x_2} + I_{(r-1)N_{x_1}} \otimes A_{x_2}) \mathbf{v} = \mathbf{g}, \quad (3.31)$$

where

$$\mathbf{g} = [Z^T B_{x_1} W_1 \otimes I_{(r-1)N_{x_2}}] \mathbf{f}^*, \quad \mathbf{v} = (Z \otimes I_{(r-1)N_{x_2}})^{-1} \mathbf{u}. \quad (3.32)$$

If we set

$$\begin{aligned} \mathbf{v} &= [\mathbf{v}_1, \dots, \mathbf{v}_{(r-1)N_{x_1}}], & \mathbf{v}_m &= [v_{m,1}, \dots, v_{m,(r-1)N_{x_2}}], \\ \mathbf{g} &= [\mathbf{g}_1, \dots, \mathbf{g}_{(r-1)N_{x_1}}], & \mathbf{g}_m &= [g_{m,1}, \dots, g_{m,(r-1)N_{x_2}}], \end{aligned}$$

then (3.31) can be written as

$$A_{x_2} \mathbf{v}_k = \mathbf{g}_k \quad (3.33)$$

since $\lambda_k = 0$ for some $1 \leq k \leq (r-1)N_{x_1}$, and

$$A_{x_2} + \lambda_i B_{x_2} \mathbf{v}_i = \mathbf{g}_i, \quad i = 1, \dots, (r-1)N_{x_1}, \quad i \neq k.$$

Note that the linear system (3.33) is singular and, moreover, that (3.33) is the matrix vector form of the 1-D collocation problem

$$-v''(\xi^{x_2}) = g(\xi^{x_2}), \quad \xi^{x_2} \in \mathcal{G}_{x_2}, \quad v \in \mathcal{M}_{x_2}^N, \quad (3.34)$$

where $g(\xi_j^{x_2}) = \mathbf{g}_{1,j}$, $j = 1, \dots, (r-1)N_{x_2}$. Since (3.33) has a solution, it follows that (3.34) has a solution. Additionally, if v satisfies (3.34), then so does v plus a constant. In light of this fact, there must exist a solution v of (3.34) such that

$$-v''(\xi^{x_2}) = g(\xi^{x_2}), \quad \xi^{x_2} \in \mathcal{G}_{x_2}, \quad v \in \mathcal{M}_{x_2}, \quad v(0) = 0, \quad v'(1) = 0. \quad (3.35)$$

Given that (3.35) satisfies a Dirichlet boundary condition on the right-hand end point of $[0, 1]$, it follows that the problem is non-singular. Moreover, there are \mathbf{v}_1 and U which are solutions to (3.33) and (3.14) (or, (3.24), as the case may be), respectively, corresponding to v satisfying (3.35).

In summary, we arrive at the following matrix decomposition algorithm.

Algorithm 1 MDA for Neumann OSC problems

- 1: Compute \mathbf{g} and \mathbf{v} using (3.32)
 - 2: **for** $i = 1 : (r - 1)N_{x_1}$ **do**
 - 3: **if** $\lambda_i = 0$ **then**
 - 4: Solve (3.35) to obtain \mathbf{v}_i
 - 5: **else**
 - 6: Solve $(A_{x_2} + \lambda_i B_{x_2})\mathbf{v}_i = \mathbf{g}_i$
 - 7: **end if**
 - 8: **end for**
 - 9: Compute $\mathbf{u} = (Z \otimes I_{(r-1)N_{x_2}})\mathbf{v}$
-

3.5 Numerical Results

We consider Problems 1, 2, and 3 (See Table 3.1) which will test the OSC-MDA method for both homogeneous and nonhomogeneous Neumann boundary conditions. For each test problem and for $r = 3, 4, 5, 6$, the error is computed in two ways. First, we compute the errors in the L^2 norm of the gradient (i.e., the H^1 semi-norm),

$$\|\nabla(u - U)\|_{L^2(\Omega)}.$$

Then, using uniform 500×500 partition of Ω , we compute the maximum norm error

$$\|u - U\|_{C(\Omega)}.$$

When computing the L^2 and maximum norm errors we select $N = 9, 16, 25, 36$ for $r = 3, 4, 5$. However, to avoid reaching machine precision, we select $N = 4, 9, 16, 25$ when $r = 6$. We

compute the corresponding convergence rates using the formula

$$\text{rate} = \frac{\log(\epsilon_{N_1}/\epsilon_{N_2})}{\log(N_1/N_2)},$$

where $N_1 < N_2$ are two consecutive values of N .

To compute the L^2 and global maximum norm errors in ∇U , we evaluate U at points of a partition of $\bar{\Omega}$. For example, if $\{\tilde{\xi}_k\}_{k=1}^{r+1}$ and $\{\tilde{\omega}_k\}_{k=1}^{r+1}$ are the nodes and weights of the $(r+1)$ -point Gauss-Legendre quadrature rule for $(0, 1)$, we define $\tilde{\mathcal{G}}_{x_1} = \{\tilde{\xi}_{i,k}^{x_1}\}_{i=1,k=1}^{N_{x_1}, r+1}$ and $\tilde{\mathcal{G}}_{x_2} = \{\tilde{\xi}_{j,l}^{x_2}\}_{j=1,l=1}^{N_{x_2}, r+1}$, where the $\tilde{\xi}_{i,k}^{x_1}$ and $\tilde{\xi}_{j,l}^{x_2}$ are given by (3.4) with ξ_k replaced by $\tilde{\xi}_k$. We introduce

$$\tilde{\mathcal{G}}_r = \{\xi = (\tilde{\xi}^{x_1}, \tilde{\xi}^{x_2}) : \tilde{\xi}^{x_1} \in \tilde{\mathcal{G}}_{x_1}, \tilde{\xi}^{x_2} \in \tilde{\mathcal{G}}_{x_2}\}. \quad (3.36)$$

Then the L^2 norm error is computed as follows. First, for each $\xi^{x_1} \in \mathcal{G}_{x_1}$, we evaluate, $U(\xi^{x_1}, \cdot) \in \mathcal{M}_{x_2}$ at the points $\tilde{\xi}^{x_2} \in \tilde{\mathcal{G}}_{x_2}$, and for each $\tilde{\xi}^{x_2} \in \tilde{\mathcal{G}}_{x_2}$, we evaluate $U(\cdot, \tilde{\xi}^{x_2}) \in \mathcal{M}_{x_1}$ at the points $\tilde{\xi}^{x_1} \in \tilde{\mathcal{G}}_{x_1}$. Thus we evaluate the components of ∇U at the points of $\tilde{\mathcal{G}}_r$ in (3.36) and then we approximate $\|\nabla(u - U)\|_{L^2(\Omega)}$ by $\|\nabla(u - U)\|_{\tilde{\mathcal{G}}_r}$, where $\|\cdot\|_{\tilde{\mathcal{G}}_r}$ is defined by (3.5) with $r - 1$, ω_k , ω_l , $\xi_{i,k}^{x_1}$, $\xi_{j,l}^{x_2}$ replaced by $r + 1$, $\tilde{\omega}_k$, $\tilde{\omega}_l$, $\tilde{\xi}_{i,k}^{x_1}$, $\tilde{\xi}_{j,l}^{x_2}$, respectively. The maximum norm errors are computed in a similar manner.

It should be noted that if $U \in \mathcal{M}_r^N$ is the OSC solution of (3.14), it will be necessary to specify the value of U at a point in order to accurately compute the maximum norm convergence rates. Specifically, we replace U by $U + c$ where $c = u(0, 0) - U(0, 0)$ so that $(U + c)(0, 0) = u(0, 0)$.

Table 3.1: Test Problems for OSC-MDA

Problem	True Solution
1	$u(x, y) = e^{\cos(\pi x) \cos(\pi y)}$
2	$u(x, y) = \sin(4\pi x) \sin(4\pi y)$
3	$u(x, y) = e^{1.2x + 1.4y} \sin(4\pi y)$

Table 3.2 and Table 3.3 show the errors and rates in the H^1 semi-norm and maximum norm, respectively, for the OSC-MDA method when applied to Problem 1. Likewise, Ta-

ble 3.4 and Table 3.5 show the errors and rates in the H^1 semi-norm and maximum norm, respectively, for the OSC-MDA method when applied to Problem 2 and Table 3.6 and Table 3.7 show the errors and rates in the H^1 semi-norm and maximum norm, respectively, for the OSC-MDA method when applied to Problem 3. In every case, the expected optimal order convergence rates are observed.

Table 3.2: OSC-MDA H^1 semi-norm errors and rates for Problem 1.

$r = 3$			$r = 4$		
N	error	rate	N	error	rate
9	2.6743e-03		9	1.3172e-04	
16	2.6743e-03	3.0045	16	1.3235e-05	3.9937
25	1.2436e-04	3.0017	25	2.2226e-06	3.9978
36	4.1637e-05	3.0007	36	5.1709e-07	3.9990
$r = 5$			$r = 6$		
N	error	rate	N	error	rate
9	6.2558e-06		4	4.6351e-05	
16	3.5426e-07	4.9903	9	2.8387e-07	6.2835
25	3.8099e-08	4.9965	16	9.0561e-09	5.9876
36	6.1611e-09	4.9964	25	6.3418e-10	5.9577

Table 3.3: OSC-MDA Maximum norm errors and rates for Problem 1.

$r = 3$			$r = 4$		
N	error	rate	N	error	rate
9	4.2482e-04		9	1.5936e-05	
16	4.5281e-05	3.8911	16	9.0926e-07	4.9773
25	7.7498e-06	3.9554	25	9.3908e-08	5.0871
36	1.8132e-06	3.9835	36	1.5992e-08	4.8547
$r = 5$			$r = 6$		
N	error	rate	N	error	rate
9	9.6265e-07		4	8.9602e-06	
16	3.5542e-08	5.7337	9	2.2700e-08	7.3720
25	2.5585e-09	5.8960	16	4.9295e-10	6.6562
36	3.9005e-10	5.1582	25	6.1684e-11	4.6570

Table 3.4: OSC-MDA H^1 semi-norm errors and rates for Problem 2.

$r = 3$			$r = 4$		
N	error	rate	N	error	rate
9	1.4298e-01		9	1.1158e-02	
16	2.5032e-02	3.0285	16	1.1209e-03	3.9941
25	6.5210e-03	3.0141	25	1.8822e-04	3.9980
36	2.1785e-03	3.0067	36	4.3787e-05	3.9991
$r = 5$			$r = 6$		
N	error	rate	N	error	rate
9	7.4792e-04		4	1.0681e-03	
16	4.2351e-05	4.9904	9	4.2533e-05	3.9749
25	4.5542e-06	4.9967	16	1.3556e-06	5.9893
36	7.3591e-07	4.9986	25	9.3330e-08	5.9958

Table 3.5: OSC-MDA Maximum norm errors and rates for Problem 2.

$r = 3$			$r = 4$		
N	error	rate	N	error	rate
9	1.7633e-02		9	5.9471e-04	
16	1.6536e-03	4.1137	16	2.9218e-05	5.2372
25	2.8384e-04	3.9488	25	2.9865e-06	5.1103
36	6.7286e-05	3.9476	36	4.5995e-07	5.1303
$r = 5$			$r = 6$		
N	error	rate	N	error	rate
9	4.4701e-05		4	7.0788e-05	
16	1.2447e-06	6.2241	9	1.1570e-06	5.0730
25	9.8296e-08	5.6884	16	1.8686e-08	7.1707
36	1.1200e-08	5.9567	25	8.5150e-10	6.9205

Table 3.6: OSC-MDA H^1 semi-norm errors and rates for Problem 3.

$r = 3$			$r = 4$		
N	error	rate	N	error	rate
9	7.2270e-01		9	5.0960e-02	
16	1.2701e-01	3.0220	16	15.2375e-03	3.9544
25	3.3201e-02	3.0063	25	8.8416e-04	3.9862
36	1.1108e-02	3.0026	36	2.0607e-04	3.9941
$r = 5$			$r = 6$		
N	error	rate	N	error	rate
9	3.9619e-03		4	2.5115e-02	
16	2.2227e-04	5.0066	9	1.9471e-04	5.9928
25	2.3859e-05	5.0007	16	6.3531e-06	5.9485
36	3.8531e-06	5.0001	25	4.3965e-07	5.9843

Table 3.7: OSC-MDA Maximum norm errors and rates for Problem 3.

$r = 3$			$r = 4$		
N	error	rate	N	error	rate
9	1.4032e-01		9	4.3253e-03	
16	1.3458e-02	4.0745	16	2.3237e-04	5.0818
25	1.3458e-02	3.9987	25	2.5856e-05	4.9201
36	5.2498e-04	4.0022	36	4.2207e-06	4.9707
$r = 5$			$r = 6$		
N	error	rate	N	error	rate
9	2.8820e-04		4	2.3162e-03	
16	8.6116e-06	6.1014	9	1.0431e-05	6.6626
25	6.4022e-07	5.8237	16	1.7855e-07	7.0697
36	7.0766e-08	6.0400	25	8.6891e-09	6.7732

CHAPTER 4

ADI+MDA ORTHOGONAL SPLINE COLLOCATION FOR THE PRESSURE POISSON REFORMULATION OF THE NAVIER-STOKES EQUATIONS IN TWO SPACE VARIABLES

We are interested in the numerical solution to the incompressible Navier-Stokes equations. Let $\Omega = (0, 1) \times (0, 1)$. Then in standard formulation these equations are given by the nonlinear system

$$\mathbf{u}_t + (\mathbf{u} \cdot \nabla) \mathbf{u} - \mu \Delta \mathbf{u} + \nabla p = \mathbf{f}(x_1, x_2, t) \quad (x_1, x_2) \in \Omega, \quad t \in (T_0, T_1], \quad (4.1)$$

$$\nabla \cdot \mathbf{u} = 0, \quad (x_1, x_2) \in \Omega, \quad t \in (T_0, T_1], \quad (4.2)$$

for the velocity field $\mathbf{u} = \begin{bmatrix} u_1 \\ u_2 \end{bmatrix}$, pressure p , kinematic viscosity μ , and forcing term $\mathbf{f} = \begin{bmatrix} f_1 \\ f_2 \end{bmatrix}$,

where $\Delta \equiv \partial^2/\partial x_1^2 + \partial^2/\partial x_2^2$, $\nabla = \begin{bmatrix} \partial/\partial x_1 \\ \partial/\partial x_2 \end{bmatrix}$. The solution \mathbf{u} of (4.1)–(4.2) is subject to the initial condition,

$$\mathbf{u}(x_1, x_2, T_0) = \mathbf{g}(x_1, x_2), \quad (x_1, x_2) \in \bar{\Omega}, \quad (4.3)$$

the nonhomogeneous Dirichlet boundary condition

$$\mathbf{u}(x_1, x_2, t) = \mathbf{d}(x_1, x_2, t), \quad (x_1, x_2) \in \partial\Omega, \quad t \in \times(T_0, T_1], \quad (4.4)$$

where $\mathbf{g} = \begin{bmatrix} g_1 \\ g_2 \end{bmatrix}$, $\mathbf{d} = \begin{bmatrix} d_1 \\ d_2 \end{bmatrix}$, $\bar{\Omega} = \Omega \cup \partial\Omega$, and $\partial\Omega$ is the boundary of Ω . Note that in what

follows (cf. the second term of (4.1)), for any functions $\mathbf{u} = \begin{bmatrix} u_1 \\ u_2 \end{bmatrix}$ in Ω we have

$$(\mathbf{u} \cdot \nabla) \mathbf{u} = \left(u_1 \frac{\partial}{\partial x_1} + u_2 \frac{\partial}{\partial x_2} \right) \begin{bmatrix} u_1 \\ u_2 \end{bmatrix} = \begin{bmatrix} u_1 \frac{\partial u_1}{\partial x_1} + u_2 \frac{\partial u_1}{\partial x_2} \\ u_1 \frac{\partial u_2}{\partial x_1} + u_2 \frac{\partial u_2}{\partial x_2} \end{bmatrix}. \quad (4.5)$$

Fully implicit discretizations of (4.1)-(4.4) by standard methods will give rise to a non-linear saddle point problem at every time step of the form

$$\begin{bmatrix} N(\mathbf{u}^{n+1}) & B \\ B^T & O \end{bmatrix} \begin{bmatrix} \mathbf{u}^{n+1} \\ p^{n+1} \end{bmatrix} = \begin{bmatrix} \mathbf{F} \\ \mathbf{0} \end{bmatrix},$$

where O denotes the zero matrix. Then, the updates for the velocity and pressure terms can be obtained through a Newton or Picard iteration [3, 4]. Despite the broad applicability and intuitive appeal of this direct approach, the cost of solving the nonlinear system is prohibitive for the time dependent problem. Of course, the above system can be linearized by making use of the velocity from a previous time step, but solving the resulting linear system come with its own complications. One early finite difference approach was the so-called Marker-and-Cell method of Harlow and Welch [40] wherein the velocity and pressure terms are solved on staggered meshes in order to avoid instabilities. Finite element methods have been popular, but in order for the numerical solution of a saddle point system to be stable and accurate, the underlying spatial discretization must satisfy the so-called inf-sup conditions [7]. Fortunately, it is well known how to construct such spatial discretizations, but, unfortunately, this approach is not without its own drawbacks. For example, in order to satisfy the inf-sup conditions, a typical finite element discretization will use pressure elements which are of one order less than those used for velocity [7]. Consequently, the order of accuracy of the pressure term will be less than that of the velocity term. Collocation schemes such as spectral [41] or B-spline [42] collocation are not immune to these restrictions due to the inf-sup conditions either.

Projection methods, beginning with pioneering work of Chorin [43] and Temam [44], can be thought of as a way of obtaining velocity and pressure updates without the need to solve a large coupled system. These methods work by, first, relaxing the incompressibility constraint (1.2) and solving for an intermediate velocity (which is not necessarily divergence free) before projecting this solution on to the space of divergence free functions. It was once thought that certain versions of these methods could avoid the need to satisfy the inf-sup

condition [45], but this supposition was later shown to be incorrect [46]. Moreover, it is well known that, in general, projection methods do not enforce the appropriate boundary conditions for either the velocity or pressure terms [46]. To that end, a considerable amount of effort has been expended in order to modify existing schemes so that they satisfy accurate tangential velocity boundary conditions [47] and consistent pressure boundary conditions [5, 48]. Despite the incremental improvements that have been made to projection methods over the years, it is still quite common for these schemes to suffer from numerical issues (e.g., “numerical boundary layers” [49]) which can limit their overall accuracy [46].

One way to avoid the inf-sup conditions and any resulting complications is to rewrite the Navier–Stokes equations in an equivalent form. Of particular interest to this chapter is the pressure Poisson reformulation due to Henshaw and Petersson [8], which was later described in the continuous setting by Johnston and Liu [9]. That is, it can be shown [8, 9, 50] that (4.1)-(4.4) can be rewritten in the following form

$$\mathbf{u}_t + (\mathbf{u} \cdot \nabla) \mathbf{u} - \mu \Delta \mathbf{u} + \nabla p = \mathbf{f}(x_1, x_2, t), \quad (x_1, x_2) \in \Omega, \quad t \in (T_0, T_1], \quad (4.6)$$

$$\mathbf{u}(x_1, x_2, T_0) = \mathbf{g}(x_1, x_2), \quad (x_1, x_2) \in \bar{\Omega}, \quad (4.7)$$

$$\mathbf{u}(x_1, x_2, t) = \mathbf{d}(x_1, x_2, t), \quad (x_1, x_2) \in \partial\Omega, \quad t \in (T_0, T_1], \quad (4.8)$$

$$\Delta p = g(\mathbf{u}, x_1, x_2, t), \quad (x_1, x_2) \in \Omega, \quad t \in (T_0, T_1], \quad (4.9)$$

$$\frac{\partial p}{\partial \mathbf{n}} = h(\mathbf{u}, x_1, x_2, t), \quad (x_1, x_2) \in \partial\Omega, \quad t \in (T_0, T_1], \quad (4.10)$$

where

$$g(\mathbf{u}, x_1, x_2, t) = -\nabla \cdot ((\mathbf{u} \cdot \nabla) \mathbf{u}) + \nabla \cdot \mathbf{f} + \gamma \nabla \cdot \mathbf{u},$$

$$h(\mathbf{u}, x_1, x_2, t) = -\mathbf{n} \cdot \mathbf{u}_t - \mathbf{n} \cdot (\mathbf{u} \cdot \nabla) \mathbf{u} - \mu \mathbf{n} \cdot \nabla \times \nabla \times \mathbf{u} + \mathbf{n} \cdot \mathbf{f},$$

γ is a nonnegative real number, \mathbf{n} is the outward unit normal vector on $\partial\Omega$, $\frac{\partial}{\partial \mathbf{n}} = \mathbf{n} \cdot \nabla$, and we define

$$\nabla \times \nabla \times \mathbf{u} = \begin{bmatrix} -\frac{\partial^2 u_1}{\partial x_2^2} + \frac{\partial^2 u_2}{\partial x_1 \partial x_2} \\ \frac{\partial^2 u_1}{\partial x_2 \partial x_1} - \frac{\partial^2 u_2}{\partial x_1^2} \end{bmatrix}. \quad (4.11)$$

Note that, for the choice of $\Omega = (0, 1) \times (0, 1)$, the normal vector \mathbf{n} is well defined on $\partial\Omega$ except at the corners. To that end, we set $\mathbf{n} = \begin{bmatrix} 0 \\ 1 \end{bmatrix}$ at the points $(1, 0)$ and $(1, 1)$, and

$\mathbf{n} = \begin{bmatrix} 0 \\ -1 \end{bmatrix}$ at the points $(0, 0)$ and $(0, 1)$. A simple derivation of (4.6)–(4.10) is given in section 4.2.

It should be noted that the discretization of (4.6)–(4.10) still gives rise to a singular linear system since if p satisfies the above equations, then so does p plus a constant. Despite this, the choice of spatial discretization does not need to satisfy the inf-sup conditions and the singularity can be dealt with using standard techniques [37, 38]. Thus, numerical schemes for the solution of (4.6)–(4.10) can be constructed such that the approximations of pressure and velocity terms are of equal order. Previous work on the numerical solution to the pressure Poisson reformulation of the Navier-Stokes equations, (4.6)–(4.10), focused on finite difference, finite element, and spectral collocation methods [8, 9]. In the present chapter, we present an orthogonal spline collocation (OSC) scheme which uses an alternating direction implicit (ADI) extrapolated Crank-Nicolson OSC method for the velocity update and an OSC matrix decomposition algorithm (MDA) for the pressure update. In what follows we will refer to the combined scheme as ADI+MDA for simplicity.

The remainder of the chapter has the following structure. Section 4.1 states some preliminary definitions and establishes the notation used throughout. A simple derivation of the pressure Poisson reformulation is given in section 4.2. The ADI+MDA scheme is outlined in section 4.3. Finally, section 4.4 gives the numerical results.

4.1 Preliminaries

In what follows, $\delta_{x_1} = \{x_1^{(i)}\}_{i=0}^{N_{x_1}}$ and $\delta_{x_2} = \{x_2^{(j)}\}_{j=0}^{N_{x_2}}$ are partitions of $[0, 1]$, such that,

$$0 = x_1^{(0)} < x_1^{(1)} < \dots < x_1^{(N_{x_1})} = 1, \quad 0 = x_2^{(0)} < x_2^{(1)} < \dots < x_2^{(N_{x_2})} = 1.$$

We define $\delta = \delta_{x_1} \times \delta_{x_2}$, and introduce

$$h_i^{x_1} = x_1^{(i)} - x_1^{(i-1)}, \quad i = 1, \dots, N_{x_1}, \quad h_j^{x_2} = x_2^{(j)} - x_2^{(j-1)}, \quad j = 1, \dots, N_{x_2}.$$

We set

$$h_{x_1} = \max_{i=1, \dots, N_{x_1}} h_i^{x_1}, \quad h_{x_2} = \max_{j=1, \dots, N_{x_2}} h_j^{x_2}, \quad h = \max(h_{x_1}, h_{x_2}).$$

It is assumed that the family of partitions δ of Ω is quasi-uniform.

Let \mathcal{M}_{x_1} and \mathcal{M}_{x_2} be the spaces of C^1 splines of degree $\leq r$ with the breaks at the $x_1^{(i)}$ and $x_2^{(j)}$, respectively, that is,

$$\mathcal{M}_{x_1} = \{v \in C^1[0, 1] : v|_{[x_1^{(i-1)}, x_1^{(i)}]} \in P_r, i = 1, \dots, N_{x_1}\},$$

$$\mathcal{M}_{x_2} = \{v \in C^1[0, 1] : v|_{[x_2^{(j-1)}, x_2^{(j)}]} \in P_r, j = 1, \dots, N_{x_2}\},$$

where P_r is the set of polynomials of degree $\leq r$. Note that $\dim \mathcal{M}_{x_i} = (r-1)N_{x_i} + 2$, $i = 1, 2$. Let $\mathcal{M}_r = \mathcal{M}_{x_1} \otimes \mathcal{M}_{x_2}$, $\mathcal{M}_r \times \mathcal{M}_r = \left\{ \begin{bmatrix} v_1 \\ v_2 \end{bmatrix} : v_1, v_2 \in \mathcal{M}_r \right\}$.

Let $\{\xi_k\}_{k=1}^{r-1}$ be the nodes of the $(r-1)$ -point Gauss-Legendre quadrature for $(0, 1)$, and let $\mathcal{G}_{x_1} = \{\xi_{i,k}^{x_1}\}_{i=1, k=1}^{N_{x_1}, r-1}$, $\mathcal{G}_{x_2} = \{\xi_{j,l}^{x_2}\}_{j=1, l=1}^{N_{x_2}, r-1}$ where

$$\xi_{i,k}^{x_1} = x_1^{(i-1)} + h_i^{x_1} \xi_k, \quad \xi_{j,l}^{x_2} = x_2^{(j-1)} + h_j^{x_2} \xi_l. \quad (4.12)$$

Then the set of collocation points in Ω is given by,

$$\mathcal{G}_r = \{\xi = (\xi^{x_1}, \xi^{x_2}) : \xi^{x_1} \in \mathcal{G}_{x_1}, \xi^{x_2} \in \mathcal{G}_{x_2}\}.$$

We introduce

$$\overline{\mathcal{G}}_r = \{\xi = (\xi^{x_1}, \xi^{x_2}) : \xi^{x_1} \in \mathcal{G}_{x_1} \cup \{0, 1\}, \xi^{x_2} \in \mathcal{G}_{x_2} \cup \{0, 1\}\},$$

so that the set of boundary collocation points is

$$\partial\mathcal{G}_r = \bar{\mathcal{G}}_r \cap \partial\Omega.$$

For $\mathbf{v} = \begin{bmatrix} v_1 \\ v_2 \end{bmatrix}$ and $\mathbf{z} = \begin{bmatrix} z_1 \\ z_2 \end{bmatrix}$ defined on \mathcal{G}_r , the inner product $\langle \mathbf{v}, \mathbf{z} \rangle$ and norm $\|\mathbf{v}\|$ are given by

$$\langle \mathbf{v}, \mathbf{z} \rangle = \langle v_1, z_1 \rangle_{\mathcal{G}_r} + \langle v_2, z_2 \rangle_{\mathcal{G}_r}, \quad \|\mathbf{v}\|_{\mathcal{G}_r} = \sqrt{\langle \mathbf{v}, \mathbf{v} \rangle_{\mathcal{G}_r}}, \quad (4.13)$$

where for v and z defined on \mathcal{G}_r , the inner product $\langle v, z \rangle_{\mathcal{G}_r}$ and norm $\|v\|_{\mathcal{G}_r}$ are defined

$$\langle v, z \rangle_{\mathcal{G}_r} = \sum_{i=1}^{N_{x_1}} \sum_{j=1}^{N_{x_2}} h_i^{x_1} h_j^{x_2} \sum_{k=1}^{r-1} \sum_{l=1}^{r-1} \omega_k \omega_l (vz)(\xi_{i,k}, \xi_{j,l}), \quad \|v\|_{\mathcal{G}_r} = \sqrt{\langle v, v \rangle_{\mathcal{G}_r}}. \quad (4.14)$$

We introduce,

$$\|\mathbf{v}\|_{C(\bar{\Omega})} = \max \left\{ \max_{x \in \bar{\Omega}} |v_1(x)|, \max_{x \in \bar{\Omega}} |v_2(x)| \right\},$$

$$\|\mathbf{v}\|_{L^2(\Omega)} = \left(\int_{\Omega} v_1^2 + \int_{\Omega} v_2^2 \right)^{1/2}, \quad \|\mathbf{v}\|_{H^1(\Omega)} = \left(\|\mathbf{v}\|_{L^2(\Omega)}^2 + \sum_{k=1}^2 \|\nabla v_k\|_{L^2(\Omega)}^2 \right)^{1/2}.$$

Let $\{t_n\}_{n=0}^{N_t}$ be a partition of $[T_0, T_1]$, where $t_n = T_0 + n\tau$ and the time step

$$\tau = \frac{T_1 - T_0}{N_t}.$$

We also introduce $t_{n+1/2} = (t_n + t_{n+1})/2$, $n = 0, \dots, N_t - 1$.

Throughout we assume that (4.6)–(4.10) has a unique, sufficiently smooth solution $[\mathbf{u}, p]^T$.

4.2 Derivation of the Pressure Poisson Reformulation

In this section, we make use of the following identity (compare (13) on page 165 in [51])

$$\nabla \times \nabla \times \mathbf{u} = \nabla(\nabla \cdot \mathbf{u}) - \Delta \mathbf{u}, \quad (4.15)$$

which follows easily by computing $\nabla(\nabla \cdot \mathbf{u})$ and simplifying the right-hand side.

Taking the divergence of (4.1) and using

$$\nabla \cdot (\mathbf{u}_t) = \frac{\partial}{\partial x_1} \left(\frac{\partial u_1}{\partial t} \right) + \frac{\partial}{\partial x_2} \left(\frac{\partial u_2}{\partial t} \right) = \frac{\partial}{\partial t} \left(\frac{\partial u_1}{\partial x_2} \right) + \frac{\partial}{\partial t} \left(\frac{\partial u_2}{\partial x_1} \right) = (\nabla \cdot \mathbf{u})_t,$$

$$\nabla \cdot (\Delta \mathbf{u}) = \frac{\partial}{\partial x_1} \left(\frac{\partial^2 u_1}{\partial x_1^2} \right) + \frac{\partial}{\partial x_2} \left(\frac{\partial^2 u_2}{\partial x_2^2} \right) = \frac{\partial^2}{\partial x_1^2} \left(\frac{\partial u_1}{\partial x_1} \right) + \frac{\partial^2}{\partial x_2^2} \left(\frac{\partial u_2}{\partial x_2} \right) = \Delta(\nabla \cdot \mathbf{u}),$$

$$\nabla \cdot (\nabla p) = \Delta p,$$

we obtain

$$(\nabla \cdot \mathbf{u})_t + \nabla \cdot ((\mathbf{u} \cdot \nabla) \mathbf{u}) - \mu \Delta(\nabla \cdot \mathbf{u}) + \Delta p = \nabla \cdot \mathbf{f}(x_1, x_2, t), \quad (x_1, x_2) \in \Omega, \quad t \in (T_0, T_1]. \quad (4.16)$$

Equations (4.16) and (4.2) yield

$$\Delta p = -\nabla \cdot ((\mathbf{u} \cdot \nabla) \mathbf{u}) + \nabla \cdot \mathbf{f}(x_1, x_2, t), \quad (x_1, x_2) \in \Omega, \quad t \in (T_0, T_1], \quad (4.17)$$

which is (4.9) with $\gamma = 0$.

Taking the dot product of \mathbf{n} with both sides of (4.1), with Ω replaced by $\bar{\Omega}$, we obtain

$$\mathbf{n} \cdot \mathbf{u}_t + \mathbf{n} \cdot ((\mathbf{u} \cdot \nabla) \mathbf{u}) - \mu \mathbf{n} \cdot \Delta \mathbf{u} + \mathbf{n} \cdot \nabla p = \mathbf{n} \cdot \mathbf{f}(x_1, x_2, t), \quad (x_1, x_2) \in \partial\Omega, \quad t \in (T_0, T_1].$$

Using (4.4) and (4.5), we have

$$\mathbf{n} \cdot \mathbf{u}_t = \mathbf{n} \cdot \mathbf{d}_t, \quad \mathbf{n} \cdot ((\mathbf{u} \cdot \nabla) \mathbf{u}) = \mathbf{n} \cdot ((\mathbf{d} \cdot \nabla) \mathbf{u}), \quad (x_1, x_2) \in \partial\Omega, \quad t \in (T_0, T_1].$$

Since $\mathbf{n} \cdot \nabla p = \frac{\partial p}{\partial \mathbf{n}}$, using the last two unnumbered equation, we arrive at

$$\frac{\partial p}{\partial \mathbf{n}} = -\mathbf{n} \cdot \mathbf{d}_t - \mathbf{n} \cdot ((\mathbf{d} \cdot \nabla) \mathbf{u}) + \mu \mathbf{n} \cdot \Delta \mathbf{u} + \mathbf{n} \cdot \mathbf{f}(x_1, x_2, t), \quad (x_1, x_2) \in \partial\Omega, \quad t \in (T_0, T_1]. \quad (4.18)$$

Using (4.15) on $\bar{\Omega} \times (T_0, T_1]$ and (4.2), with Ω replaced by $\bar{\Omega}$, we have

$$\Delta \mathbf{u} = -\nabla \times \nabla \times \mathbf{u} \quad (x_1, x_2) \in \partial\Omega, \quad t \in (T_0, T_1].$$

Substituting the last equation into (4.18), we arrive at

$$\frac{\partial p}{\partial \mathbf{n}} = -\mathbf{n} \cdot \mathbf{d}_t - \mathbf{n} \cdot ((\mathbf{d} \cdot \nabla) \mathbf{u}) - \mu \mathbf{n} \cdot (\nabla \times \nabla \times \mathbf{u}) + \mathbf{n} \cdot \mathbf{f}(x_1, x_2, t), \quad (x_1, x_2) \in \partial\Omega, \quad t \in (T_0, T_1], \quad (4.19)$$

which is (4.10).

Hence, one possibility for the pressure Poisson equation (PPE) reformulation is given by (4.6)-(4.10). To understand, how the PPE reformulation enforces the divergence free condition (4.2), we set $\phi = \nabla \cdot \mathbf{u}$ and consider the following. Substituting (4.17) into (4.16), we have

$$\phi_t - \mu \Delta \phi = 0, \quad (x_1, x_2) \in \Omega, \quad t \in (T_0, T_1].$$

Equating the right-hand sides of (4.18) and (4.19) and using (4.15), we obtain

$$\frac{\partial \phi}{\partial \mathbf{n}} = 0, \quad (x_1, x_2) \in \partial\Omega, \quad t \in (T_0, T_1].$$

Assuming that (4.2) holds for $t = T_0$, we have

$$\phi(x_1, x_2, T_0) = 0, \quad (x_1, x_2) \in \Omega.$$

Thus the last three unnumbered equations yield (4.2). Of course, in the discrete setting the same cannot be said. That is, we are no longer guaranteed that any discrete approximation to the initial condition will be divergence free. From which it follows that the divergence free constraint will be enforced by the last two unnumbered equations. If, for instance, μ is small, then the proposed PPE reformulation will enforce the divergence free constraint rather weakly since μ is itself the diffusion coefficient controlling the dissipation of the divergence. Previous authors have suggested [8, 50] an improvement to PPE reformulation by incorporating an additional term the PPE which depends on $\nabla \cdot \mathbf{u}$. In particular, in Remark 5 of [50] and the unnumbered equation above (3) in [8], it has been suggested that (4.17) be replaced with

$$\Delta p = -\nabla \cdot ((\mathbf{u} \cdot \nabla) \mathbf{u}) + \gamma \nabla \cdot \mathbf{u} + \nabla \cdot \mathbf{f}(x_1, x_2, t), \quad (x_1, x_2) \in \Omega, \quad t \in (T_0, T_1], \quad (4.20)$$

for an arbitrary non-negative constant γ . Clearly, in the continuous setting, the additional term does not affect the PPE reformulation. Any \mathbf{u} satisfying (4.1)–(4.4) satisfies (4.1), (4.4), (4.20), and (4.19) since $\nabla \cdot \mathbf{u} = 0$ by (4.2). However, the divergence free constraint of the modified PPE reformulation will instead be enforced by the following parabolic problem

$$\phi_t - \mu \Delta \phi = -\gamma \phi, \quad (x_1, x_2) \in \Omega, \quad t \in (T_0, T_1],$$

$$\frac{\partial \phi}{\partial \mathbf{n}} = 0, \quad (x_1, x_2) \in \partial \Omega, \quad t \in (T_0, T_1].$$

Hence, for small μ , the appearance of the additional term in (4.20) will help to ensure that the divergence free constraint is enforced adequately.

4.3 ADI+MDA OSC Scheme for Navier-Stokes

The ADI+MDA OSC scheme for (4.6)–(4.10) consists in finding $\mathbf{U}^n \in \mathcal{M}_r \times \mathcal{M}_r$ and $P^n \in \mathcal{M}_r$, $n = 2, \dots, N_t$ such that for $n = 1, \dots, N_t - 1$

$$\begin{aligned} \frac{\mathbf{U}^{n, \frac{1}{2}}(\xi) - \mathbf{U}^n(\xi)}{0.5\tau} + \left[\left(\tilde{\mathbf{U}}^n \cdot \nabla \right) \tilde{\mathbf{U}}^n \right] (\xi) \\ - \mu \mathbf{U}_{x_1 x_1}^{n, \frac{1}{2}}(\xi) - \mu \mathbf{U}_{x_2 x_2}^n(\xi) + \nabla \tilde{P}^n(\xi) = \mathbf{f}^{n+1/2}(\xi), \quad \xi \in \mathcal{G}_r, \end{aligned} \quad (4.21)$$

$$\begin{aligned} \frac{\mathbf{U}^{n+1}(\xi) - \mathbf{U}^{n, \frac{1}{2}}(\xi)}{0.5\tau} + \left[\left(\tilde{\mathbf{U}}^n \cdot \nabla \right) \tilde{\mathbf{U}}^n \right] (\xi) \\ - \mu \mathbf{U}_{x_1 x_1}^{n, \frac{1}{2}}(\xi) - \mu \mathbf{U}_{x_2 x_2}^{n+1}(\xi) + \nabla \tilde{P}^n(\xi) = \mathbf{f}^{n+1/2}(\xi), \quad \xi \in \mathcal{G}_r, \end{aligned} \quad (4.22)$$

$$\Delta P^{n+1}(\xi) = g^{n+1}(\mathbf{U}^{n+1}, \xi), \quad \xi \in \mathcal{G}_r, \quad (4.23)$$

where

$$\tilde{\varphi}^n = \frac{3\varphi^n - \varphi^{n-1}}{2}, \quad \varphi^{n+1/2} = \frac{\varphi^{n+1} + \varphi^n}{2},$$

and where $\mathbf{U}^0, \mathbf{U}^1 \in \mathcal{M}_r \times \mathcal{M}_r$, $P^0, P^1 \in \mathcal{M}_r$ will be specified later. We assume the following boundary conditions. For $n = 2, \dots, N_t$, we assume

$$\mathbf{U}^n = \mathbf{d}^n(\xi), \quad \xi \in \partial \mathcal{G}_r,$$

which determines \mathbf{U}^n on $\partial\Omega$. For $n = 1, \dots, N_t - 1$, $\xi^{x_2} \in \mathcal{G}_{x_2}$, and $\mathbf{U}^{n, \frac{1}{2}}(\cdot, \xi^{x_2}) \in \mathcal{M}_{x_1} \times \mathcal{M}_{x_1}$, we assume

$$\mathbf{U}^{n, \frac{1}{2}}(x_1, \xi^{x_2}) = \mathbf{U}^{n+1/2}(x_1, \xi^{x_2}) - \frac{\tau^2 \mu}{4} (d_t \mathbf{U}^n)_{x_2 x_2}(x_1, \xi^{x_2}), \quad x_1 = 0, 1, \quad (4.24)$$

where

$$d_t \mathbf{U}^n = \frac{\mathbf{U}^{n+1} - \mathbf{U}^n}{\tau}.$$

Also, for $n = 1, \dots, N_t - 1$, we assume

$$\frac{\partial P^{n+1}}{\partial \mathbf{n}}(\xi) = h^{n+1}(\mathbf{U}^{n+1}, \xi), \quad \xi \in \partial\mathcal{G}_r. \quad (4.25)$$

In order to initialize the scheme (4.21)–(4.21) we use $\mathbf{U}^0 \in \mathcal{M}_r \times \mathcal{M}_r$ such that

$$\mathbf{U}^0 = \mathbf{g}^0(\xi), \quad \xi \in \bar{\mathcal{G}}_r$$

and compute $\mathbf{U}^1 \in \mathcal{M}_r \times \mathcal{M}_r$ using the predictor-corrector method to be described shortly.

However, assuming that only the initial velocity field \mathbf{U}^0 is known, we must first calculate the initial pressure P^0 . That is, we begin by finding $P^0 \in \mathcal{M}_r$ satisfying

$$\Delta P^0(\xi) = g^0(\mathbf{U}^0, \xi), \quad \xi \in \mathcal{G}_r,$$

$$\frac{\partial P^0}{\partial \mathbf{n}}(\xi) = h^0(\mathbf{U}^0, \xi), \quad \xi \in \partial\mathcal{G}_r.$$

Thus, setting $\mathbf{V}^0 = \mathbf{U}^0$ and $Q^0 = P^0$ the ADI predictor step is,

$$\begin{aligned} \frac{\mathbf{V}^{0, \frac{1}{2}}(\xi) - \mathbf{V}^0(\xi)}{0.5\tau} + [(\mathbf{V}^0 \cdot \nabla) \mathbf{V}^0](\xi) \\ - \mu \mathbf{V}_{x_1 x_1}^{0, \frac{1}{2}}(\xi) - \mu \mathbf{V}_{x_2 x_2}^0(\xi) + \nabla Q^0(\xi) = \mathbf{f}^{1/2}(\xi), \quad \xi \in \mathcal{G}_r, \end{aligned} \quad (4.26)$$

$$\begin{aligned} \frac{\mathbf{V}^1(\xi) - \mathbf{V}^{0, \frac{1}{2}}(\xi)}{0.5\tau} + [(\mathbf{V}^0 \cdot \nabla) \mathbf{V}^0](\xi) \\ - \mu \mathbf{V}_{x_1 x_1}^{0, \frac{1}{2}}(\xi) - \mu \mathbf{V}_{x_2 x_2}^1(\xi) + \nabla Q^0(\xi) = \mathbf{f}^{1/2}(\xi), \quad \xi \in \mathcal{G}_r, \end{aligned} \quad (4.27)$$

where

$$\mathbf{V}^1 = \mathbf{d}^1(\xi), \quad \xi \in \partial\mathcal{G}_r,$$

and for each $\xi^{x_2} \in \mathcal{G}_{x_2}$, $\mathbf{V}^{0,\frac{1}{2}}(\cdot, \xi^{x_2}) \in \mathcal{M}_{x_1} \times \mathcal{M}_{x_1}$, and

$$\mathbf{V}^{0,\frac{1}{2}}(x_1, \xi^{x_2}) = \mathbf{V}^{1/2}(x_1, \xi^{x_2}) - \frac{\tau^2 \mu}{4} (d_t \mathbf{V}^0)_{x_2 x_2}(x_1, \xi_{j,l}^{x_2}), \quad x_1 = 0, 1. \quad (4.28)$$

Once $\mathbf{V}^1 \in \mathcal{M}_r \times \mathcal{M}_r$ is obtained, the pressure update is the $Q^1 \in \mathcal{M}_r$ satisfying

$$\Delta Q^1(\xi) = g^1(\mathbf{V}^1, \xi), \quad \xi \in \mathcal{G}_r,$$

$$\frac{\partial Q^1}{\partial \mathbf{n}}(\xi) = h^1(\mathbf{V}^1, \xi), \quad \xi \in \partial\mathcal{G}_r.$$

Next, the ADI corrector step is,

$$\begin{aligned} \frac{\mathbf{U}^{0,\frac{1}{2}}(\xi) - \mathbf{U}^0(\xi)}{0.5\tau} + [(\mathbf{V}^{1/2} \cdot \nabla) \mathbf{V}^{1/2}](\xi) \\ - \mu \mathbf{U}_{x_1 x_1}^{0,\frac{1}{2}}(\xi) - \mu \mathbf{U}_{x_2 x_2}^0(\xi) + \nabla Q^{1/2}(\xi) = \mathbf{f}^{1/2}(\xi), \quad \xi \in \mathcal{G}_r, \end{aligned} \quad (4.29)$$

$$\begin{aligned} \frac{\mathbf{U}^1(\xi) - \mathbf{U}^{0,\frac{1}{2}}(\xi)}{0.5\tau} + [(\mathbf{V}^{1/2} \cdot \nabla) \mathbf{V}^{1/2}](\xi) \\ - \mu \mathbf{U}_{x_1 x_1}^{0,\frac{1}{2}}(\xi) - \mu \mathbf{U}_{x_2 x_2}^1(\xi) + \nabla Q^{1/2}(\xi) = \mathbf{f}^{1/2}(\xi), \quad \xi \in \mathcal{G}_r, \end{aligned} \quad (4.30)$$

where

$$\mathbf{U}^1 = \mathbf{d}^1(\xi), \quad \xi \in \partial\mathcal{G}_r$$

and for each $\xi^{x_2} \in \mathcal{G}_{x_2}$, $\mathbf{U}^{0,\frac{1}{2}}(\cdot, \xi^{x_2}) \in \mathcal{M}_{x_1} \times \mathcal{M}_{x_1}$, and

$$\mathbf{U}^{0,\frac{1}{2}}(x_1, \xi^{x_2}) = \mathbf{U}^{1/2}(x_1, \xi^{x_2}) - \frac{\tau^2 \mu}{4} (d_t \mathbf{U}^0)_{x_2 x_2}(x_1, \xi_{j,l}^{x_2}), \quad x_1 = 0, 1. \quad (4.31)$$

Once $\mathbf{U}^1 \in \mathcal{M}_r \times \mathcal{M}_r$ is obtained, this leads to the final pressure update of the predictor-corrector scheme. Namely, we seek $P^1 \in \mathcal{M}_r$ satisfying

$$\Delta P^1(\xi) = g^1(\mathbf{U}^1, \xi), \quad \xi \in \mathcal{G}_r,$$

$$\frac{\partial P^1}{\partial \mathbf{n}}(\xi) = h^1(\mathbf{U}^1, \xi) \quad \xi \in \partial\mathcal{G}_r.$$

It should be noted that this scheme differs from that in [9] since we use an ADI method to obtain \mathbf{U}^{n+1} , we include the “divergence damping” in (4.25) and in our treatment of the nonlinear term. That is, in [9],

$$\frac{3}{2} (\mathbf{U}^n \cdot \nabla) \mathbf{U}^n - \frac{1}{2} (\mathbf{U}^{n-1} \cdot \nabla) \mathbf{U}^{n-1}$$

is used in place of

$$\left(\tilde{\mathbf{U}}^n \cdot \nabla \right) \tilde{\mathbf{U}}^n.$$

This approach splits the updates for \mathbf{U}^{n+1} and P^{n+1} in to two distinct steps. First, the update for \mathbf{U}^{n+1} using (4.21)-(4.22), is nothing other than the ADI-ECN scheme for Burgers’ equation in two space variables with an explicit forcing term (cf. (2.35)-(2.36)). Then, the update for P^{n+1} , (4.23)-(4.25), is simply a Poisson equation with nonhomogeneous Neumann boundary conditions which is solved by MDA (cf. section 3.2.2). In this manner, the updates for \mathbf{U}^{n+1} and P^{n+1} can be obtained by solving a sequence of independent two-point boundary value problems. For example, we first solve for $\mathbf{U}^{n,1/2}(\cdot, \xi_{x_2})$, $\xi_{x_2} \in \mathcal{G}_{x_2}$, along the x_1 direction (Figure 4.1(a)), then solve for $\mathbf{U}^{n+1}(\xi_{x_1}, \cdot)$, $\xi_{x_1} \in \mathcal{G}_{x_1}$, along the x_2 direction (Figure 4.1(b)). A schematic of the ADI scheme with the choice of $N = 4$ and $r = 3$ is shown in Figure 4.1.

4.4 Numerical Results

In what follows we set

$$\mathbf{f} = \mathbf{u}_t + (\mathbf{u} \cdot \nabla) \mathbf{u} - \mu \Delta \mathbf{u} + \nabla p$$

so that

$$\begin{aligned} u_1(x_1, x_2, t) &= \pi \cos(t) \sin^2(\pi x_1) \sin(2\pi x_2) \\ u_2(x_1, x_2, t) &= -\pi \cos(t) \sin(2\pi x_1) \sin^2(\pi x_2) \\ p(x_1, x_2, t) &= -\cos(t) \cos(\pi x_1) \sin(\pi x_2) \end{aligned}$$

is the exact solution of (4.1)–(4.4). In our first test we take $\mu = 1$ and $\gamma = 0$.

Based on the theoretical analysis of Burgers’ equation in Chapter 2, we expect the ADI scheme (4.21)–(4.22) to yield an approximation $\mathbf{U}^{N_t} \in \mathcal{M}_r \times \mathcal{M}_r$ to $\mathbf{u}(\cdot, T_1)$ on $\bar{\Omega}$ such that

$$\|\mathbf{u}(\cdot, T_1) - \mathbf{U}^{N_t}\|_{H^1(\Omega)} \leq C(\tau^2 + h^r).$$

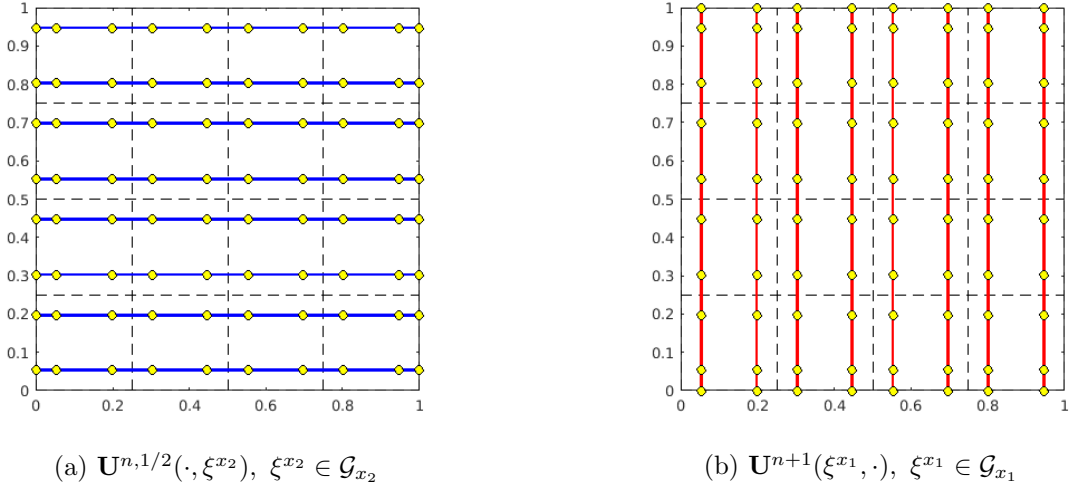


Figure 4.1: A schematic of the ADI scheme with $N = 4$ and $r = 3$. The OSC solutions are found along the solid lines at the collocation points denoted as circles. The dashed lines denote the breaks.

Furthermore, based on the theoretical analysis of OSC solutions to Neumann Poisson problems in Chapter 3, we expect the MDA scheme applied to (4.23)–(4.25) to yield an approximation $P^{N_t} \in \mathcal{M}_r$ to $p(\cdot, T_1)$ on $\bar{\Omega}$ such that

$$\|\nabla(p(\cdot, T_1) - P^{N_t})\|_{L^2(\Omega)} \leq C(\tau^2 + h^r).$$

For the values of $N = 4, 9, 16, 25$, we use the uniform partitions δ of $[0, 1] \times [0, 1]$. For $r = 3, 4, 5, 6$, we select $N_t = N^{r/2}$ so that we expect the overall convergence rates to be $O(N^{-r})$ for both the velocity and pressure terms. In addition to confirming the expected convergence results, we check how well the velocity at the final time step \mathbf{U}^{N_t} satisfies divergence free condition by calculating

$$\|\nabla \cdot \mathbf{U}^{N_t}\|_{C(\bar{\Omega})},$$

by the evaluation of \mathbf{U}^{N_t} on a uniform 500×500 partition of Ω .

To compute, for example, the L^2 , norm errors in \mathbf{U}^{N_t} , we evaluate \mathbf{U}^{N_t} at points of a partition of $\bar{\Omega}$. For example, if $\{\tilde{\xi}_k\}_{k=1}^{r+1}$ and $\{\tilde{\omega}_k\}_{k=1}^{r+1}$ are the nodes and weights of the $(r + 1)$ -point Gauss-Legendre quadrature rule for $(0, 1)$, we define $\tilde{\mathcal{G}}_{x_1} = \{\tilde{\xi}_{i,k}^{x_1}\}_{i=1, k=1}^{N_{x_1}, r+1}$ and

$\tilde{\mathcal{G}}_{x_2} = \{\tilde{\xi}_{j,l}^{x_2}\}_{j=1,l=1}^{N_{x_2},r+1}$, where the $\tilde{\xi}_{i,k}^{x_1}$ and $\tilde{\xi}_{j,l}^{x_2}$ are given by (4.12) with ξ_k replaced by $\tilde{\xi}_k$. We introduce

$$\tilde{\mathcal{G}}_r = \{\xi = (\tilde{\xi}^{x_1}, \tilde{\xi}^{x_2}) : \tilde{\xi}^{x_1} \in \tilde{\mathcal{G}}_{x_1}, \tilde{\xi}^{x_2} \in \tilde{\mathcal{G}}_{x_2}\}. \quad (4.32)$$

Then the L^2 norm error is computed as follows. First, for each $\xi^{x_1} \in \mathcal{G}_{x_1}$, we evaluate, $\mathbf{U}^{N_t}(\xi^{x_1}, \cdot) \in \mathcal{M}_{x_2} \times \mathcal{M}_{x_2}$ at the points $\tilde{\xi}^{x_2} \in \tilde{\mathcal{G}}_{x_2}$, and for each $\tilde{\xi}^{x_2} \in \tilde{\mathcal{G}}_{x_2}$, we evaluate $\mathbf{U}^{N_t}(\cdot, \tilde{\xi}^{x_2}) \in \mathcal{M}_{x_1} \times \mathcal{M}_{x_1}$ at the points $\tilde{\xi}^{x_1} \in \tilde{\mathcal{G}}_{x_1}$. Thus we evaluate \mathbf{U}^{N_t} at the points of $\tilde{\mathcal{G}}_r$ in (4.32) and then we approximate $\|\mathbf{u}^{N_t} - \mathbf{U}^{N_t}\|_{L^2(\Omega)}$ by $\|\mathbf{u}^{N_t} - \mathbf{U}^{N_t}\|_{\tilde{\mathcal{G}}_r}$, where $\|\cdot\|_{\tilde{\mathcal{G}}_r}$ is defined by (4.13) and (4.14) with $r - 1$, ω_k , ω_l , $\xi_{i,k}^{x_1}$, $\xi_{j,l}^{x_2}$ replaced by $r + 1$, $\tilde{\omega}_k$, $\tilde{\omega}_l$, $\tilde{\xi}_{i,k}^{x_1}$, $\tilde{\xi}_{j,l}^{x_2}$, respectively. The H^1 and maximum norm errors are computed in a similar manner. We also computed the corresponding convergence rates using the formula

$$\text{rate} = \frac{\log(\epsilon_{N_1}/\epsilon_{N_2})}{\log(N_2/N_1)},$$

where $N_1 < N_2$ are two consecutive values of N . Table 4.1 and Table 4.2 show that the ADI+MDA scheme obtains the expected convergence rates in the L^2 norm of ∇p and the H^1 norm of \mathbf{u} , respectively. Table 4.3 demonstrates the scheme also obtains the expected convergence rates in the maximum norm of $\nabla \cdot \mathbf{u}$, and, hence, gives evidence for how well the scheme enforces the incompressibility constraint (4.2).

Next, we test the effect of the divergence damping term $\gamma \nabla \cdot \mathbf{u}$ on the ADI+MDA OSC scheme. To that end, we repeat the above numerical experiments for fixed $r = 3, 4$, but use $\mu = 1/100$. For $r = 3$ we use $N = 64, 81, 100, 121$ and choose $N_t = 8^3, 9^3, 10^3, 11^3$ and for $r = 4$ we use $N = 25, 36, 49, 64$ and choose $N_t = 5^4, 6^4, 7^4, 8^4$. We run the code once using $\gamma = 0$ and again using $\gamma = 100$. The results for $r = 3$ can be found in Table 4.4 and the results for $r = 4$ are given in Table 4.5. Optimal convergence rates were obtained in every case with $\gamma = 0$ and with $\gamma = 100$, but the presence of the divergence damping term leads to smaller errors in $\nabla \cdot \mathbf{u}$, as expected.

Table 4.1: L^2 norm errors and rates for ∇p using $\mu = 1$.

$r = 3$			$r = 4$		
N	err_p	rate	N	err_p	rate
4	2.8466e+00		4	1.3117e+00	
9	4.6323e-01	2.9044	9	7.7131e-02	3.9529
16	1.1288e-01	2.9527	16	1.0526e-02	3.9752
25	3.7677e-02	2.9716	25	2.2286e-03	3.9842
$r = 5$			$r = 6$		
N	err_p	rate	N	err_p	rate
4	4.3340e-01		4	1.3682e-01	
9	1.1593e-02	4.9759	9	1.6203e-03	5.9848
16	8.8049e-04	4.9863	16	6.8947e-05	5.9910
25	1.1882e-04	4.9909	25	5.9455e-06	5.9940

Table 4.2: H^1 norm errors and rates for \mathbf{u} using $\mu = 1$.

$r = 3$			$r = 4$		
N	$err_{\mathbf{u}}$	rate	N	$err_{\mathbf{u}}$	rate
4	5.0179e-01		4	1.5594e-01	
9	5.5430e-02	2.7167	9	6.2551e-03	3.9659
16	1.0270e-02	2.9301	16	6.2606e-04	4.0004
25	2.7258e-03	2.9723	25	1.0496e-04	4.0017
$r = 5$			$r = 6$		
N	$err_{\mathbf{u}}$	rate	N	$err_{\mathbf{u}}$	rate
4	3.9712e-02		4	9.9526e-03	
9	6.8929e-04	4.9989	9	7.6549e-05	6.0026
16	3.8772e-05	5.0020	16	2.4217e-06	6.0022
25	4.1608e-06	5.0013	25	1.6632e-07	6.0014

Table 4.3: Maximum norm errors and rates for $\nabla \cdot \mathbf{u}$ using $\mu = 1$.

$r = 3$			$r = 4$		
N	$err_{\nabla \cdot \mathbf{u}}$	rate	N	$err_{\nabla \cdot \mathbf{u}}$	rate
4	6.6150e-01		4	1.7603e-01	
9	7.7225e-02	2.9277	9	8.3395e-03	3.9530
16	1.6791e-02	2.9277	16	9.7781e-04	3.9792
25	4.8414e-03	2.9052	25	1.7741e-04	3.9841
$r = 5$			$r = 6$		
N	$err_{\nabla \cdot \mathbf{u}}$	rate	N	$err_{\nabla \cdot \mathbf{u}}$	rate
4	5.2750e-02		4	1.3682e-02	
9	9.8426e-04	4.9763	9	1.1785e-04	5.9798
16	6.1954e-05	4.9822	16	4.0305e-06	5.9916
25	7.0057e-06	4.9811	25	2.8702e-07	5.9936

Table 4.4: Errors and rates for $\nabla \cdot \mathbf{u}$, \mathbf{u} , and p using $\mu = 1/100$ and $r = 3$. Two different values of the divergence damping coefficient γ are shown: $\gamma = 0$ (left) and $\gamma = 100$ (right).

$\mu = 1/100$					
$\gamma = 0$			$\gamma = 100$		
N	$err_{\nabla \cdot \mathbf{u}}$	rate	N	$err_{\nabla \cdot \mathbf{u}}$	rate
64	8.9234e-04		64	4.6205e-05	
81	4.4227e-04	2.9797	81	2.3000e-05	2.9613
100	2.3551e-04	2.9905	100	1.2246e-05	2.9911
121	1.3321e-04	2.9893	121	6.9035e-06	3.0069
N	$err_{\mathbf{u}}$	rate	N	$err_{\mathbf{u}}$	rate
64	1.8867e-03		64	7.3682e-05	
81	9.3666e-04	2.9728	81	3.6343e-05	3.0003
49	4.9955e-04	2.9831	100	1.9310e-05	3.0009
121	2.8292e-04	2.9826	121	1.0902e-05	2.9993
N	err_p	rate	N	err_p	rate
64	2.8637e-03		64	6.2991e-05	
81	1.4219e-03	2.9720	81	3.1052e-05	3.0027
100	7.5847e-04	2.9824	100	1.6491e-05	3.0033
121	4.2961e-04	2.9820	121	6.9035e-06	2.9969

Table 4.5: Errors and rates for $\nabla \cdot \mathbf{u}$, \mathbf{u} , and p using $\mu = 1/100$ and $r = 4$. Two different values of the divergence damping coefficient γ are shown: $\gamma = 0$ (left) and $\gamma = 100$ (right).

$\mu = 1/100$					
$\gamma = 0$			$\gamma = 100$		
N	$err_{\nabla \cdot \mathbf{u}}$	rate	N	$err_{\nabla \cdot \mathbf{u}}$	rate
25	6.0624e-04		25	1.8754e-05	
36	1.4148e-04	3.9906	36	4.7158e-06	3.7858
49	4.1209e-05	4.0009	49	1.4248e-06	3.8822
64	1.4177e-05	3.9956	64	4.9507e-07	3.9583
N	$err_{\mathbf{u}}$	rate	N	$err_{\mathbf{u}}$	rate
25	1.2920e-03		25	3.3641e-05	
36	3.0148e-04	3.9908	36	7.8783e-06	3.9810
49	8.7966e-05	3.9953	49	2.3038e-06	3.9881
64	3.0255e-05	3.9964	64	7.9327e-07	3.9921
N	err_p	rate	N	err_p	rate
25	1.9621e-03		25	4.2355e-05	
36	4.5796e-04	3.9901	36	9.8629e-06	3.9966
49	1.3363e-04	3.9951	49	2.8749e-06	3.9986
64	4.5960e-05	3.9964	64	9.8821e-07	3.9986

CHAPTER 5
LID-DRIVEN CAVITY FLOW

In this chapter we are interested in the numerical solution of the lid-driven cavity flow problem given by the Navier-Stokes equations

$$\mathbf{u}_t + (\mathbf{u} \cdot \nabla) \mathbf{u} - \mu \Delta \mathbf{u} + \nabla p = \mathbf{0} \quad (x_1, x_2) \in \Omega, \quad t \in (T_0, T_1], \quad (5.1)$$

$$\nabla \cdot \mathbf{u} = 0, \quad (x_1, x_2) \in \Omega, \quad t \in (T_0, T_1],$$

$$\mathbf{u}(x_1, x_2, T_0) = \mathbf{0}, \quad (x_1, x_2) \in \bar{\Omega},$$

$$\mathbf{u}(x_1, x_2, t) = \mathbf{d}(x_1, x_2, t), \quad (x_1, x_2) \in \partial\Omega, \quad t \in \times(T_0, T_1],$$

where $\Omega = (0, 1) \times (0, 1)$, $\mathbf{d} = \mathbf{0}$ on the bottom and vertical sides of $\partial\Omega$ (including endpoints),

and $\mathbf{d} = \begin{bmatrix} 1 \\ 0 \end{bmatrix}$ on the top boundary $\{(x_1, 1) : 0 < x_1 < 1\}$; see figure Figure 5.1. Notice that for this choice of boundary conditions $\mathbf{d}_t = \mathbf{0}$. Moreover, since $\mathbf{d} = \mathbf{0}$ on the bottom

and vertical sides of $\partial\Omega$ (including endpoints), and $\mathbf{d} = \begin{bmatrix} 1 \\ 0 \end{bmatrix}$ on the top boundary $\{(x_1, 1) :$

$0 < x_1 < 1\}$, the nonlinear term $(\mathbf{u} \cdot \nabla)\mathbf{u} = \mathbf{0}$ on $\partial\Omega$ except at the two corners $(0, 1)$ and $(1, 1)$ where $\frac{\partial u_1}{\partial x_1}$ in (4.5) does not exist. It is with this difficulty in mind that we define

$\mathbf{n} = \begin{bmatrix} 0 \\ 1 \end{bmatrix}$ at $(0, 1)$ and $(1, 1)$ so that at these points $\mathbf{n}(\mathbf{u} \cdot \nabla)\mathbf{u} = \mathbf{0}$. (The normal vector \mathbf{n}

is well defined on $\partial\Omega$ except at the corners and we set $\mathbf{n} = \begin{bmatrix} 0 \\ -1 \end{bmatrix}$ at the points $(0, 0)$ and $(0, 1)$.)

Due to these simplifications and $\mathbf{0}$ on the right-hand side in (5.1), the pressure Poisson equation reformulation of the cavity problem seems to consist of

$$\mathbf{u}_t + (\mathbf{u} \cdot \nabla) \mathbf{u} - \mu \Delta \mathbf{u} + \nabla p = \mathbf{0}, \quad (x_1, x_2) \in \Omega, \quad t \in (T_0, T_1],$$

$$\begin{aligned}
\mathbf{u}(x_1, x_2, T_0) &= 0, \quad (x_1, x_2) \in \overline{\Omega}, \\
\mathbf{u}(x_1, x_2, t) &= \mathbf{d}(x_1, x_2, t), \quad (x_1, x_2) \in \partial\Omega, \quad t \in (T_0, T_1], \\
\Delta p &= g(\mathbf{u}, x_1, x_2, t), \quad (x_1, x_2) \in \Omega, \quad t \in (T_0, T_1], \\
\frac{\partial p}{\partial \mathbf{n}} &= h(\mathbf{u}, x_1, x_2, t), \quad (x_1, x_2) \in \partial\Omega, \quad t \in (T_0, T_1],
\end{aligned} \tag{5.2}$$

where

$$g(\mathbf{u}, x_1, x_2, t) = -\nabla \cdot ((\mathbf{u} \cdot \nabla) \mathbf{u}) + \gamma \nabla \cdot \mathbf{u},$$

$$h(\mathbf{u}, x_1, x_2, t) = -\mu \mathbf{n} \cdot \nabla \times \nabla \times \mathbf{u},$$

γ is a nonnegative real number, and

$$\nabla \times \nabla \times \mathbf{u} = \begin{bmatrix} -\frac{\partial^2 u_1}{\partial x_2^2} + \frac{\partial^2 u_2}{\partial x_1 \partial x_2} \\ \frac{\partial^2 u_1}{\partial x_2 \partial x_1} - \frac{\partial^2 u_2}{\partial x_1^2} \end{bmatrix}. \tag{5.3}$$

However, the second entry of (5.3) does not seem to exist at the corners (0, 1) and (1, 1).

Hence at (0, 1) and (1, 1) we replace (5.2) with

$$\frac{\partial p}{\partial \mathbf{n}} = 0, \quad t \in (T_0, T_1],$$

which follows from (5.1) and $\mathbf{n} = \begin{bmatrix} 0 \\ 1 \end{bmatrix}$ and $\Delta u_2 = 0$ at (0, 1) and (1, 1). (Note that we could use the same equation at the other two corners (0, 0) and (1, 0).)

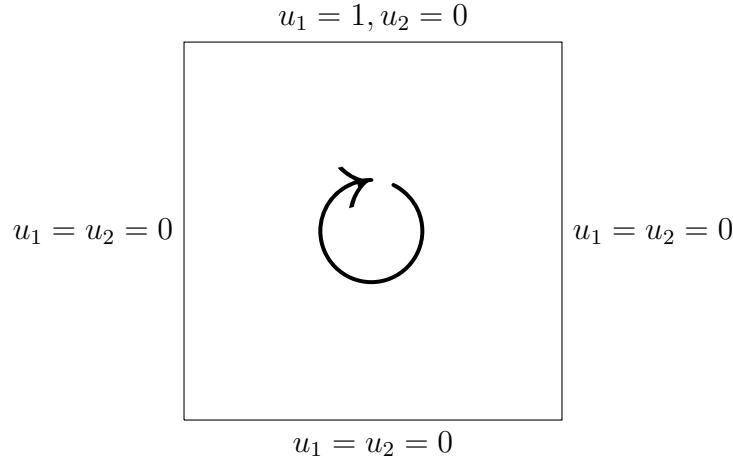


Figure 5.1: Boundary conditions for the lid-driven cavity problem.

The lid-driven cavity flow is a typical test problem for Navier-Stokes solvers [52]. This is an ideal test of a method's veracity because it is easily implementable, but does not have a closed form solution. The difficulty at the corners extends beyond the practical necessity of defining the boundary condition for the pressure term. Solutions to the cavity problems are known to be discontinuous at these points, yet the problem remains as a standard benchmark for numerical solvers of the Navier-Stokes equations [53, 54]. Additionally, these boundary conditions will cause eddies (i.e., regions where the fluid is rotating in the opposite direction from the main body of the flow [55]) to form within the cavity and the size and shape of these eddies is dependent on the coefficient μ . In particular, for the values of $\mu = 1/100, 1/1000$, the Navier-Stokes equations will reach a steady state solution [53, 54]. To investigate these steady state solutions using the time dependent Navier-Stokes equations it is necessary to integrate over $(T_0, T_1]$, where $T_0 = 0$ and T_1 is large. Then, from the resulting velocity field, we can compute the stream function, ψ , from the following Poisson equation

$$-\Delta\psi = \frac{\partial u_2}{\partial x_1} - \frac{\partial u_1}{\partial x_2}, \quad \text{in } \Omega,$$

subject to

$$\psi = 0, \quad \text{on } \partial\Omega.$$

The level curves of the stream function, $L_c(\psi)$, defined by

$$L_c(\psi) = \{(x_1, x_2) : \psi(x_1, x_2) = c\},$$

are referred to as the “streamlines” and they show the path traced out by a massless particle moving through the flow. The qualitative features of the flow can be easily visualized from the streamlines, allowing us to compare our method with existing benchmark solutions [7, 53, 54]. For example, the values of the stream function near the corner eddies are exponentially small compared to those near the center of the flow [55]. Thus, obtaining the streamlines from the computed velocity gives us means to inspect the accuracy of the solution on both large and small scales simultaneously in a way that plotting simply the velocity surfaces cannot. In addition, various authors have applied accurate steady state solvers to the cavity problem, allowing us directly compare the computed velocities at certain locations along the center lines of the domain [53, 54]. In what follows, we consider $\mu = 1/100, 1/1000$ for which steady state solutions are known to occur and accurate reference solutions exist.

For the lid-driven cavity problem we solve the pressure Poisson reformulation of Navier-Stokes equations of this section using the ADI+MDA OSC scheme of section 4.3 and run simulations for the prescribed values of μ . Given that the solution to the lid-driven cavity problem is not smooth and that the coefficient μ is chosen to be relatively small, we select $r = 3$ and $N = 144$ to ensure reasonable results. We integrate over the interval $(0, 50]$ and with $\tau = 1/12^3$ corresponding to $N_t = 50 * 12^3$. For this N_t we have

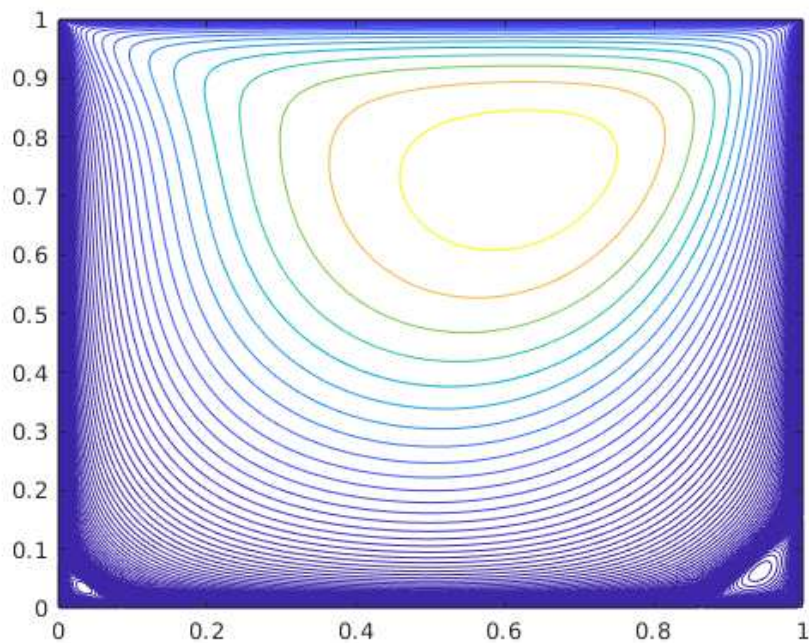
$$\frac{\|\mathbf{U}^{N_t} - \mathbf{U}^{N_t-1}\|_{C(\bar{\Omega})}}{\tau \|\mathbf{U}^{N_t}\|_{C(\bar{\Omega})}} < 10^{-6},$$

which indicates no further improvement. The presence of a small coefficient μ suggests that the addition of the diffusion damping term $\gamma \nabla \cdot \mathbf{u}$ will help the scheme enforce the incompressibility constraint. We select $\gamma = 100$ and $\gamma = 1000$ for $\mu = 1/100$ and $\mu = 1/1000$, respectively. Once the final velocity $\mathbf{U}^{N_t} \in \mathcal{M}_r \times \mathcal{M}_r$ is obtained, the OSC approximation

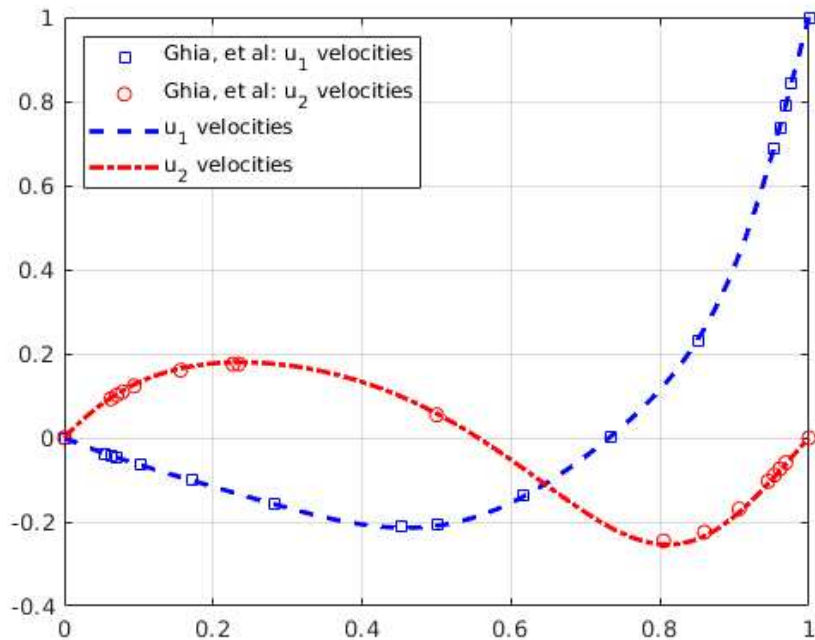
to the stream function is defined by $\Psi \in \mathcal{M}_r^0$ such that

$$-\Delta\Psi(\xi) = [U_2^{N_t}]_{x_1}(\xi) - [U_1^{N_t}]_{x_2}(\xi), \quad \xi \in \mathcal{G}_r.$$

The results for $\mu = 1/100$ are shown in Figure 5.2. In particular Figure 5.2(a) shows the streamlines computed from the final velocity \mathbf{U}^{N_t} and a comparison to standard benchmark values [53] is given in Figure 5.2(b). The benchmark comparisons are based on velocities through the center line of each component of \mathbf{U}^{N_t} . The blue line shows $U_1(0.5, \cdot)$ with the benchmark values given as blue squares and the red line shows $U_2(\cdot, 0.5)$ the benchmark values shown as red circles. A detail of the corner eddies is shown in Figure 5.3 with Figure 5.3(a) and Figure 5.3(b) displaying the lower left and lower right corners, respectively. Likewise, the results for $\mu = 1/1000$ are shown in Figure 5.4 with streamlines in Figure 5.4(a) and benchmark comparisons in Figure 5.4(b). Details of the corner eddies for $\mu = 1/1000$ are in Figure 5.5 with Figure 5.5(b) and Figure 5.5(a) displaying the lower left and lower right corners, respectively. The results presented closely match those in the literature (cf. Figure 3 in [53]).

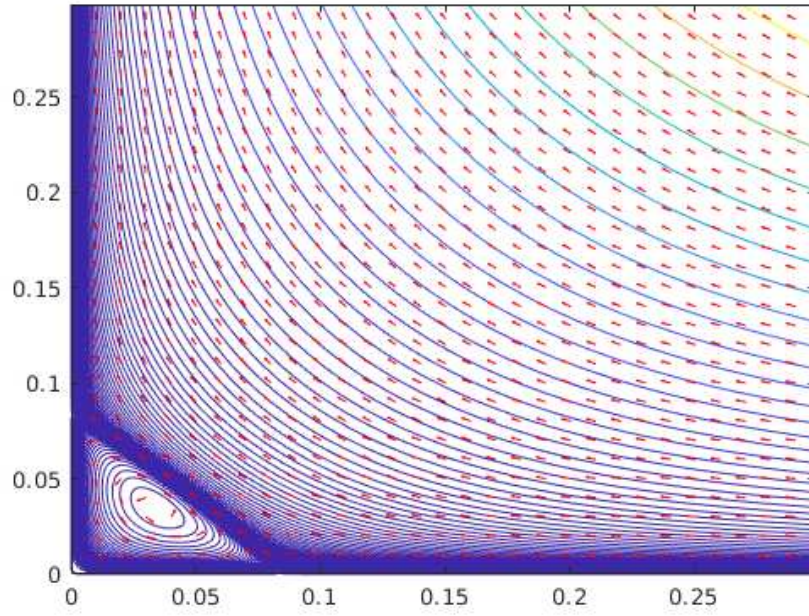


(a) Streamlines

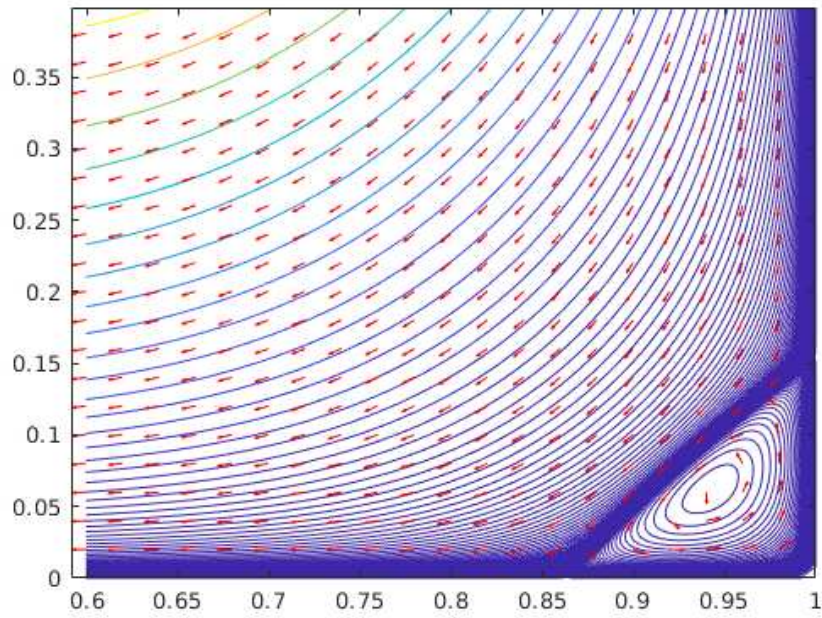


(b) Benchmarks

Figure 5.2: Streamlines and benchmarks of the lid-driven cavity problem for $\mu = 1/100$

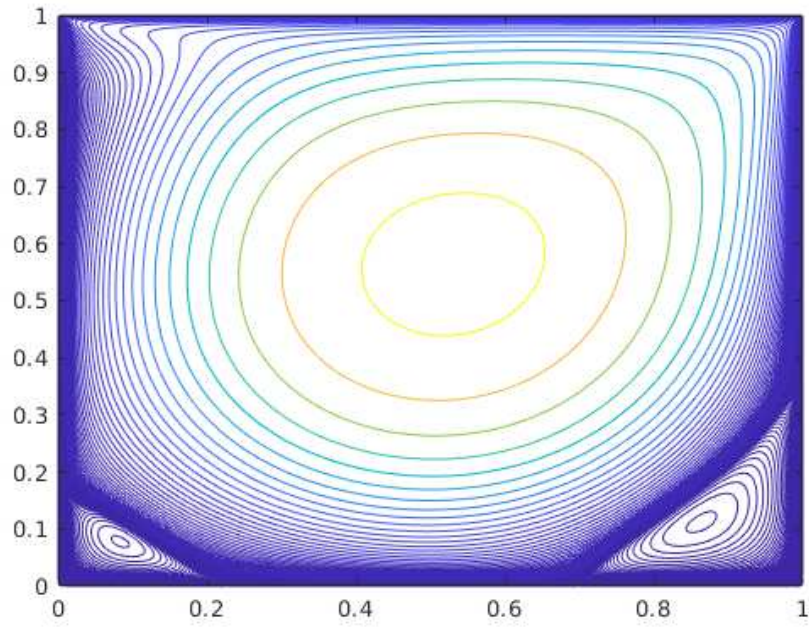


(a) Lower left corner

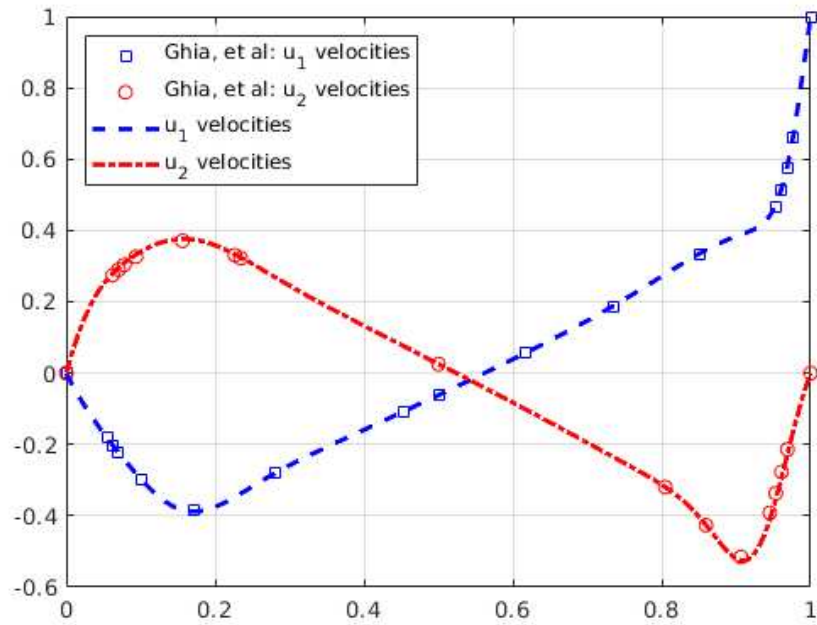


(b) Lower right corner

Figure 5.3: A detail of the counter rotating eddies in the lower corners of the lid-driven cavity flow problem for $\mu = 1/100$ with the normalized velocity field given by the red arrows.

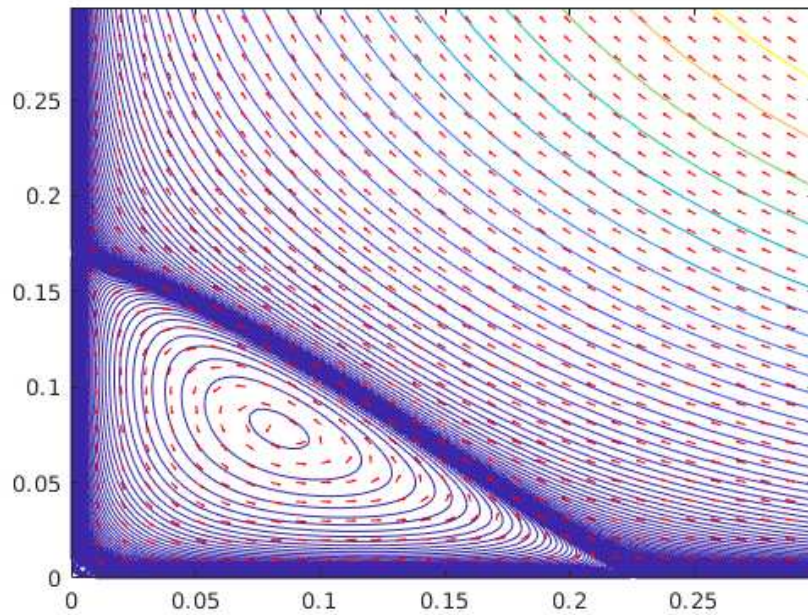


(a) Streamlines

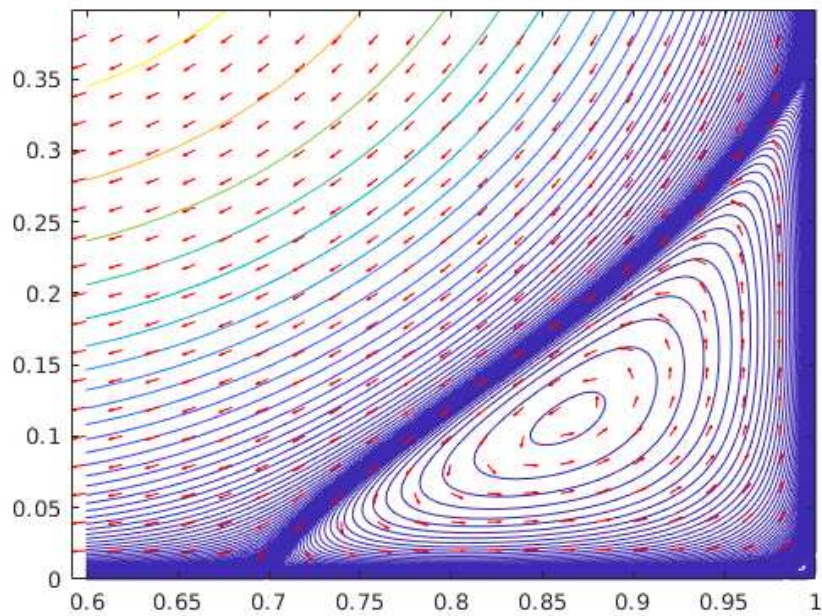


(b) Benchmarks

Figure 5.4: Streamlines and benchmarks of the lid-driven cavity problem for $\mu = 1/1000$



(a) Lower left corner



(b) Lower right corner

Figure 5.5: A detail of the counter rotating eddies in the lower corners of the lid-driven cavity flow problem for $\mu = 1/1000$ with the normalized velocity field given by the red arrows.

CHAPTER 6

CONCLUSION

In this dissertation, we studied the numerical solution to the pressure Poisson equation reformulation of the Navier–Stokes equations. Accordingly, we investigated the ADI-ECN-OSC scheme for Burgers’ equation and the OSC MDA method for Poisson’s equation with Neumann boundary conditions in two space variables. We proved that the ADI-ECN-OSC scheme for Burgers’ equation is $O(\tau^2 + h^r)$ in the H^1 norm and we proved that the OSC method for Poisson’s equation with homogeneous Neumann boundary conditions is $O(h^r)$ in the H^1 semi-norm. Numerical experiments confirmed these theoretical results. Then, we introduced an ADI+MDA OSC scheme for the pressure Poisson equation reformulation of the Navier–Stokes equations. Numerical experiments confirmed the expected optimal order convergence rates. Finally, we applied the ADI+MDA OSC scheme to the lid-driven cavity flow and demonstrated the scheme’s accuracy by comparing the results to standard benchmark values.

REFERENCES CITED

- [1] G.A. Baker. Galerkin approximations for the Navier–Stokes equations. Technical report, Harvard University, 1976.
- [2] R. Ingram. A new linearly extrapolated Crank–Nicolson time–stepping scheme for the Navier–Stokes equations. *Math. Comp.*, **82**:1953–1973, 2013.
- [3] R. Hunt. The numerical solution of the laminar flow in a constricted channel at moderately high Reynolds number using Newton iteration. *Int. J. Numer. Meth. Fluids*, **11**: 247–259, 1990.
- [4] S.A. Jordan. An iterative scheme for numerical solution of steady incompressible viscous flows. *Computers & Fluids*, **21**:503–517, 1992.
- [5] S.A. Orszag, M. Israeli, and M. Deville. Boundary conditions for incompressible flows. *J. Sci. Comp.*, **1**:75–111, 1986.
- [6] N.A. Petersson. Stability of pressure boundary conditions for Stokes and Navier–Stokes equations. *J. Comp. Phys.*, **172**:40–70, 2001.
- [7] H. Elman, D. Silvester, and A. Wathen. *Finite Elements and Fast Iterative Solvers with Applications in Incompressible Fluid Dynamics*. Oxford University Press, New York, 2005.
- [8] H.D. Henshaw and N.A. Petersson. A split-step scheme for the incompressible Navier–Stokes equations. In M.M. Hafez, editor, *Numerical Simulation of Incompressible Flows*, pages 108–125. World Scientific, 2003.
- [9] H. Johnston and J.-G. Liu. Accurate, stable and efficient Navier–Stokes solvers based on explicit treatment of the pressure term. *J. Comput. Phys.*, **199**:221–259, 2004.
- [10] B. Bialecki and R. Fernandes. An orthogonal spline collocation alternating direction implicit Crank–Nicolson method for linear parabolic problems on rectangles. *SIAM J. Numer. Anal.*, **36**:1414–1434, 1999.
- [11] B. Bialecki and G. Fairweather. An alternating direction implicit orthogonal spline collocation scheme for nonlinear parabolic problems on rectangular polygons. *SIAM J. Sci. Comput.*, **28**:1054–1077, 2006.

- [12] A. Refik Bahadir. A fully implicit finite difference scheme for two-dimensional Burgers' equations. *App. Math. and Comp.*, **137**:131–137, 2003.
- [13] C. A. J. Fletcher. A comparison of finite element and finite difference solutions of the one- and two-dimensional Burgers' equations. *J. Comp. Phys.*, **61**:159–188, 1983.
- [14] S. F. Radawan. On the fourth-order accurate compact adi scheme for solving the unsteady nonlinear coupled Burgers' equations. *J. Nonlinear Math. Phys.*, **6**:13–34, 1999.
- [15] S. F. Radawan. Comparison of higher-order accurate schemes for solving the two-dimensional unsteady Burgers equation. *Journal of Computational and Applied Mathematics*, **174**:383–397, 2005.
- [16] P. Arminjon and C. Beauchamp. Numerical solution of Burgers' equation in two space dimensions. *Comp. Meth. in App. Mechanics and Engineering*, **19**:361–365, 1979.
- [17] Siraj ul Islam, B. Šarler, R. Vertnik, and G. Kosec. Radial basis function collocation method for the numerical solution of the two-dimensional transient nonlinear coupled Burgers equations. *Applied Mathematical Modeling*, **36**:1148–1160, 2012.
- [18] A. H. Khater, R. S. Temsah, and M. M. Hassan. A Chebyshev spectral collocation method for solving Burgers-type equations. *Journal of Computational and Applied Mathematics*, **222**:333–350, 2008.
- [19] R. Fernandes and G. Fairweather. An ADI extrapolated Crank-Nicolson orthogonal spline collocation method for nonlinear reaction diffusion systems. *J. Comp. Phys.*, **231**:6248–6267, 2012.
- [20] R. Fernandes, B. Bialecki, and G. Fairweather. An ADI extrapolated Crank-Nicolson orthogonal spline collocation method for nonlinear reaction diffusion systems on evolving domains. *J. Comp. Phys.*, **299**:561–580, 2015.
- [21] B. Bialecki and N. Fisher. Maximum norm convergence analysis of extrapolated Crank–Nicolson orthogonal spline collocation for Burgers' equation in one space variable. *Journal of Difference Equations and Applications*, 2018. doi: 10.1080/10236198.2018.1512981.
- [22] P. Percell and M. F. Wheeler. A C^1 finite element collocation method for elliptic equations. *SIAM J. Numer. Anal.*, **17**:605–622, 1980.
- [23] J. Douglas Jr. and T. Dupont. *Collocation Methods for Parabolic Equations in a Single Space Variable*. Springer-Verlag, New York, 1974.

- [24] P.G. Ciarlet. *The Finite Element Method for Elliptic Problems*. North-Holland, New York, 1978.
- [25] B. Bialecki and X. Cai. H^1 -norm error bounds for piecewise hermite bicubic orthogonal spline collocation schemes for elliptic boundary value problems. *SIAM J. Numer. Anal.*, **31**:1128–1146, 1994.
- [26] B. Bialecki. Convergence analysis of orthogonal spline collocation for elliptic boundary value problems. *SIAM J. Numer. Anal.*, **35**:617–631, 1998.
- [27] G. Fairweather and R. Fernandes. Analysis of alternating direction collocation methods for parabolic and hyperbolic problems in two space variables. *Num. Meth. for PDE's*, **9**:191–211, 1993.
- [28] D. Dillery. *Higher Order Orthogonal Spline Collocation Schemes for Elliptic and Parabolic Problems*. PhD thesis, University of Kentucky, Lexington, KY, 1994.
- [29] A. Zenisek. *Nonlinear Elliptic Evolution Problems and Their Finite Element Approximation*. Academic Press, London, 1990.
- [30] B. Li, G. Fairweather, and B. Bialecki. Discrete time orthogonal spline collocation methods for vibration problems. *SIAM J. Numer. Anal.*, **39**:2045–2065, 2002.
- [31] M. Lees. A priori estimates for the solutions of difference approximations to parabolic partial differential equations. *Duke Math. J.*, **27**:297–311, 1960.
- [32] C. de Boor. Package for calculating with B-splines. *SIAM J. Numer. Anal.*, **14**:471–472, 1977.
- [33] J. C. Diaz, G. Fairweather, and P. Keast. FORTRAN packages for solving certain almost block diagonal linear systems by modified alternate row and column elimination. *ACM Trans. Math. Software*, **9**:358–375, 1983.
- [34] J. C. Diaz, G. Fairweather, and P. Keast. Algorithm 603 COLROW and ARCECO: FORTRAN packages for solving certain almost block diagonal linear systems by modified alternate row and column elimination. *ACM Trans. Math. Software*, **9**:376–380, 1983.
- [35] P. Keast. Private communication.
- [36] C. A. J. Fletcher. Generating exact solutions of the two-dimensional Burgers' equation. *Int. J. Numer. Methods Fluids*, **3**:213–216, 1983.

- [37] B. Bialecki and G. Fairweather. Matrix decomposition algorithms in orthogonal spline collocation for separable elliptic boundary value problems. *SIAM J. Sci. Comp.*, **16**: 330–347, 1995.
- [38] B. Bialecki and K. Remington. Fourier matrix decomposition methods for the least squares solution of singular Neumann and periodic hermite bicubic collocation problems. *SIAM J. Sci. Comput.*, **16**:431–451, 1995.
- [39] S.D. Conte and C. de Boor. *Elementary Numerical Analysis, An Algorithmic Approach*. McGraw-Hill Book Company, New York, 1980.
- [40] F.H. Harlow and J.E. Welch. Numerical calculation of time-dependent viscous incompressible flow of fluid with a free surface. *Phys. Fluids*, **8**:2182–2189, 1965.
- [41] C. Canuto, M.Y. Hussaini, A. Quateroni, and T.A. Zang. *Spectral Methods: Evolution to Complex Geometries and Applications to Fluid Dynamics*. Springer, New York, 2007.
- [42] O. Botella. On a collocation B-spline method for the solution of the Navier–Stokes equations. *Computers & Fluids*, **31**:397–420, 2002.
- [43] A.J. Chorin. Numerical solution of the Navier–Stokes equations. *Math. Comput.*, **22**: 745–762, 1968.
- [44] R. Temam. Sur l’approximation de la solution des équations de Navier–Stokes par la méthode de pas fractionnaires, II. *Arch. Ration. Mech. Anal.*, **33**:337–385, 1969.
- [45] L.J.P. Timmermans, P.D. Mineev, and F.N. van de Vosse. An approximate projection scheme for incompressible fluid using spectral elements. *Int. J. for Numer. Meth. in Fluids*, **22**:673–688, 1996.
- [46] J.L. Guermond, P. Mineev, and J. Shen. An overview of projection methods for incompressible flows. *Comput. Methods App. Mech. and Engrg.*, **195**:6011–6045, 2006.
- [47] D.L. Brown, R. Cortez, and M.L. Minion. Accurate projection methods for the incompressible Navier–Stokes equations. *J. Comput. Phys.*, **168**:464–499, 2001.
- [48] J.L. Guermond and J. Shen. On the error estimates for the rotational pressure-correction projection methods. *Math. Comp.*, **73**:1719–1737, 2003.
- [49] W. E and J.G. Liu. Projection method I: Convergence and numerical boundary layers. *SIAM J. Numer. Anal.*, **32**:1017–1057, 1995.

- [50] D. Shirokoff and R.R. Rosales. An efficient method for the incompressible Navier–Stokes equations on irregular domains with no-slip boundary conditions, high order up to the boundary. *J. Comput. Phys.*, **230**:8619–8646, 2011.
- [51] A.J. Chorin and J.E. Marsden. *A Mathematical Introduction to Fluid Mechanics*. Springer–Verlag, New York, 1990.
- [52] O.R. Burggraf. Analytical and numerical studies of the structure of steady separated flows. *Journal of Fluid Mechanics*, **24**:113–151, 1966.
- [53] U. Ghia, K.N. Ghia, and C.T. Shin. High-Re solutions for incompressible flow using Navier-Stokes equations and a multigrid method. *J. Comput. Phys.*, **48**:387–411, 1982.
- [54] O. Botella and R. Peyret. Benchmark spectral results on the lid-driven cavity flow. *Computers & Fluids*, **27**:421–433, 1998.
- [55] D.J. Acheson. *Elementary Fluid Dynamics*. Oxford University Press, New York, 1990.